

AD-A094 771

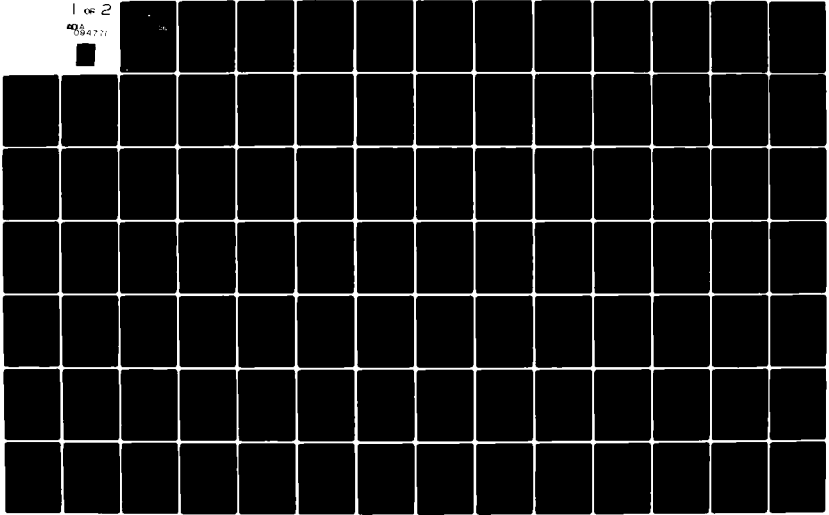
AIR FORCE INST OF TECH WRIGHT-PATTERSON AFB OH SCHOO--ETC F/G 9/2
COMPUTER SIMULATION OF SOLAR AIR HEATING SYSTEMS USING ROCK BED--ETC(U)
DEC 80 D B FANT
AFIT/GAE/AA/80D-4

UNCLASSIFIED

NL

1 of 2

4084771



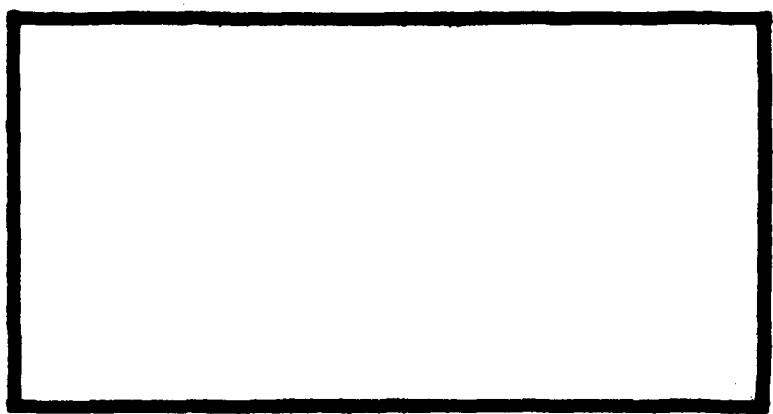
AD A09471

Handwritten marks

(1)



LEVEL II



DTIC
ELECT
FEB 10 1981

S **D**

F

DISTRIBUTION STATEMENT A
 Approved for public release;
 Distribution Unlimited

DEPARTMENT OF THE AIR FORCE
 AIR UNIVERSITY (ATC)
AIR FORCE INSTITUTE OF TECHNOLOGY

Wright-Patterson Air Force Base, Ohio

DC FILE COPY

23 JAN 1981

APPROVED FOR PUBLIC RELEASE AFR 190-17.

Laurel A. Lampela
LAUREL A. LAMPELA, 2Lt, USAF
Deputy Director, Public Affairs

Air Force Institute of Technology (AFIT)
Wright-Patterson AFB, OH 45433

(11) Doc 80

(1) Master's thesis

Accession For	
NTIS GRA&I	<input checked="" type="checkbox"/>
DTIC TAB	<input type="checkbox"/>
Unannounced	<input type="checkbox"/>
Justification	
By _____	
Distribution/	
Availability Codes	
Avail and/or	
Dist	Special
A	

(6) COMPUTER SIMULATION OF SOLAR
AIR HEATING SYSTEMS USING
ROCK BED THERMAL STORAGE UNITS

DTIC ELECTED
FEB 10 1981

THESIS

F

(14) AFIT/GAE/AA/80D-4

(15) DANIEL B. FANT
2LT USAF

anthology

(12) 144

012225

81 2 09 094

COMPUTER SIMULATION OF
SOLAR AIR HEATING SYSTEMS
USING ROCK BED THERMAL STORAGE UNITS

THESIS

Presented to the Faculty of the School of Engineering
of the Air Force Institute of Technology
Air Training Command
in Partial Fulfillment of the
Requirements for the Degree of
Master of Science

by

Daniel B. Fant

2Lt USAF

Graduate Aeronautical Engineering

December 1980

Approved for public release, distribution unlimited.

Preface

Rapid interest in solar energy has come about as a result of increasing costs of energy from conventional fuels. However, due to the intermittent and diffuse nature of solar energy some unique problems have also arisen. One in particular is thermal storage, and this motivated the study of solar air heating systems utilizing rock beds as thermal storage units. A computer simulation model capable of estimating the long-term performance of an air heating system is described in this work, along with complete instructions on how to operate the program. Various systems can be simulated by simply making the appropriate change in input parameters.

I wish to thank the Air Force for accepting me into this program and providing the exceptional staff and faculty which made this educational experience most worthwhile. I also wish to thank Mr. Stan Boyd for obtaining research material that was not readily available from the AFIT library.

I would especially like to thank Dr. James E. Hitchcock, my thesis advisor, for his many hours of assistance, encouragement and suggestions which made this thesis possible. But most of all I would like to thank my parents for their reassurance and support which in so many ways kept me going and made me strong.

Daniel B. Fant

Contents

Preface	11
List of Figures	v
List of Tables	vi
List of Symbols	vii
Abstract	xii
I Introduction	1
Background	1
Purpose	2
Approach	2
II Heat Transfer Analysis of Packed Beds	5
Rock Bed Geometry	5
Rock Bed Assumptions	5
Heat Transfer Coefficients	7
Internal Resistance	11
Development of Differential Equations	13
Solution of Equations Using a Finite-Difference Scheme	15
Analytical Solution for Constant Inlet Air Temperatures	18
III Pressure Drop Equations	25
Power Calculation	25
Rock Bed	25
Collector	26
Duct Work	29
IV Performance Simulation of an Air Heating System	33
Control Strategy (Modes 1, 2 and 3)	33
Space Heating Loads	36
Auxiliary Energy	37
V Results and Conclusions	38
Rock Bed Simulation Results	38
System Simulation Results	55
General Remarks on Rock Bed Air System	62
Conclusions	63

References	66
Appendix A: Review of Method for Determining Useful Energy Collected.	68
Appendix B: Alternate Methods for Determining Heat Transfer Coefficients and Pressure Drop	71
Appendix C: Duct Heat Transfer Relationships	76
Appendix D: Explicit and Modified-Implicit Schemes	81
Appendix E: Program Instructions	84
Appendix F: Air System Flowchart	90
Appendix G: Computer Program Listing	99
Vita	128

List of Figures

<u>Figures</u>		<u>Page</u>
1	Rock Bed Geometry	6
2	Spherical Rock Resistances	11
3	Differential Bed Segment	13
4	Bed Control Volume	14
5	The function F_1 versus δ	23
6	The function f_1 versus δ	24
7	Collector Geometry	27
8	Duct Elbow	30
9	Schematic Diagram of a Solar Air System	34
10	Three Modal Control Box	35
11-12	Air and Bed Temperature Profiles	40
13-17	Comparison of Analytical and Numerical Results	45
18	Bed Pressure Drop	50
19	Collector Pressure Drop	51
20	Duct Work Pressure Drop	52
21-22	Total Monthly Cost	53
23	Net Savings	58
24	Per Cent Solar Energy	59
B1	Staggered Tube Arrangement	73
B2	Tube Bundle	73
C1	Duct Cross Section	76
C2	Duct Length Section	79

List of Tables

<u>Table</u>		<u>Page</u>
1	Temperature Convergence Data	39
2	Solar Energy Savings	60
3	Solar Energy Data	61
4	Types of Rocks and Their Densities	64
5	Some Common Heat Storage Materials	65
B1	Particle Shape Factors	72
E1	Degree-Days, Vandalia, Ohio	89

List of Symbols

<u>English Symbols</u>	<u>Meaning</u>	<u>Units</u>
a	Collector air gap spacing	ft
A	Cross sectional area of bed	ft ²
A _{col}	Air duct cross sectional area in collector	ft ²
A _D	Duct cross sectional area	ft ²
A _{ins}	Surface area for insulation	ft ²
A _m	Minimum flow area	ft ²
A _p	Surface area of particles	ft ²
A _s	Surface area of spherical rock	ft ²
A _{void}	Void area	ft ²
A _w	Wetted-surface area	ft ²
B	Width of collector	ft
B _i	Biot number	dimensionless
C _o	Pressure loss coefficient	dimensionless
c _{pa}	Specific-heat of air	B/lbm-F
c _{ps}	Specific-heat of solid	B/lbm-F
DD	Degree-Days	F
D _h	Hydraulic-diameter	ft
D _m	Minimum clearance distance	ft
D _p	Particle diameter	ft
D _T	Duct diameter	ft
EFFP	Fan efficiency	dimensionless
EG	Void fraction	dimensionless
EPSIL	Discharge tolerance	hours
f	Fanning-friction factor	dimensionless

<u>English Symbols</u>	<u>Meaning</u>	<u>Units</u>
f^l	D'arcy friction factor	dimensionless
FTC1	Primary Federal tax credit percentage/100	dimensionless
FTC2	Secondary Federal tax credit percentage/100	dimensionless
g_c	Newton's second law, 32.174	lbm-ft/lbf-sec ²
G	Mass velocity	lbm/ft ² -sec
G_{rD}	Grashof number	dimensionless
h	Heat transfer coefficient	B/hr-ft ² -F
HB	Bed height	ft
h_i	Forced-convection heat-transfer coefficient	B/hr-ft ² -F
h_o	Free-convection heat-transfer coefficient	B/hr-ft ² -F
h	Volumetric heat-transfer coefficient	B/hr-ft ³ -F
i	Position subscript	dimensionless
j	Time superscript	dimensionless
K_f	Conductivity of fluid	B/hr-ft-F
K_{ins}	Conductivity of insulation	B/hr-ft-F
KJ	Number of bed segments	dimensionless
K_s	Conductivity of solid	B/hr-ft-F
L	Length of collector	ft
L*	Characteristic Bed Length	ft
LB	Bed length	ft
LC	Collector length	ft
LD	Duct length	ft
LTCA	Secondary tax credit amount	\$
\dot{m}_a	Mass flowrate of air	lbm/hr
N	Number of bed nodes & number of transverse rows	dimensionless
NH	Number of hours of operation	hours

<u>English Symbols</u>	<u>Meaning</u>	<u>Units</u>
Nu*	Characteristic Nusselt number	dimensionless
OTC	Ohio tax credit percentage/100	dimensionless
P _c	Air duct perimeter for collector	ft
P _r	Prandtl number	dimensionless
P _w	Wetted perimeter of rock	ft
P	Power	B/hr
Q	Volumetric flowrate	ft ³ /hr
QAUX	Auxiliary energy requirements	Btu
QAVE	Useful energy collected	Btu
Q _L	Energy lost from bed	Btu
QMIN	Minimum blowing energy requirements	Btu
QSHL	Space heating load requirements	Btu
Re*	Characteristic Reynolds number	dimensionless
R _i	Internal rock resistance	hr-F/B
R _o	External rock resistance	hr-F/B
R _h	Hydraulic-radius	ft
R _p	Rock radius	ft
S _L	Center to center longitudinal distance	ft
S _T	Center to center transverse distance	ft
STCA	Initial tax credit amount	\$
t	Time parameter	hours
T _a	Air temperature	F
\bar{T}_a	Average ambient monthly temperature	F
T _{a,o}	Initial air temperature	F
T _b	Bed temperature	F

<u>English Symbols</u>	<u>Meaning</u>	<u>Units</u>
$T_{b,0}$	Initial bed temperature	F
t_f	Film-temperature	F
TIB	Bed temperature initially	F
t_{ic}	Air temperature into collector	F
t_{id}	Air temperature into duct	F
TIN	Air temperature into bed	F
t_{ins}	Bed insulation thickness	ft
t_o	Rock temperature	F
TOB	Air temperature outside bed	F
t_{oc}	Air temperature coming out of collector	F
t_{od}	Air temperature coming out of duct	F
TMAXC	Maximum credit return	\$
TMIN	Discharge time increment	minutes
TN	Number of elbows	dimensionless
t_w	Wall temperature	F
t_∞	Free stream air temperature	F
U	Overall heat transfer coefficient	B/hr-ft ² -F
UA	Structure conductance	B/hr-F
U*	Characteristic velocity	ft/hr
U_I	Insulation conductance	B/hr-F
V	Oncoming air velocity	ft/hr
V_g	Void volume	ft ³
V_o	Superficial velocity	ft/hr
V_p	Rock volume	ft ³
WB	Width of bed	ft

English Symbols

	<u>Meaning</u>	<u>Units</u>
w_k	Blowing work	Btu
x	Bed position parameter	ft

Greek Symbols

	<u>Meaning</u>	<u>Units</u>
α	Collector aspect ratio	dimensionless
β	Coefficient of volumetric expansion	1/R
δ	Analytical solution parameter or declination angle	dimensionless, degrees
ϵ_g	Void fraction	dimensionless
ϵ_p	Rock fraction	dimensionless
η	Analytical heat loss parameter	dimensionless
ρ_a	Air density	lbm/ft ³
ρ_s	Solid density	lbm/ft ³
μ	Dynamic viscosity	lbf/hr-ft ²
ν	Momentum diffusivity	ft ² /hr
$\Delta\tau$	Time increment	hours
ϕ	Shape factor or latitude	dimensionless, degrees

ABSTRACT

This thesis is concerned with the analysis and design of solar air heating systems utilizing rock beds as thermal storage units. A computer simulation model capable of estimating the response of both the solar collector and the rock bed is described. Differential equations describing the rock bed were approximated in a finite-difference form and solved numerically on a digital computer. The temperature of both the solid (rock) and the fluid (air) is determined as a function of time and distance along the bed. The simulation required both charging and discharging of the rock bed for time-varying inlet fluid temperatures. The numerical method used to solve the rock bed equations proved to be stable and convergent and showed satisfactory agreement in comparison to an analytical solution for constant-inlet air temperatures. A cost analysis was also incorporated within this program, by varying the collector area one could determine the optimum collector size for maximum savings. Pressure drop relationships for flat-plate collectors, duct work and packed beds were used to determine operating costs. The particular air system tested proved to be cost effective when compared with natural gas fuel costs for an economic term of 20 years.

COMPUTER SIMULATION OF SOLAR
AIR HEATING SYSTEMS USING
ROCK BED THERMAL STORAGE UNITS

I Introduction

Background

The incident solar energy on earth is approximately 1.2×10^{19} Btu per year, while the world's total energy consumption is about 7×10^{16} Btu per year (Ref 17). However, solar energy is a variable source of energy. Here on earth, the sun shines only during the day; and on cloudy days it is intermittent. Therefore, proper storage of this abundant, cheap, and pollution free energy is necessary for its efficient utilization.

The idea of thermal storage goes way back to the caveman or Roman era when they brought sun heated stones or bricks to bed to supply them with warmth during the night. The Romans also dug deep cellars in the side of hills which they filled with snow during the winter and it would remain throughout the summer to be used when needed. These above happenings can best be explained by the fact that rocks act as a good storage material (Ref 17).

The direct mode of operation of air heating systems is to transfer heated air directly from the collector to the heated space. When more energy is collected than needed, it is stored sensibly in a storage bed by blowing heated air from the collector through the bed. This is referred to as the bed charging mode. When energy is not available from the collector to satisfy the space heating loads, sensible energy is removed from the rock bed. This is known as the bed discharging mode. Discharging is normally accomplished by a reversal of the air flow, thus, causing the outlet air temperature to approach the temperature at the hot end of the bed.

Purpose

The purpose of this thesis was to develop a computer program which completely simulates the three-modal operation of a solar air heating system utilizing rock beds for thermal storage. This involves a numerical method for computing the temperatures of both the air and rock as functions of time and distance for the charging and discharging modes of the bed.

With a proper theoretical analysis of rock beds, duct work and collectors, a simulation model would provide the useful purpose of estimating the performance of a solar air heater much more quickly and cheaply than would be possible by experimentation. In order to simulate various systems, a change in only certain parameters is necessary.

Approach

Before simulating an air system along with the thermal performance of a rock bed storage unit with varying inlet air temperatures, one must first develop a scheme for solar energy collection. Fortunately, this was accomplished by utilizing the previous work of Captain Prins (Ref 16) on solar water heating systems. His long term analysis of flat-plate collectors was used for determining the useful amount of solar energy collected per unit time. Here, long term is defined to be that period of time necessary to describe the performance of a heating system in any particular climate, normally a one to two year period is sufficient for long term simulations (Ref 12).

The amount of useful energy collected is the difference between the solar energy absorbed and the energy lost by the collector. It is a function of the collector area (AC), the collector heat removal efficiency (FR), the monthly average instantaneous total radiation (\bar{I}_{Tt}), the utilizability (UT) and the effective transmittance-absorptance product ($\overline{\tau\alpha}$).

$$Q = AC \times FR \times \bar{I}_{Tt} \times UT \times (\overline{\tau\alpha}) \quad (1)$$

FR is a function of the fluid flowrate and the absorber plate design. \bar{T}_{Tt} depends on the location and orientation of the collector, also on the hour of day and the time of year. The utilizability is a function of variability of the incident solar energy and the loss coefficient of the collector, which in turn is a function of the number of cover plates, cover material and amount of insulation. Lastly, $(\bar{\tau\alpha})$ also depends on absorber plate properties, the number of cover plates and the angle at which solar radiation strikes the collector.

The useful energy collected in equation (1) also determines the temperature rise of the collector air.

$$Q = (\dot{m}_a c_{pa}) (T_{oc} - T_{ic}) \quad (2)$$

where \dot{m}_a is the mass flowrate of air into the collector, c_{pa} is the specific heat of air at the constant pressure, T_{ic} is the air temperature into the collector and T_{oc} is the air temperature out of the collector. Therefore, if Q is determined from equation (1), one can then solve for T_{oc} from equation (2).

$$T_{oc} = [Q/\dot{m}_a c_p] + T_{ic} \quad (3)$$

Equation (3) is utilized in the program to determine the varying air temperatures into the rock bed during the charging mode.

Flat-plate collector results must be combined with a rock bed performance analysis to completely simulate air heating systems. This involved describing a control strategy for the various operational modes of the system; along with developing an adequate space heating model and determining auxiliary energy requirements.

A slight modification of Prins' cost analysis was also necessary to deal with air system simulations.

The heart of this thesis remains to follow, it deals with the theoretical heat transfer analysis of rock beds in Chapter II, pressure drop relationships in Chapter III and a control strategy in Chapter IV. Finally, the results of a typical computer simulation are presented and discussed in Chapter V.

II Heat Transfer Analysis of Packed Beds

In this chapter, the study of the flowrate of air through rock beds is examined. Heat transfer coefficient formulas are discussed and the differential equations which describe the response of the bed are developed. A finite-difference numerical solution to these equations is also presented.

Rock Bed Geometry

The rock bed is a relatively simply looking storage unit, for its geometry refer to Fig 1. The bed consists of a container to hold the rocks plus an inlet and outlet for the flow of air through the unit. For computer purposes it is divided into N-equal segments, all assumed isothermal and of length Δx ; this assumption becomes better as the number of segments is increased. Also, insulation surrounds all sides of the bed to minimum energy losses.

A well designed bed is cubical in shape and utilizes rocks that may vary between .5 and 2.5 inches in diameter; these two facts result from pressure drop and heat transfer considerations (Ref 17).

Rock Bed Assumptions

- a. Rocks are spherical with void fractions of 30 to 60 per cent.
- b. Fluid must be a gas such as air.
- c. Constant fluid and material properties (for air this is a very good approximation for the temperature range, 70-200 F).
- d. For practical purposes, it is advisable to deal with a uniform or average volumetric heat transfer coefficient, rather than focus on local values.
- e. Constant volumetric flowrates.
- f. Fluid flow and heat conduction in the solid material are one-dimensional in the flow direction.

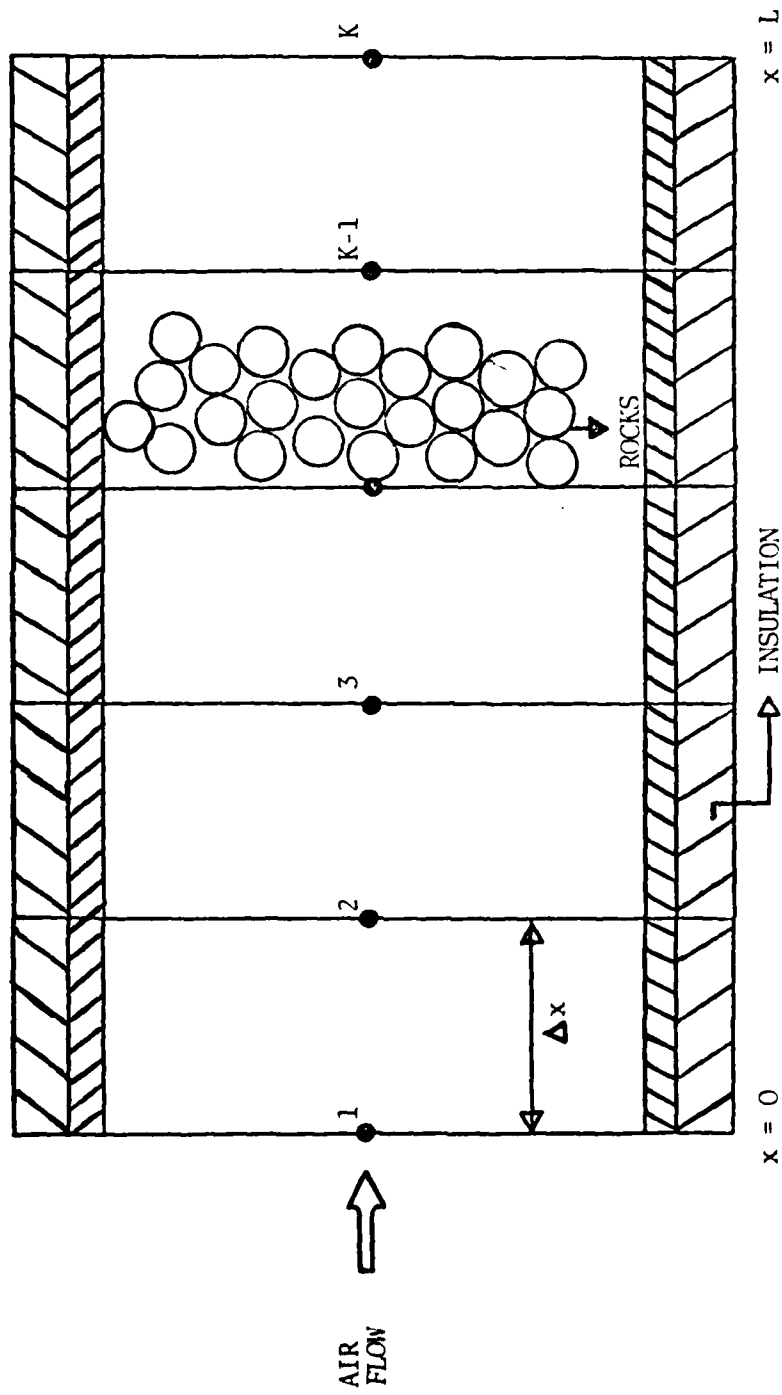


Fig 1. Rock Bed Geometry

- g. Thermal storage within the fluid (air) is neglected.
- h. Heat conduction within the fluid (air) is neglected.
- i. Fluid properties are evaluated at a film temperature, t_f , where

$$t_f = \frac{t_o + t_\infty}{2}$$

and

t_∞ = free stream air temperature

t_o = rock temperature

Heat Transfer Coefficients

There are several methods for determining the heat transfer coefficient between the air and the solid. However, in this section a relationship which takes into account both laminar and turbulent flow contributions will be considered. The following expressions and equations were cited from Ref 18.

For alternate methods refer to Appendix B.

The void fraction, ϵ_g , is defined as

$$\epsilon_g = \frac{\text{void volume of bed}}{\text{total volume of bed}} = \frac{V_g}{V} \quad (4)$$

therefore, the particle or rock fraction, ϵ_p , is

$$\epsilon_p = \frac{\text{rock volume}}{\text{total volume of bed}} = 1 - \epsilon_g \quad (5)$$

For a bed with N particles which have a volume, V_p , the volume occupied by the rocks is

$$V_p N = V - \epsilon_g V = V(1 - \epsilon_g) \quad (6)$$

Then, the number of particles per unit volume is

$$\frac{N}{V} = (1 - \epsilon_g)/V_p \quad (7)$$

The hydraulic radius, R_h , is defined as

$$R_h = \frac{\text{void volume of bed}}{\text{surface area of particles}} = \frac{\epsilon gV}{A_p N} \quad (8)$$

where A_p is the surface area of a particle. Substituting for $\frac{N}{V}$ from equation (7) yields

$$R_h = \frac{Vp}{A_p} \frac{\epsilon g}{(1 - \epsilon g)} \quad (9)$$

For heat transfer purposes, a characteristic length and velocity are needed. Ref 18 used six times the hydraulic radius for the characteristic length, L^* . Substituting for R_h from equation (9) yields

$$L^* = 6R_h = \frac{6Vp}{A_p} \frac{\epsilon g}{1 - \epsilon g} \quad (10)$$

A spherical particle diameter, D_p , is defined as

$$D_p = 6Vp/A_p \quad (11)$$

where

$$Vp = \pi D_p^3 / 6$$

$$A_p = \pi D_p^2$$

So now the characteristic length becomes

$$L^* = D_p \frac{\epsilon g}{1 - \epsilon g} \quad (12)$$

The characteristic velocity, u^* , is defined as the average velocity of the fluid flowing through the voids. From continuity

$$\rho A_{\text{void}} u^* = \rho V_0 A \quad (13)$$

where V_0 is the superficial or free-stream velocity. The void area, A_{void} , is related to A , the cross sectional area of the bed by

$$A_{\text{void}} = \epsilon_g A \quad (14)$$

Combining equation (14) and equation (13) the characteristic velocity becomes

$$u^* = V_0 / \epsilon_g \quad (15)$$

This is also referred to as the institutional velocity.

Finally, an expression for the characteristic Reynolds number can be written as

$$\text{Re}^* = u^* L^* / \nu \quad (16)$$

where ν , the momentum diffusivity, is

$$\nu = \mu_g c / \rho \quad (17)$$

Combining equations (12), (15), (17) and (16) yields

$$\text{Re}^* = D_p G / \mu_g c (1 - \epsilon_g) \quad (18)$$

where G = superficial mass velocity = ρV_0 .

The characteristic Nusselt number is defined as

$$\text{Nu}^* = h L^* / K_f \quad (19)$$

Substituting for L^* from equation (12) into equation (19) gives

$$\text{Nu}^* = \frac{hD_p}{K_f} \frac{\epsilon_g}{1-\epsilon_g} \quad (20)$$

where h is the average coefficient of heat transfer and K_f , the thermal conductivity of the fluid.

The empirical formulation of the Nusselt number is represented by the following equation (Ref 18):

$$\text{Nu}^* = (1.5 \text{Re}^{*1/2} + 0.2 \text{Re}^{*2/3}) \text{Pr}^{1/3} \quad (21)$$

Reynolds number to the one-half power accounts for laminar flow effects while $\text{Re}^{*2/3}$ is its turbulent counterpart.

Combining equations (20) and (21) and solving for h gives

$$h = \frac{(1 - \epsilon_g)}{\epsilon_g} \frac{K_f}{D_p} (0.5\text{Re}^{*1/2} + 0.2 \text{Re}^{*2/3}) \text{Pr}^{1/3} \quad (22)$$

where Pr is the Prandtl number of the fluid. Remember, all fluid properties are evaluated at a film temperature as discussed earlier.

Equation (22) is valid for void fractions less than .65 and Reynolds numbers greater than or equal to 100. This equation can be used for either spherical or cylindrical shaped objects, and it can be modified for staggered tube arrangements. For quick approximations of h , an experimental curve of Nusselt number versus Reynolds number is provided in Ref 18.

To determine the volumetric heat transfer coefficient, h_v , the following expression is used

$$h_v = h d A_h / A_{dx} \quad (23)$$

where

A = cross sectional area of bed segment

A_{dx} = total volume of bed segment

dA_h = total surface area of particles.

Therefore,

$$\begin{aligned} dA_h &= 4\pi R_p^2 \text{ [number of particles]} \\ &= 4\pi R_p^2 \text{ [Adx (1 - } \epsilon_g) / \pi D_p^3 / 6] \end{aligned}$$

or

$$dA_h = \frac{6}{D_p} \text{ Adx (1 - } \epsilon_g) \quad (24)$$

After substituting dA_h from equation (24) into equation (23), h_v becomes

$$h_v = 6h (1 - \epsilon_g) / D_p \quad (25)$$

Internal Resistance

To account for internal temperature gradients within the rocks a non-dimensional heat transfer parameter known as the Biot number must first be described.

The Biot number, Bi , is defined as

$$Bi = \frac{\text{internal resistance}}{\text{external resistance}} = \frac{R_i}{R_o} \quad (26)$$

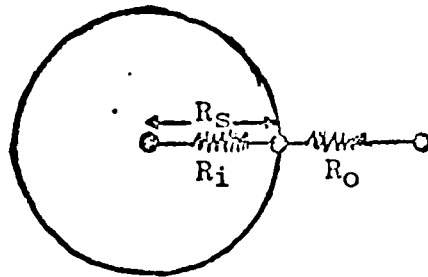


Fig 2. Spherical Rock Resistances

where, the internal resistance is

$$R_i = R_s / K_s A_s \quad (27)$$

and

K_s = thermal conductivity of solid

A_s = surface area of rock.

R_o , the external resistance is

$$R_o = \frac{1}{hA_s} \quad (28)$$

where h is determined by equation (22). Combining equations (26), (27) and (28) yields

$$Bi = \frac{R_i}{R_o} = \frac{hR_p}{K_s} \quad (29)$$

It is only when the Biot number is less than 0.1 can heat conduction in the solid material be neglected. In this case, the thermal resistance of the solid particles is small in comparison to the thermal resistance of the convective film between the air and solid. Therefore, for $Bi < .1$ the effect of temperature gradients within the solid particles can be ignored.

A Biot number correction proposed by "Babcock" in an article written by Jefferson (Ref 9) is a factor which can be incorporated into the heat transfer coefficient to account for the following effects: axial (static) fluid-solid-fluid conduction, fluid phase axial dispersion, fluid-solid heat transfer resistance, and most importantly, internal particle thermal resistance. The result according to Babcock is

$$h_{veff} = \frac{hv}{(1 + Bi/5)} \beta^2 \quad (30)$$

where

$$\beta = \frac{HCS}{HCS + HCA}$$

and

$$HCS = \text{heat capacity of solid} = \rho_s c_{ps} (1 - \epsilon_g)$$

$$\text{HCA} = \text{heat capacity of air} = \rho_a c_{pa} \epsilon g$$

Note that HCA is much less than HCS since the density of air is much less than the rock density, therefore β is approximately one; so for air the effect of β on equation (30) can be neglected.

Also, the formula proposed by "Babcock" was proven experimentally for Biot numbers up to about 4.

Development of Differential Equations

To develop the equations which describe the response of a rock bed, two energy balances on the following control volume must be made. (A similar set of equations can also be found in Ref 6). The first energy balance is for the fluid (air) equation while the other is for the solid.

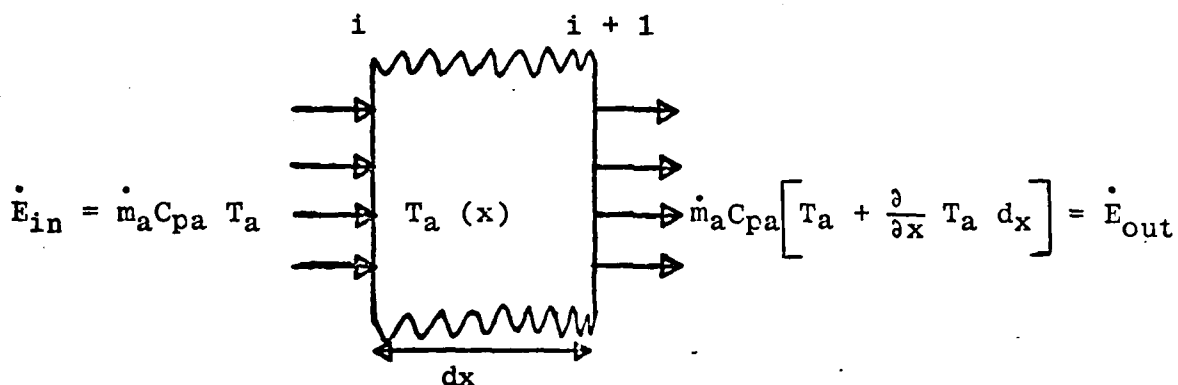


Fig 3. Differential Bed Segment

The time rate of change of energy within the control volume is

$$\dot{E}_{\text{stored}} = \epsilon g \rho_a c_{pa} A dx \frac{\partial T_a}{\partial t} \quad (31)$$

where, $\epsilon_g A dx$ is the void volume. Applying the conservation of energy law

$$\dot{E}_{in} = \dot{E}_{out} + \dot{E}_{stored} = h \frac{dA_h}{Adx} (T_a - T_b) Adx \quad (32)$$

where

$$\frac{hdA_h}{Adx} = h_v \text{ as seen from equation (23).}$$

With some rearrangement and substituting for \dot{E}_{in} , \dot{E}_{out} and \dot{E}_{stored} , equation (32) simplifies to

$$-\rho_a V_o c_{pa} \frac{\partial T_a}{\partial x} dx - \epsilon_g \rho_a c_{pa} dx \frac{\partial T_a}{\partial t} = h_v (T_a - T_b) dx \quad (33)$$

Now, dividing through by $\rho_a c_{pa} \epsilon_g dx$ and substituting u^* for V_o / ϵ_g yields

$$\frac{\partial T_a}{\partial t} + u^* \frac{\partial T_a}{\partial x} = \frac{-h_v}{\rho_a c_{pa} \epsilon_g} (T_a - T_b) \quad (34)$$

But since the heat capacity of the bed ($\rho_s dvol c_{ps}$) is much greater than the heat capacity of the air ($\rho_a dvol c_{pa}$), the temperature of the air as a function of time may be neglected. Therefore, equation (34) becomes:

$$\frac{\partial T_a}{\partial x} = \frac{-h_v A}{\dot{m}_a c_{pa}} (T_a - T_b) \quad (35)$$

where $\dot{m}_a = \rho_a A \epsilon_g u^*$.

The following control volume will again be used to represent the bed temperature as a function of time.

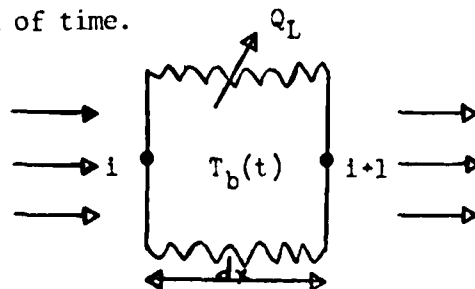


Fig 4. Bed Control Volume

Energy equations for this case are

$$\dot{E}_{\text{into bed}} = \dot{m}_a c_{pa} [T_{a,i} - T_{a,i+1}] \quad (36)$$

$\dot{E}_{\text{out of bed}} = Q_L$; where Q_L , the amount of energy lost from the bed is

$$Q_L = U_I (T_b - \text{TOB}) \quad (37)$$

and

$$U_I = \frac{K_{\text{ins}} A_{\text{ins}}}{t_{\text{ins}}}$$

where

K_{ins} = conductivity of the insulation

A_{ins} = surface area of the bed

t_{ins} = thickness of insulation surrounding bed

and, TOB = air temperature outside the bed. Also,

$$\dot{E}_{\text{stored}} = (1 - \epsilon_g) \rho_s c_{ps} A \Delta x \frac{\partial T_b}{\partial t} \quad (38)$$

where; $(1 - \epsilon_g) A \Delta x$ is the solid volume.

Therefore, again applying the conservation law and rearranging gives

$$(1 - \epsilon_g) \rho_s c_{ps} A \Delta x \frac{\partial T_b}{\partial t} = \dot{m}_a c_{pa} [T_{a,i} - T_{a,i+1}] - Q_L \quad (39)$$

Solving for $\frac{\partial T_b}{\partial t}$ yields

$$\frac{\partial T_b}{\partial t} = \frac{\dot{m}_a c_{pa}}{(1 - \epsilon_g) \rho_s c_{ps} A \Delta x} [T_{a,i} - T_{a,i+1}] - \frac{Q_L}{(1 - \epsilon_g) \rho_s c_{ps} A \Delta x} \quad (40)$$

Solution of Equations

The two equations now derived can be approximated in a finite-difference

form. In this section an implicit solution scheme will be presented. This scheme provides stability and thus allows for larger time steps, therefore, computer costs are reduced while still maintaining reasonable results. Refer to Appendix C if an explicit or a modified-implicit scheme is desired. For the equations that follow, the subscript "i" refers to the distance increment and superscript "j" refers to the time step. As mentioned before, the bed is broken up into N-equal segments. Therefore, the equations are used to solve for N-unknown bed and N-unknown fluid temperatures.

Our partial differential equations in an implicit form, as functions of new time and position, become

$$\left(\frac{\partial T_a}{\partial x}\right)^{j+1} = \frac{-h_v A}{\dot{m}_a c_{pa}} \left(T_{a,i+1}^{j+1} - T_{b,i+1}^{j+1}\right) \quad (41)$$

and

$$\left(\frac{\partial T_b}{\partial t}\right)_{i+1} = \frac{\dot{m}_a c_{pa}}{(1 - \epsilon_g) \rho_s c_{ps} A \Delta x} \left(T_{a,i}^{j+1} - T_{a,i+1}^{j+1}\right) - Q_L [(1 - \epsilon_g) \rho_s c_{ps} A \Delta x] \quad (42)$$

Finite-differencing equation (41) yields

$$\left(\frac{T_{a,i+1} - T_{a,i}}{\Delta x}\right)^{j+1} = \frac{-h_v A}{\dot{m}_a c_{pa}} \left(T_{a,i+1}^{j+1} - T_{b,i+1}^{j+1}\right) \quad (43)$$

After some more rearrangement and letting $C_1 = \frac{h_v A \Delta x}{\dot{m}_a c_{pa}}$

$$T_{a,i+1}^{j+1} = \frac{1}{1+C_1} T_{a,i}^{j+1} + \frac{C_1}{1+C_1} T_{b,i+1}^{j+1} \quad (44)$$

Since C_1 is always positive, the quantity $(1/1 + C_1)$ will never become negative; therefore, this particular form of the air equation will remain

stable for any Δx . In both the explicit and modified-implicit solution schemes, Appendix C, a Δx stability criteria is required.

Equation (42) in a fully-implicit form becomes:

$$\frac{T_{b,i+1}^{j+1} - T_{b,i+1}^j}{\Delta\tau} = \frac{\dot{m}_a c_{pa}}{Q^*} T_{a,i}^{j+1} - \frac{\dot{m}_a c_{pa}}{Q^*} T_{a,i+1}^{j+1} - Q_L/Q^* \quad (45)$$

where: $Q^* = (1 - \epsilon_g) \rho_s c_{ps} A \Delta x$.

Multiplying through by $\Delta\tau$ and letting $C_2 = \frac{\dot{m}_a c_{pa} \Delta\tau}{Q^*}$

$$T_{b,i+1}^{j+1} = T_{b,i+1}^j + C_2 \left(T_{a,i}^{j+1} - T_{a,i+1}^{j+1} \right) - \frac{Q_L \Delta\tau}{Q^*} \quad (46)$$

This form of the bed equation will always be stable, for any $\Delta\tau$. Now substituting for $T_{b,i+1}^{j+1}$ from equation (46) into equation (44) and doing some more manipulation yields:

$$T_{a,i+1}^{j+1} = \frac{1+C_1 C_2}{1+C_1+C_1 C_2} T_{a,i}^{j+1} + \frac{C_1}{1+C_1+C_1 C_2} T_{b,i+1}^j - \frac{C_1}{1+C_1+C_1 C_2} \frac{Q_L \Delta\tau}{Q^*} \quad (47)$$

where $Q_L = U_I (T_{b,i+1}^j - TOB)$ as in equation (37). Equation (47) represents the fully-implicit finite-differenced air equation as a function of time and position in the bed.

Substituting for $T_{a,i+1}^{j+1}$ from equation (47) into equation (46) yields the final bed equation.

$$T_{b,i+1}^{j+1} = \frac{C_1 C_2}{1+C_1+C_1 C_2} T_{a,i}^{j+1} + \frac{1+C_1}{1+C_1+C_1 C_2} \left[T_{b,i+1}^j - \frac{Q_L \Delta\tau}{Q^*} \right] \quad (48)$$

Equations (47) and (48) will completely describe the response of the rock bed for nodes 2 through k.

However, in the discharging mode where a complete reversal of the bed temperature distribution is required, the bed temperature at node 1 must also be determined. To do this, a second-order, polynomial curve fit is used. The curve is as follows:

$$\begin{aligned}
 T_{b_1} + B\Delta x + C\Delta x^2 &= T_{b_2}^{j+1} \\
 T_{b_1} + 2B\Delta x + 4C\Delta x^2 &= T_{b_3}^{j+1} \\
 T_{b_1} + 3B\Delta x + 9C\Delta x^2 &= T_{b_4}^{j+1}
 \end{aligned}
 \tag{49}$$

These equations were solved using the Gauss-Siedel Reduction method; the resultant bed temperature at node 1 is

$$T_{b_1} = T_{b_4} - 3T_{b_3} + 3T_{b_2}^{j+1}
 \tag{50}$$

Since monotonic temperature curves were usually present in both modes, equation (50) proved to be a fairly accurate extrapolation.

Analytical Solution

An analytical result serves the useful purpose of evaluating the completeness and validity of the numerical method.

The analytical solution proposed by Clark and Arpaci in Ref 5 is as follows: For the air temperature

$$\begin{aligned}
 T_a(S, \delta) - T_{a,0} &= D(0)F_1(S, \delta) + \\
 &\frac{D(\delta) - D(0)}{\delta} G_1(S, \delta)
 \end{aligned}
 \tag{51}$$

and for the bed temperature

$$T_b(S, \delta) - T_{b,o} = D(o) f_1(S, \delta) + \frac{D(\delta_1) - D(o)}{\delta_1} g_1(S, \delta) \quad (52)$$

The initial and boundary conditions are:

$$T_a(x, 0) = T_{a,o} = \text{initial air temperature}$$

$$T_b(x, 0) = T_{b,o} = \text{initial bed temperature}$$

$$T_a(0, t) = T_a(t) = \text{inlet air temperature}$$

For stability purposes these equations were only valid for small time steps and small distance increments. Also, the equations were derived assuming negligible heat loss from the bed. In equations (51) and (52)

$$D(o) = T_a(o) - T_{a,o}$$

$$D(\delta_1) = T_a(\delta_1) - T_{a,o}$$

and

$$S = \frac{\bar{h} P_w}{\rho_a c_{pa} A_{\text{void}}} \left(\frac{x}{u^*} \right) \quad (53)$$

$$\delta = \frac{\bar{h} P_w}{\rho_s c_{ps} A^1} \left(t - \frac{x}{u^*} \right) \quad (54)$$

where

u^* = interstitial velocity

A_{void} = flow area

$A^1 = (1 - \epsilon_g) A$ = rock area

t = time in bed

x = position in bed

\bar{h} = average heat transfer coefficient

P_w = wetted perimeter of rock

and $P_w/A_{\text{void}} = \frac{\text{wetted perimeter}}{\text{flow area}}$; but since R_h , the hydraulic radius, can

also be written as the ratio of flow area to wetted perimeter, one obtains from equation (10)

$$P_w/A_{\text{void}} = \delta/L^* \quad (55)$$

Substituting for L^* from equation (12) into equation (55) and letting $A^* = dA_h/dx$ from equation (24) yields

$$P_w/A_{\text{void}} = A^*/\epsilon g \quad (56)$$

Also note that in Figs 5 and 6

$$V = u^*$$

$$\theta = t$$

$$\rho^l = \rho_s$$

$$C_p^l = c_{ps}$$

$$\rho = \rho_a$$

$$C_p = c_{pa}$$

$$\Lambda = \Lambda_{\text{void}}$$

The functions, F_1 , G_1 and f_1 and g , from equations (51) and (52) can be determined graphically as functions of S and δ , or they can be obtained mathematically with the use of Bessel functions. To check the validity of the numerical program, a constant inlet air temperature was tested, and the graphical method was employed.

For a constant inlet air temperature case

$$T_a(\delta_n) = T_a(o); n = 1, 2, 3...$$

and

$$D(\delta_n) = D(o)$$

Equation (51) becomes

$$T_a - T_{a,o} = (T_g(o) - T_{a,o}) F_1 \quad (57)$$

Equation (57) represents the analytical air equation for constant-inlet air temperatures. Equation (52) yields the analytical bed equation.

$$T_b - T_{b,o} = f_1 (T_g(o) - T_{b,o})$$

For the graphs of F_1 and f_1 refer to Figs 5 and 6.

An analytical result (Ref 7) for the bed temperature at node 1 ($x=0$) can be obtained from the explicit bed equation in Appendix D, namely:

$$\frac{\partial T_b}{\partial t} = \frac{-hA^* (T_b - T_a)}{(1 - \epsilon_g) \rho_s c_{ps}} ; \quad (58)$$

integrating and rearranging we get:

$$\int_{T_{b,o}}^{T_b} \frac{\partial T_b}{(T_b - T_{a,o})} = \frac{-hA^*}{(1 - \epsilon_g) \rho_s c_{ps}} \int_{t_0}^t \partial t \quad (59)$$

At $x=0$, T_a is constant for a particular $\Delta\tau$, therefore equation (59) becomes:

$$\ln(T_b - T_{a,o}) \Big|_{T_{b,o}}^{T_b} = \frac{-hA^*}{(1 - \epsilon_g) \rho_s c_{ps}} \Delta\tau \quad (60)$$

and again rearranging yields:

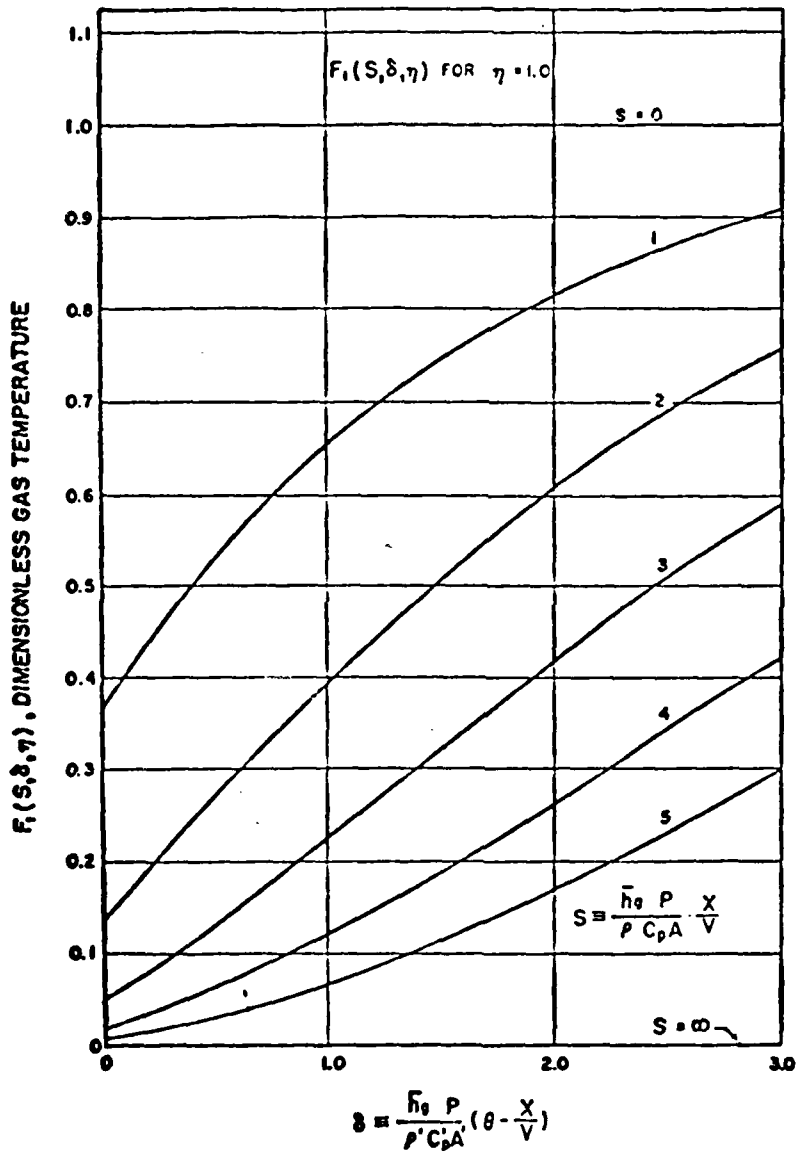
$$\frac{T_b - T_{a,o}}{T_{b,o} - T_{a,o}} = \exp \left(\frac{-hA^* \Delta\tau}{(1 - \epsilon_g) \rho_s c_{ps}} \right) \quad (61)$$

where :

$T_{a,0}$ = initial air temperature

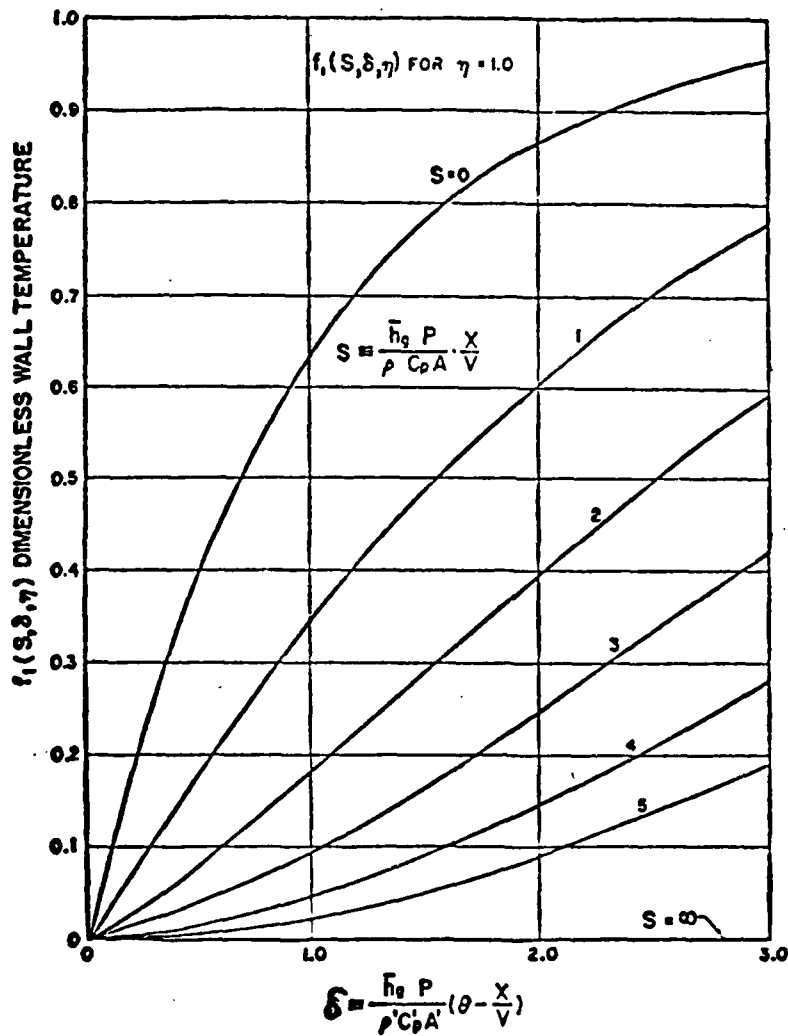
$T_{b,0}$ = initial bed temperature

Equation (61) represents the analytical response of the bed at $x=0$. This result can be used for comparison purposes with the numerical curve fit solution at node 1.



($\eta = 1$ signifies no heat loss)

Fig 5. The function F_1 versus δ (Fe²)



($\eta = 1$ signifies no heat loss)

Fig 6 . The function f_1 versus δ (Pe⁰)

III Pressure Drop Equations

This chapter deals with the discussion of pressure drop relationships for rock beds, flat plate collectors, and duct work.

Power Calculation

Once pressure drop has been determined a power calculation is necessary to obtain fan blowing costs. The theoretical work per unit mass, w_k , is given by the pressure drop divided by the air density.

$$w_k = \frac{\Delta P}{\rho_a} \quad (62)$$

Power, the rate of doing work, is therefore

$$P = \text{power} = w_k \dot{m}_a = w_k (\rho_a AV) \quad (63)$$

In terms of the volumetric flowrate, $Q = VA$

$$P = \rho_a Q w_k \quad (64)$$

Power estimates can be easily converted to operating costs by using standard utility prices and a fan efficiency factor.

Rock Bed

Ergun's equation (Ref 3) was used to determine rock bed pressure drop. His particular relationship is valid for both laminar and turbulent flows and for void fractions between .40 and .65.

$$\frac{-\Delta P}{L} = \frac{\rho V_o^2}{D_p} \left(\frac{1-\epsilon}{\epsilon} \frac{g}{3} \right) \left[170 \frac{1-\epsilon}{R_{ep}} \frac{g}{g} + 1.75 \right] \quad (65)$$

where

ρ = density of fluid (air)

V_o = free-stream velocity

$R_{e_p} = V_o D_p / \nu_f$ = Reynolds number

Ergun's equation can also be written in the following form which accents the presence of both a viscous term and a dynamic pressure term.

$$-\Delta P = a \mu_g V_o + b \rho V_o^2 \quad (66)$$

where

$a \mu_g V_o$ = viscous term

$b \rho V_o^2$ = pressure term

After some algebraic manipulation

$$a = \left[\frac{170}{\epsilon_g^3} \left(\frac{1-\epsilon_g}{D_p} \right)^2 L \right] \quad (67)$$

and

$$b = \left[\frac{1.75 (1-\epsilon_g) L}{\epsilon_g^3 D_p} \right] \quad (68)$$

A tube bundle pressure drop expression is included in Appendix B.

Collector

A flat-plate collector consists of an absorber plate, made of metal for strength and good thermal conduction, insulation to reduce energy losses from both the bottom and sides of the collector, and one or more cover plates of either glass or plastic to reduce heat losses from the top of the collector (Fig 7).

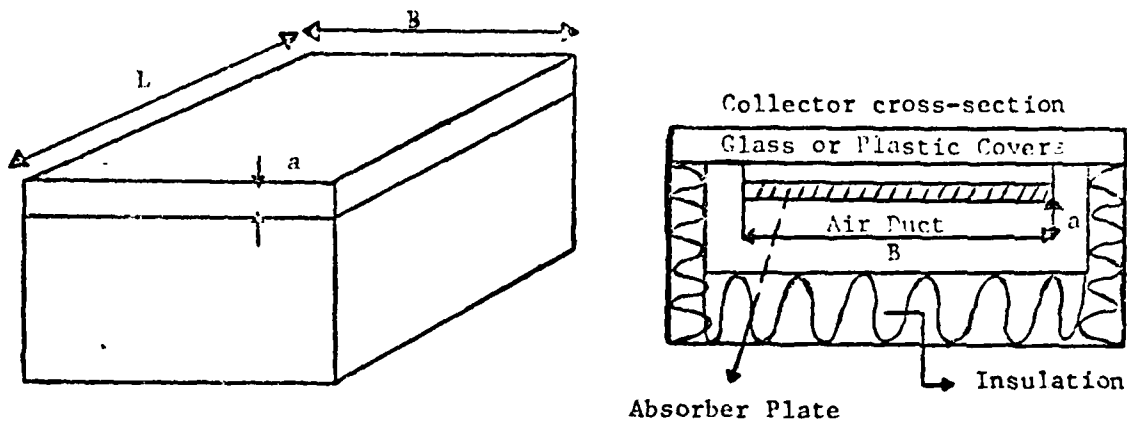


Fig 7. Collector Geometry

For this simple flat-plate air heater:

$A_{col} = aB =$ air duct cross sectional area

$P_c = 2(a+b) =$ air duct perimeter

$\alpha = B/a =$ aspect ratio of collector

$L =$ length of collector

$B =$ width of collector

$a =$ collector air gap

The collector pressure drop can be expressed in terms of a friction factor, f , (Ref 10).

$$-\Delta p = \frac{4fL\rho V^2}{2g_c D_h} \quad (69)$$

where:

$f =$ Fanning-friction factor

$\rho =$ air density

$D_h =$ hydraulic-diameter

For parallel flat plates:

$$D_h = \frac{4A_w}{P} = \frac{2aB}{a+b}, \quad (70)$$

Substituting for D_h in equation (69) gives

$$\Delta P = \frac{fL\rho V^2}{g_c aB} \quad (a+B) \quad (71)$$

For fully developed turbulent flow in tubes (this is also valid for parallel plates if the hydraulic diameter is used) and a Reynolds number range of 5,000 to 30,000, the following Fanning friction factor may be used (Ref 10):

$$f = .079Re^{-.25} \quad (72)$$

and for $30,000 < Re < 1,000,000$:

$$f = .046Re^{-.20} \quad (73)$$

where $Re = \rho V D_h / \mu g_c$ and $V = Q/A_{col}$. Now substituting equations (72) and (73) into equation (71) yields:

$$\Delta P = \frac{.079L}{g_c aB} \rho V^2 \left(\frac{1}{Re} \right)^{.25} (a+b) \quad (74)$$

for $5,000 < Re < 30,000$; or

$$\Delta p = \frac{.046}{g_c aB} \rho V^2 \left(\frac{1}{Re} \right)^{.20} (a+b) \quad (75)$$

for $30,000 < Re < 1,000,000$.

The Reynolds number for collectors is normally less than 30,000 since "a" is usually quite small; therefore equation (74) is frequently used in calculations. This equation can also be written as

$$\Delta P = \frac{.079L}{g_c \rho (aB)^3} (m)^2 \left(\frac{1}{Re} \right)^{.25} (a+b) \quad (76)$$

And since power = $P = \dot{m} \frac{\Delta P}{\rho}$

$$P = \frac{.079L(a+b)}{g_c \rho^{.25}} \left(\frac{\dot{m}}{aB} \right)^3 \frac{1}{Re} \quad .25 \quad (77)$$

Pressure drop is extremely sensitive to variations in "a" or the collector air gap spacing. As "a" increases, ΔP decreases; but since "a" is much less than "B", the increase in surface area for heat loss is minimal. Therefore, since the shape of the air duct is normally arbitrary, a somewhat larger gap spacing is recommended when one considers the significant reduction in pressure drop and blowing power requirements.

Duct Work

Our design analysis consists of:

- a. straight, round smooth radius ducts
- b. 90° - elbows, smooth and round.

For most solar energy applications, the duct design is fairly simple, involving mainly straight channels and elbows. Therefore, pressure drop calculations will be considered for these two important and essential cases only.

90° elbows: To determine pressure drop in elbows one needs to know the loss coefficient which is represented by the ratio of the total pressure loss to dynamic pressure at a referenced cross section, "o" usually at the beginning of the configuration.

$$C_o = \text{loss coefficient} = \frac{-\Delta P}{\frac{\rho V^2}{2g_c}} \quad (78)$$

or

$$\Delta P = C_o \left(\frac{\rho V^2}{2g_c} \right) \quad (79)$$

where " C_o " can be found in the ASHRAE Handbook of Fundamentals. The geometry for elbows as depicted in ASHRAE (Ref 1) is shown in Fig 8.

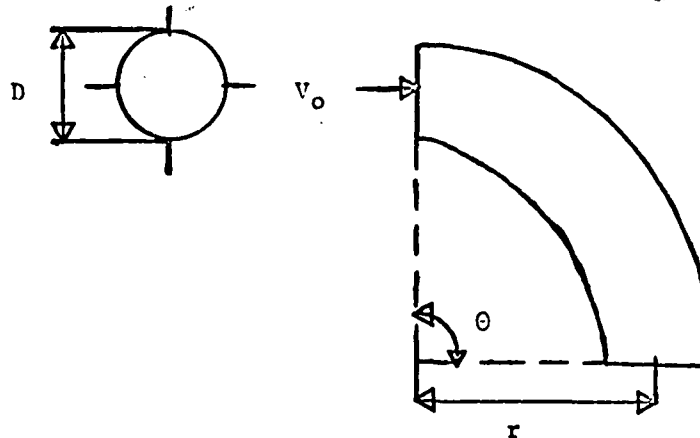


Fig 8. Duct Elbow

$$C_o = KC_o^1 \quad (80)$$

where C_o^1 is dependent on r/D ratios and K is dependent on θ .

Note that $K = 1$ when $\theta = 90^\circ$.

Coefficients for 90° Elbows

r/D	0.5	0.75	1.0	1.5	2.0	2.5
C_o^1	0.71	0.33	0.22	0.15	0.13	0.12

For angles other than 90° multiply by the following factors:

θ	0	20	30	45	60	75	90	110	130	150	180
K	0	0.31	0.45	0.60	0.78	0.90	1.00	1.13	1.20	1.28	1.40

For design purposes each straight channel is referred to as a "length" and each 90° elbow, a "turn". The motivation for circular ducts as opposed to rectangular ducts is:

- a. simpler to manufacture
- b. less leakage and easier to insulate
- c. less costly
- d. most important; less surface area, therefore, less pressure drop and thus less blowing power required.

Therefore, for these reasons, it should prove likely that ones final decision would be to use circular cross sections. The only real advantage with rectangular ducts is probably that they fit neatly in between beams, thus creating somewhat of a hideaway design.

Straight lengths: Pressure drop in straight channels can again be expressed in terms of the Fanning friction factor, f .

$$-\Delta P = \frac{4fL\rho V^2}{2g_c D_h} \quad (81)$$

where $D_h = \frac{4Aw}{P} = D_T$; or simply the actual tube diameter when dealing with circular ducts.

As before,

$$f = \frac{.079}{Re} \quad \text{for } 5,000 < Re < 30,000$$

and

$$f = \frac{.046}{Re} \quad \text{for } 30,000 < Re < 1,000,000.$$

Therefore,

$$\Delta P = \frac{4 \left(\frac{.079}{Re \cdot 25} \right) L \rho V^2}{2g_c D_h} \quad (82)$$

or

$$\Delta P = \frac{4 \left(\frac{.046}{Re} \right) L \rho V^2}{2g_c D_h} \quad (83)$$

where:

L = duct length

$$Re = \rho V D_h / \mu g_c$$

After substituting equation (82) into equation (63)

$$P = \frac{\rho \pi D_T^3 V^3 \left(\frac{.079}{Re^{.25}} \right) L}{2g_c} \quad (84)$$

A rule of thumb (ASHRAE, Ref 1) for duct work is that duct velocity should not exceed 700 fpm for low noise purposes;

$$\text{Duct velocity} = V = \frac{\text{volumetric flowrate}}{\text{cross sectional area of duct}} = \frac{Q}{A_D}$$

where: $A_D = \pi D_T^2 / 4$

Design recommendations for pressure drop in all three configurations are (Ref 2):

- a. rock beds - .1 to .4 in H_2O
- b. collectors - .2 to .8 in H_2O
- c. duct work - .08 in H_2O /100 ft duct length

Note that duct heat losses had to be minimal to validate the assumption that the inlet air temperature for the bed during its charging mode was nearly the same as the air temperature out of the collector. This involved the prediction of heat transfer from ducts as presented and discussed in Appendix C.

IV Performance Simulation of an Air Heating System

This chapter is concerned with developing a model to predict the operational modes of an air heating system. Also, a space heating load model along with auxiliary energy requirements are discussed.

Control Strategy

A suitable method for long term simulations, is to assume that during any time period, the system operates in whatever modes necessary to maintain the building temperature at the desired level. During each time period, the amount of energy collected is compared with the amount of energy required to meet the load (Ref 13).

To fully complete a simulation model there are three modes that must be satisfied for a solar air heating system. For the workings of an air system refer to the schematic diagrams in Figs 9 and 10, note that only one fan is necessary for its operation.

In the first mode of operation solar energy is available but not enough is collected to meet the space heating load; therefore, the collected energy is delivered directly from the collector to the house. In mode two, solar energy is sufficient to meet the space load; therefore, the energy collected is delivered to the house until the load is satisfied; then for the remaining time period the rest of the energy is transferred to the storage bed. This is commonly referred to as the charging mode. The third mode becomes operational when solar energy is no longer available (usually at night); then hot air is drawn from the hot end of the bed until the space load is met and room temperature **air** is returned. This is known as the discharging mode. In modes one and three, auxiliary energy may be required if the amount of energy transported from either the collector or the storage unit is depleted before satisfying the load.

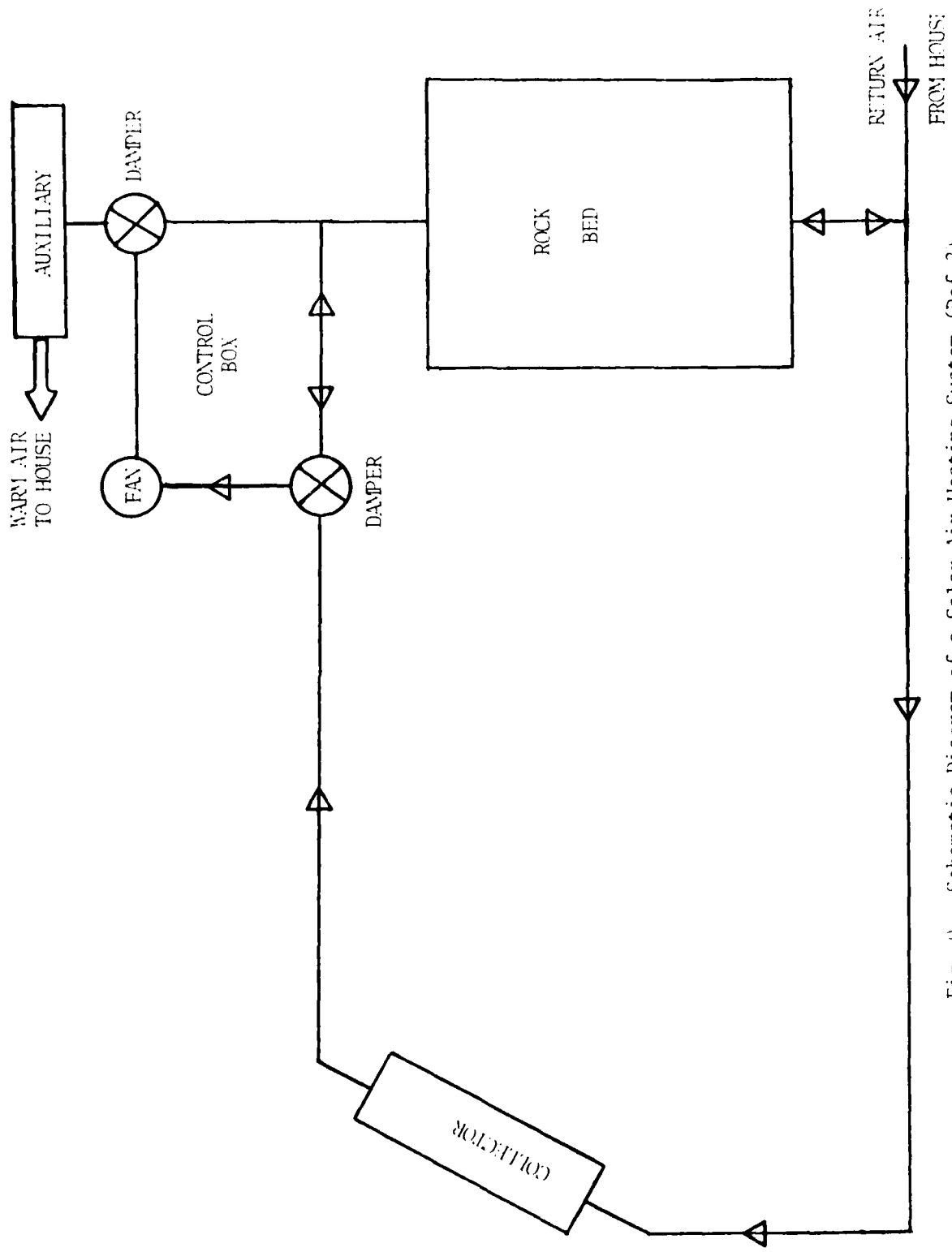


Fig 9. Schematic Diagram of a Solar Air Heating System (Ref 2)

Space Heating Loads

A variety of factors influence space heating requirements such as the location of the building, its design, orientation and particular habits of the occupants.

Many space heating models have been proposed, ranging in detail from simple to relatively complex approaches. However, due to computer time and costs, complex models for load calculations are not justified. Therefore, a simple space heating load model, the degree-day model, expresses the heating load, QSHL, as a function of the difference between the inside temperature of the building (reduced to account for heat generation due to lights, people, etc; usually about 65F) and the mean ambient (outside) temperature (Ref 12).

$$QSHL = UA (T_{\text{inside}} - \bar{T}_a) \quad (85)$$

where:

UA = the building overall loss coefficient-area product

The number of degree-days in a month, DD, is

$$DD = \sum_{i=1}^N (65F - \bar{T}_a)_i \quad (86)$$

where N is the number of days in a month and $(65F - \bar{T}_a)_i$ is taken to be zero for mean daily temperatures above 65F.

Therefore, a monthly space heating load, QSHLM, can be written as

$$QSHLM = UADD \quad (87)$$

For simulation purposes, an hourly heating load was used, namely:

$$QSHL = \frac{QSHLM}{24 N} \quad (88)$$

Auxiliary Energy

Auxiliary energy is provided for space heating whenever the amount of solar energy collected is insufficient to meet the space heating load. In practice, this condition is detected by a thermostat monitoring the temperature within the building. In the present space heating model however, the temperature within the building is assumed to be constant and auxiliary energy is supplied whenever the rate at which solar energy can be provided, Q_{AVG} , is less than the space heating load, Q_{SHL} . Therefore, the amount of auxiliary energy, Q_{AUX} , needed is:

$$Q_{AUX} = Q_{SHL} - Q_{AVG} - Q_{LOST} \quad (80)$$

where it has been assumed that any bed losses (Q_{LOST}) actually reduce the space heating load (Ref 12).

In the discharging mode, when energy is taken from the storage unit, the auxiliary energy needed is:

$$Q_{AUX} = Q_{SHL} - Q_{BEDH} \quad (90)$$

where, Q_{BEDH} , the amount of energy drawn from the bed is:

$$Q_{BEDH} = \dot{m} c_{pa} (T_{EB} - T_{ROOM}) \quad (91)$$

and

T_{EB} = Exit air temperature of bed

T_{ROOM} = Room air temperature

The Q_{AUX} calculations were used to determine backup energy costs in the air system simulation.

For the complete logic of an air system simulation, a flowchart of the computer program is presented in Appendix F.

V Results and Conclusions

Rock Bed Simulation Results

The major objective in using a fully-implicit finite-difference solution scheme was to be able to use time steps as large as one hour and still obtain adequate results for realistic simulations. In order to justify this criteria the rock bed was tested separately for a constant inlet air temperature and specified initial conditions as indicated in Table 1.

For this particular rock bed simulation, the air and bed temperatures are somewhat more sensitive to changes in Δx than to changes in time step. The corresponding temperatures for a Δx of six inches and a Δt of one hour were reasonably close for engineering purposes to the temperatures for a one inch distance increment and a .1 hour time step. Therefore, these particular increments were used in the air system simulation

To further appreciate this selection, the air and bed temperatures were plotted as functions of position and time in the bed at various time steps. In Fig 11 one notices that for a Δt of one hour the air temperatures near the beginning of the bed were slightly lower than those corresponding to a Δt of .1 hour. However, at $x=2$ feet the trend began to reverse itself as it should, since energy must be conserved. But for all positions in the bed, the temperature difference between the largest and smallest time increments were again relatively small. In Fig 12, the same general trend is observed. Only for this case, the bed temperatures are a bit lower than the corresponding air temperatures of Fig 11, but as the volumetric heat transfer coefficient approaches infinity, the air and bed temperatures at a particular point in the bed become nearly equal. Note that in both these figures a Δx of 1 foot was used; therefore, a smaller Δx would obviously result in reducing the temperature difference

Table 1. Temperature Convergence Data

Case Tested: Rock Diameter = 1 inch

Initial Bed Temperature = 70F

Inlet Air Temperature = 140F

Volumetric Flowrate = 1200 CFM

Average Heat Transfer Coefficient = $3.22^B/\text{hr-ft}^2\text{-F}$

<u>Δx (inches)</u>	<u>Δt (hours)</u>	<u>*TA (F)</u>	<u>*TB (F)</u>
1.0	0.1	96.1	91.1
1.0	0.5	94.94	91.3
1.0	1.0	93.37	90.5
4.0	1.0	96.5	93.3
**6.0	1.0	98.2	94.7

* - air & bed temperatures at $x=1$ foot after one hour of charging

** - increments used for the simulation runs

AIR TEMP VERSUS BED POSITION

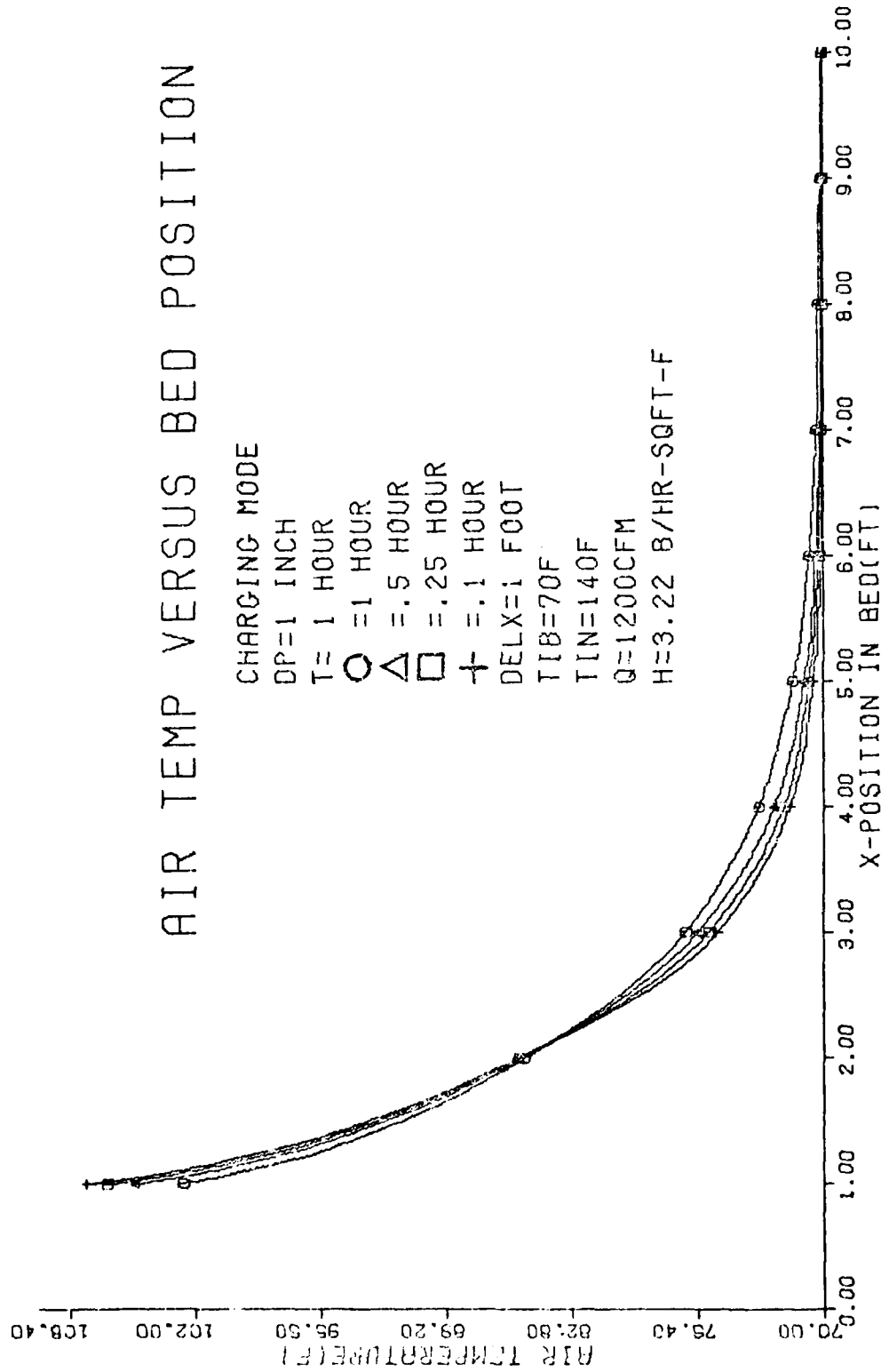


Fig 11. Air Temperature Profile (function of x)

BED TEMP VERSUS BED POSITION

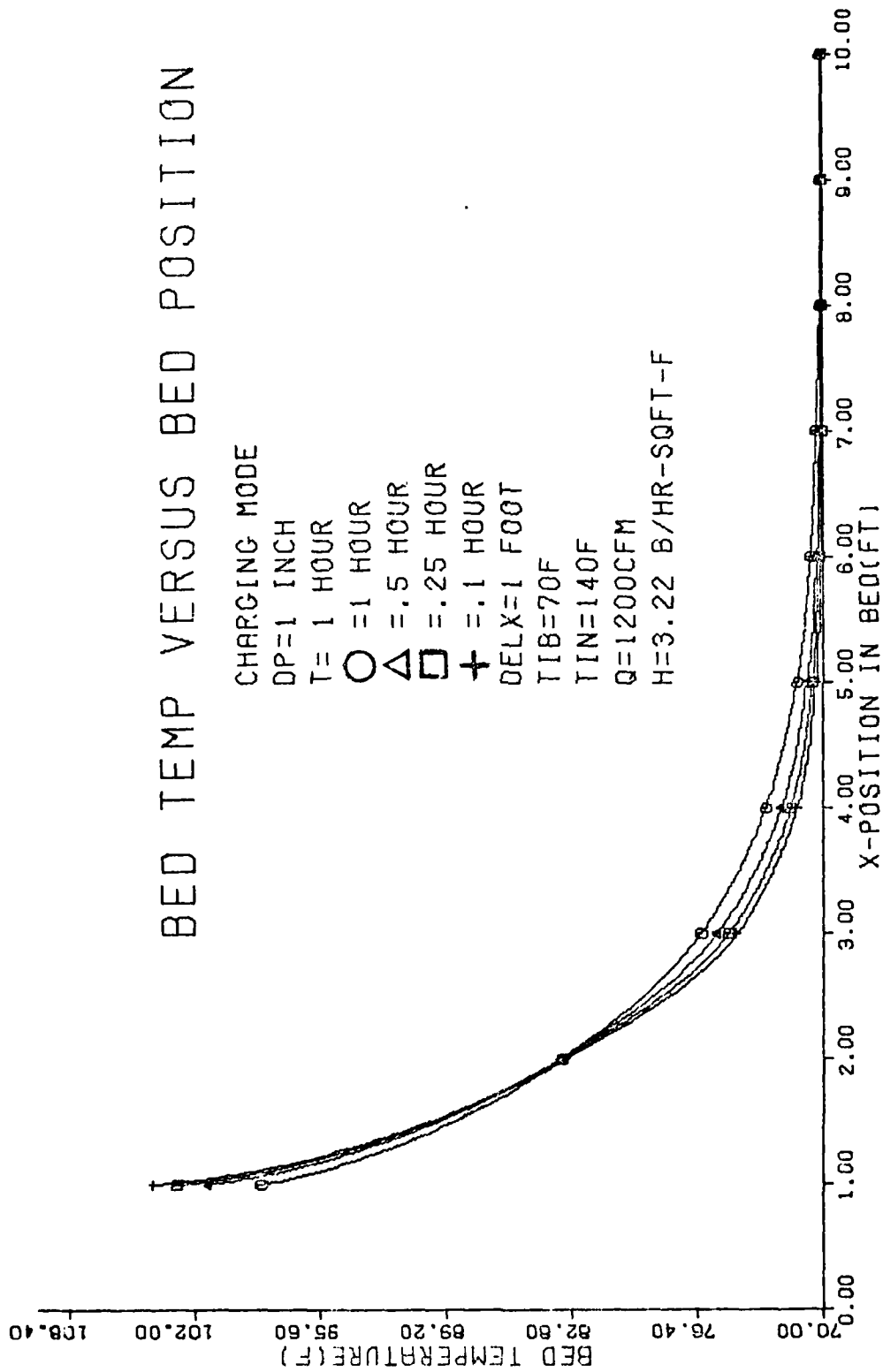


Fig 12. Bed Temperature Profile (function of x)

between the various time steps. This again reinforces the choice of selecting a Δx of six inches and a time step increment of one hour.

In Fig 13, the air temperatures were plotted as a function of time for a particular x-location in the bed ($x=1$ foot). With increasing time, the air temperatures at $x=1$ foot began approaching 140F, the inlet air temperature, T_{IN} . Also, the air temperatures for the one hour time step were all slightly lower than the corresponding air temperatures at the other three time increments. These two occurrences followed both a natural and expected trend.

To test the validity of the numerical scheme an analytical solution as discussed in Chapter II was used for comparison purposes. The analytical solution was limited to relatively small time and distance increments, for stability purposes. The solution also assumed negligible heat loss from the bed; this was simulated in the numerical case by simply setting the conductivity of the insulation, K_{INS} , to zero. In Figs 14 and 15, the air and bed temperatures were plotted as functions of x for a charging period of only .1 hour. In both graphs the numerical solution, represented by the circles, was extremely close to the analytical result. Also note that for the first few inches of the bed the air temperatures were significantly larger than the corresponding bed temperatures, and at $x=12$ inches, both the temperatures approached 70F, the initial bed temperature.

In Figs 16 and 17, the air and bed temperatures were plotted as functions of time at $x=1$ inch, for a Δt of .1 hour. Again, the numerical temperatures were quite similar in comparison to the analytical ones. Also for increasing time the air and bed temperatures approached 140F, the constant-inlet air temperature; at $t=1$ hour the air temperature was approximately 139F while the corresponding bed temperature was around 138F.

In addition, in Fig 15 the numerical curve fit extrapolation at $x=0$ resulted in a bed temperature of 98F; and the dotted line joining the bed temperatures at $x=1$ and $x=0$ obviously displayed a rather nice consistency with the natural extension of the solid analytical curve.

Therefore, Figs 14 - 17 essentially prove the validity of the numerical scheme and also the second-order polynomial curve fit solution at $x=0$.

The next three figures, Figs 18, 19 and 20, represent the bed, collector and duct work pressure drops, respectively. The bed pressure drop is plotted as a function of rock diameter for various flowrates, while the collector and duct work pressure drops are plotted as functions of Q , the volumetric flowrate. It can be seen from Fig 18 that the bed pressure drop varies directly with Q and is inversely proportional to the rock diameter. For rock diameters less than one inch significant pressure drop may result, especially at the higher flowrates. In Figs 19 and 20, both the collector and the duct work pressure drop vary directly and almost linearly with the flowrate. Here, it is worthwhile to mention that even though heat transfer coefficients increase with Q , pressure drop and thus blowing costs also increase. However, this cost increase generally outweighs any possible gain in the thermal performance of the rock bed that results due to increasing flowrates. Therefore, one is normally advised to use existing rules of thumb which provide the satisfactory range of flowrates per square foot of collector area.

The last two figures represent total monthly blowing costs as related to various rock diameters. Total cost refers to the combination of bed, collector and duct work blowing costs. Monthly costs are also directly related to Q but inversely related to rock diameter. Blowing costs remain relatively constant for rock diameters of one inch or more. However, for larger diameter rocks the rate of heat transfer is substantially reduced, since the heat transfer

coefficient is inversely proportional to rock size. Therefore, these two considerations alone appear to suggest that rock diameters of approximately one inch should prove most economical. According to Fig 21, for one inch rocks, the blowing costs at 1200 CFM correspond to approximately two dollars per month and at 1800 CFM, about six dollars per month; these results were based on an eight hour period of operation.

In the air system simulation, a volumetric flowrate of 1200 CFM with a bed of one inch diameter rocks was used. Therefore, for this particular simulation one could safely assume that the total operating costs of two dollars per month contributes rather insignificantly when determining the life cycle cost effectiveness of the air heating system. Also, with the above conditions but for 24 hours of operation, the resulting blowing cost, as indicated in Fig 22, is approximately \$5.50 per month; this however is still a relatively small amount when one considers the total investment costs required per square foot of collector area.

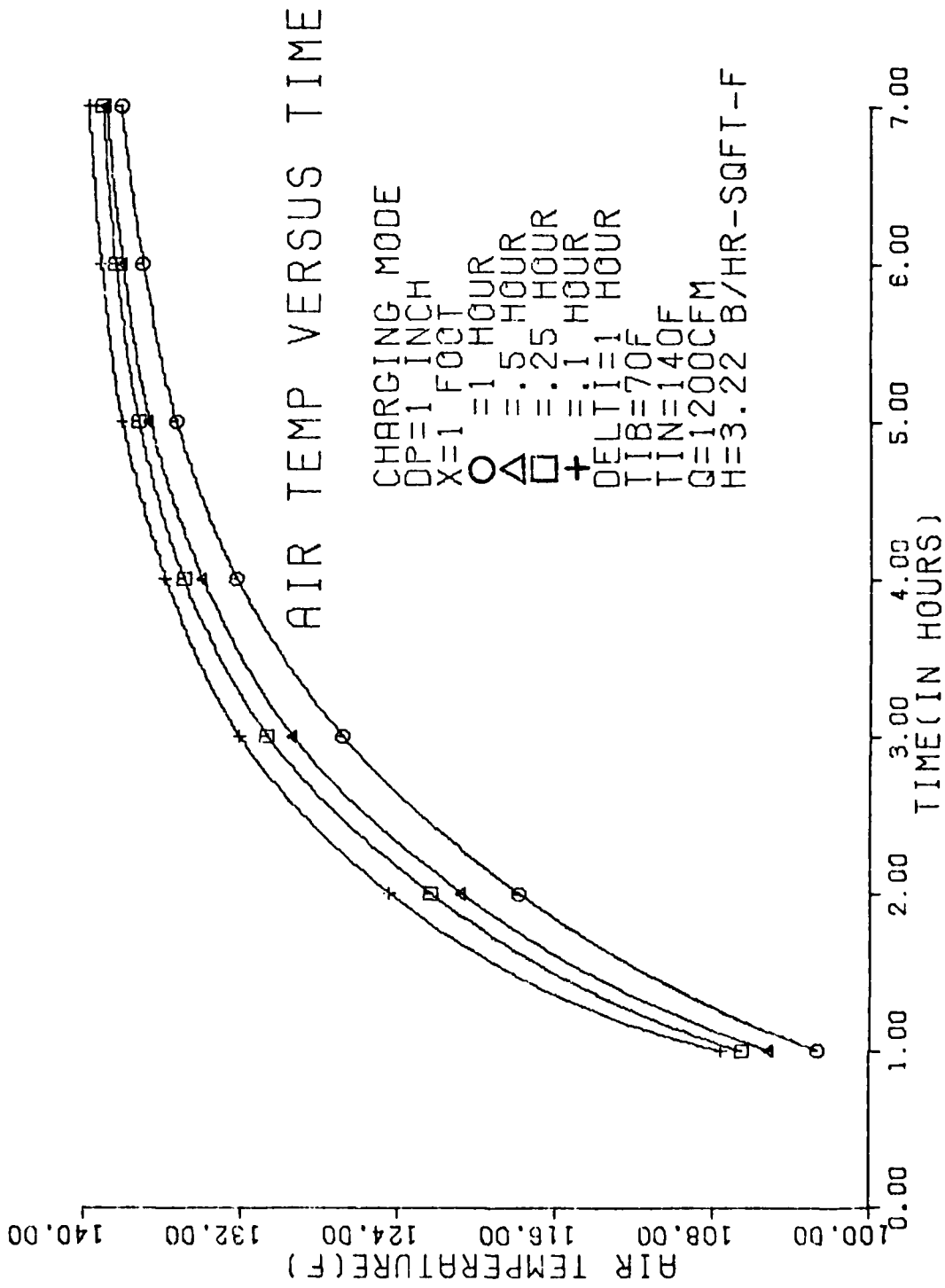


Fig 13. Air Temperature Profile (function of time)

AIR TEMP VERSUS BED POSITION

CHARGING MODE
 CP=1 INCH
 T=.1 HOUR
 DELX=1 INCH
 TIB=70F
 TIN=140F
 Q=1200CFM
 H=3.22 B/HR-SQFT-F
 KINS=0.0 B/HR-FT-F
 C=NUMERICAL
 ---=ANALYTICAL

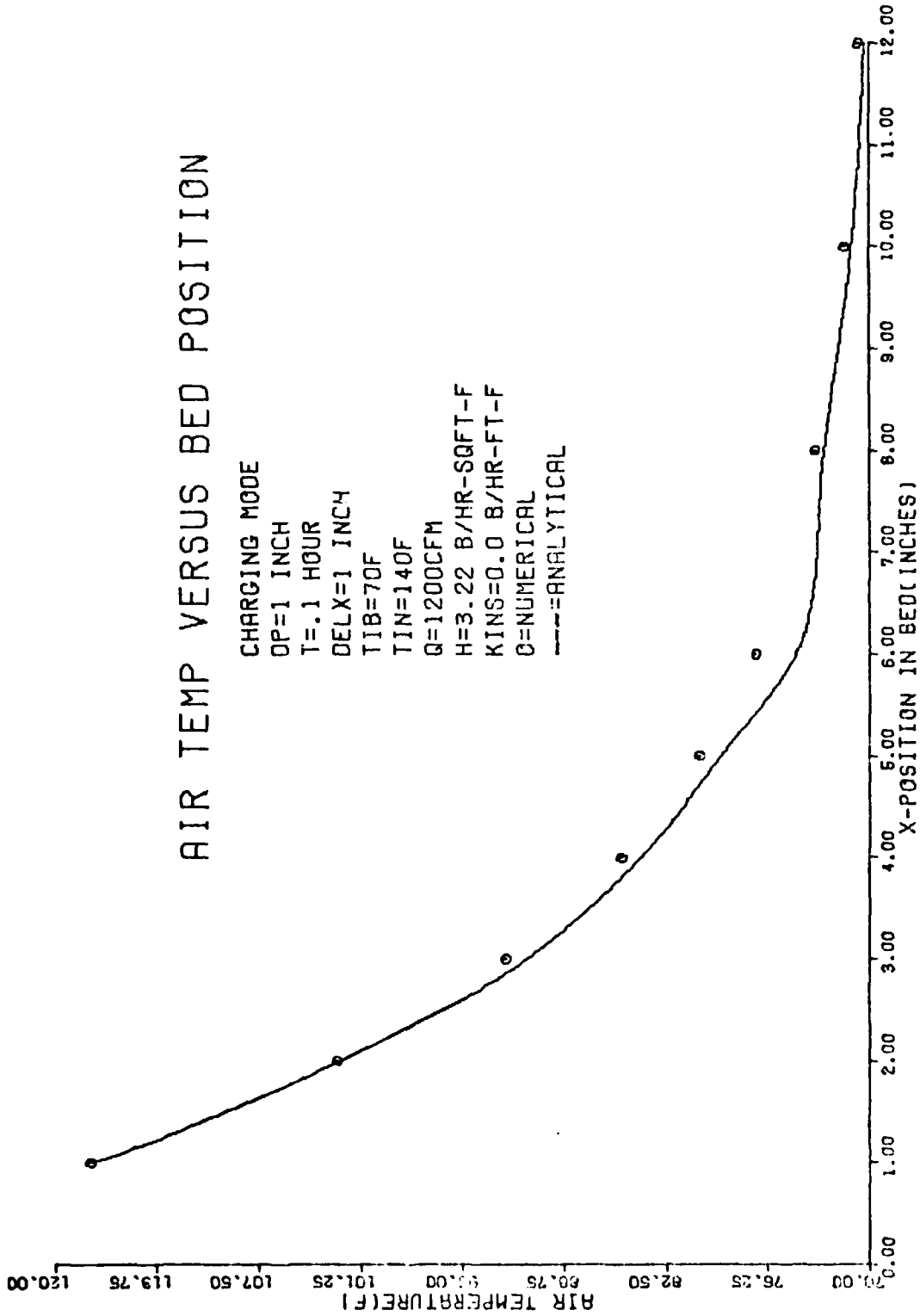


Fig 14. Comparison of Analytical and Numerical Air Temperatures (function of x)

BED TEMP VERSUS BED POSITION

CHARGING MODE
 DP=1 INCH
 T=.1 HOUR
 DELX=1 INCH
 TIB=70F
 TIN=140F
 Q=1200CFM
 H=3.22 B/HR-SQFT-F
 KINS=0.0 B/HR-FT-F
 O=NUMERICAL
 —=ANALYTICAL
 ---=EXTRAPOLATED

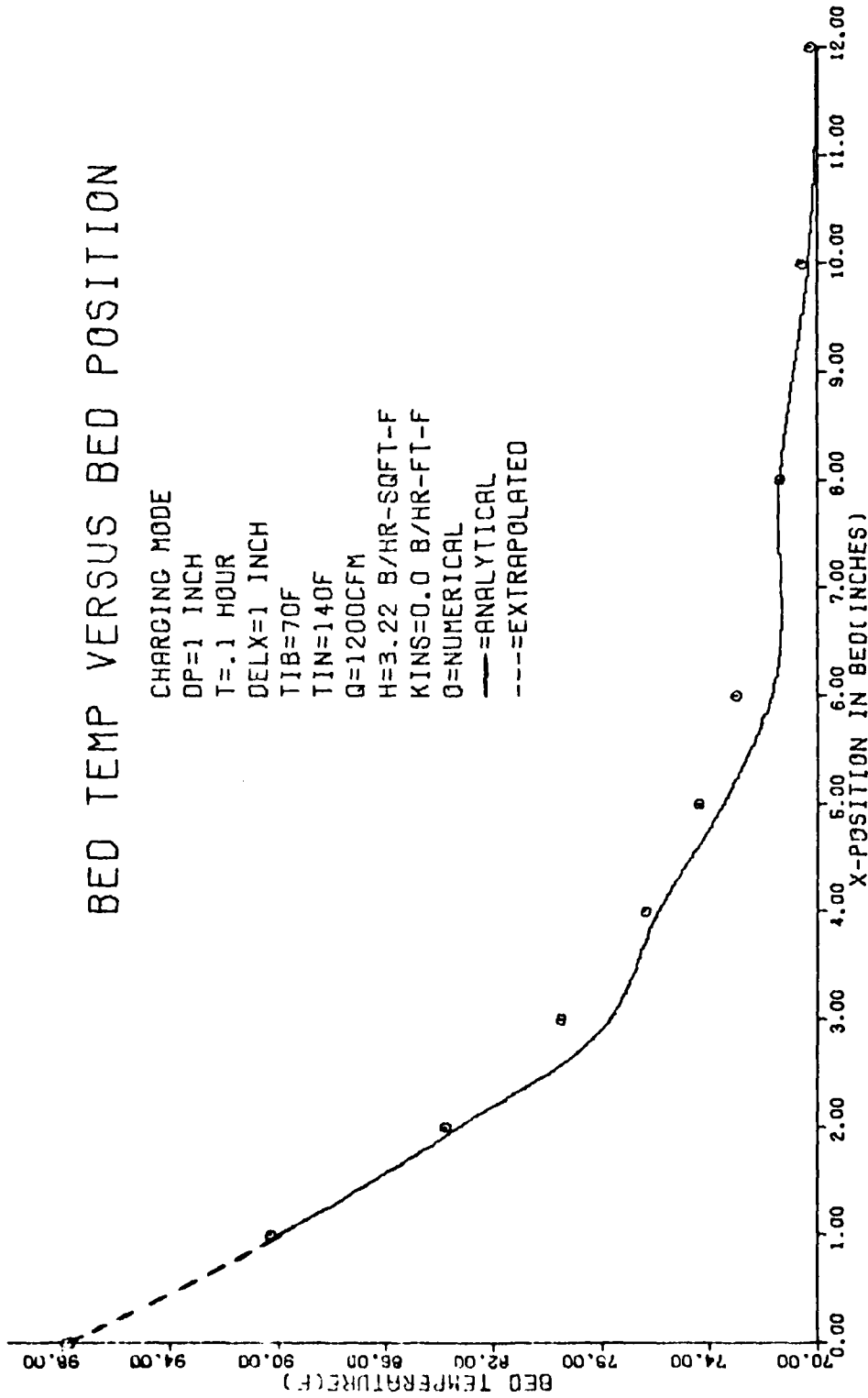


Fig 15. Comparison of Analytical and Numerical Bed Temperatures (function of x)

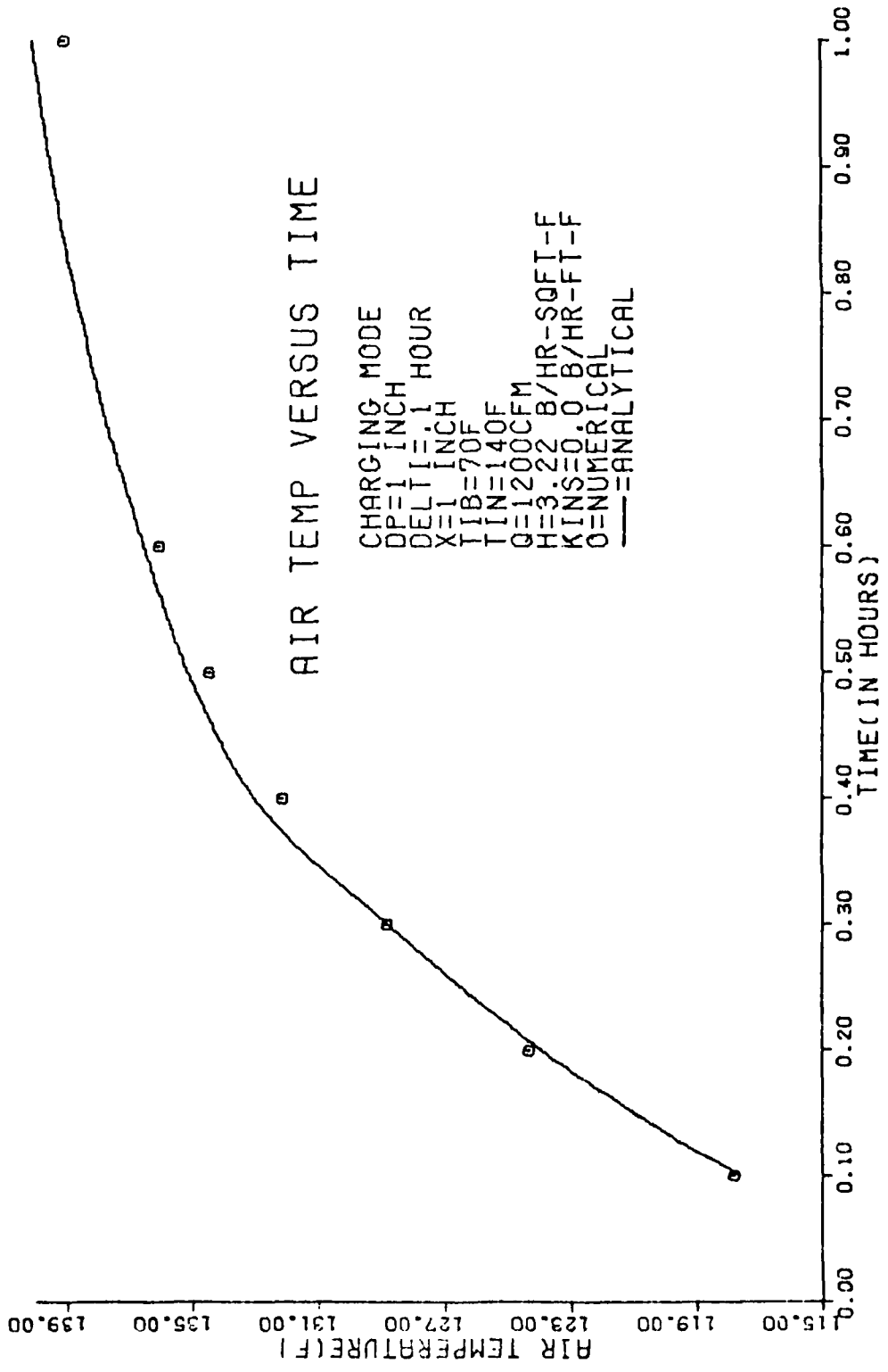


Fig 16. Comparison of Analytical and Numerical Air Temperatures (function of time)

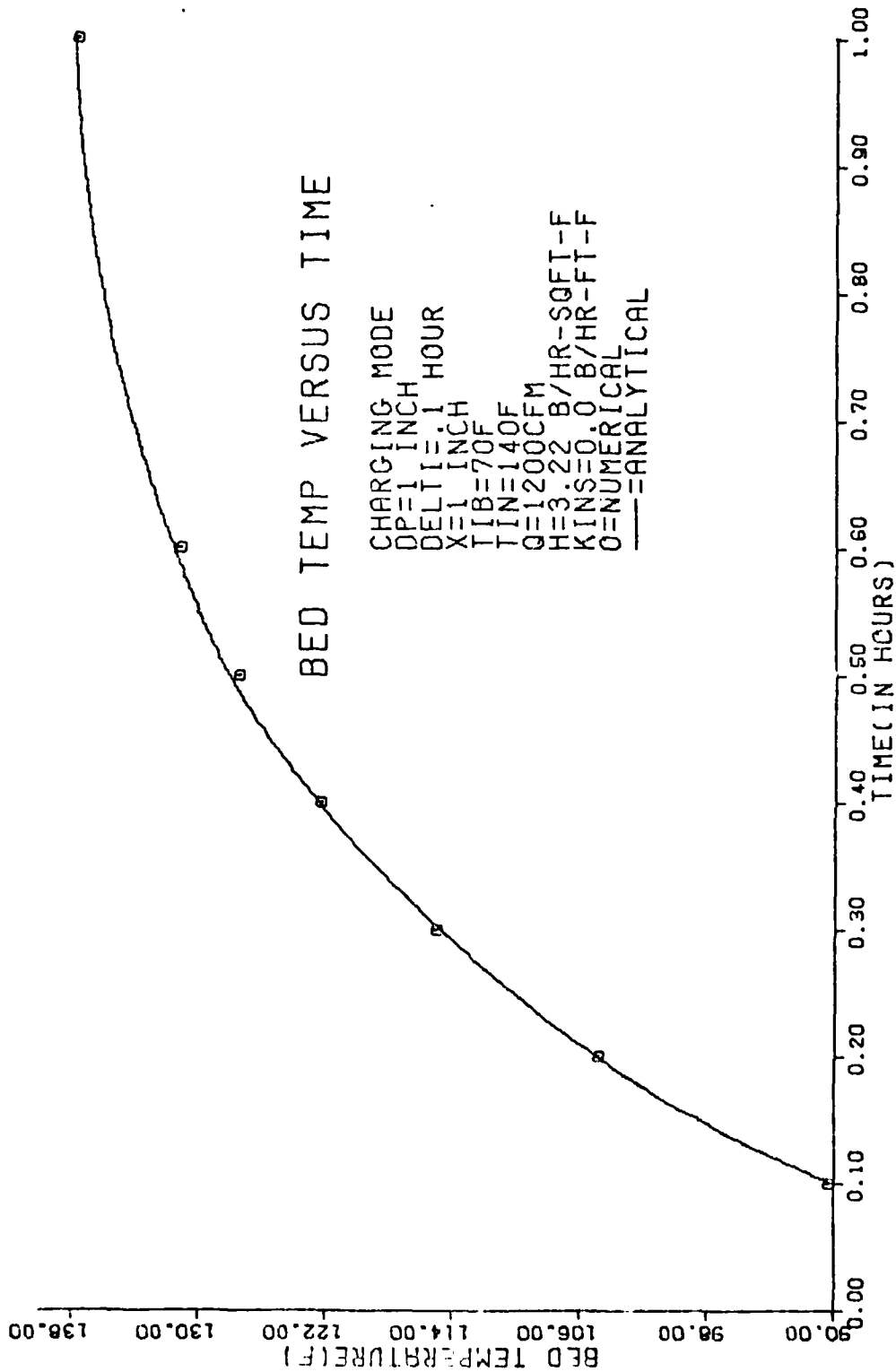


Fig 17. Comparison of Analytical and Numerical Bed Temperatures (function of time)

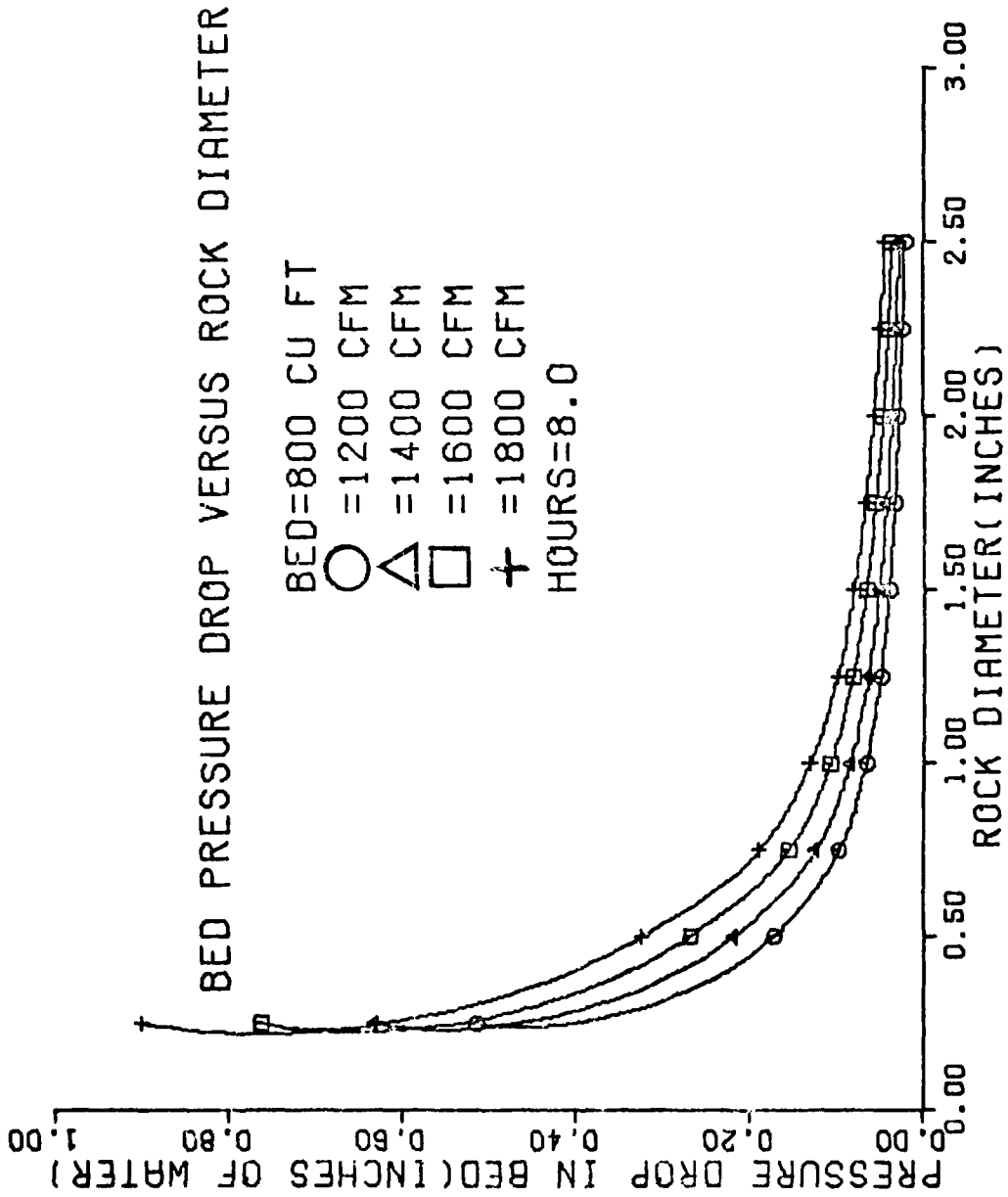


Fig 18. Bed Pressure Drop

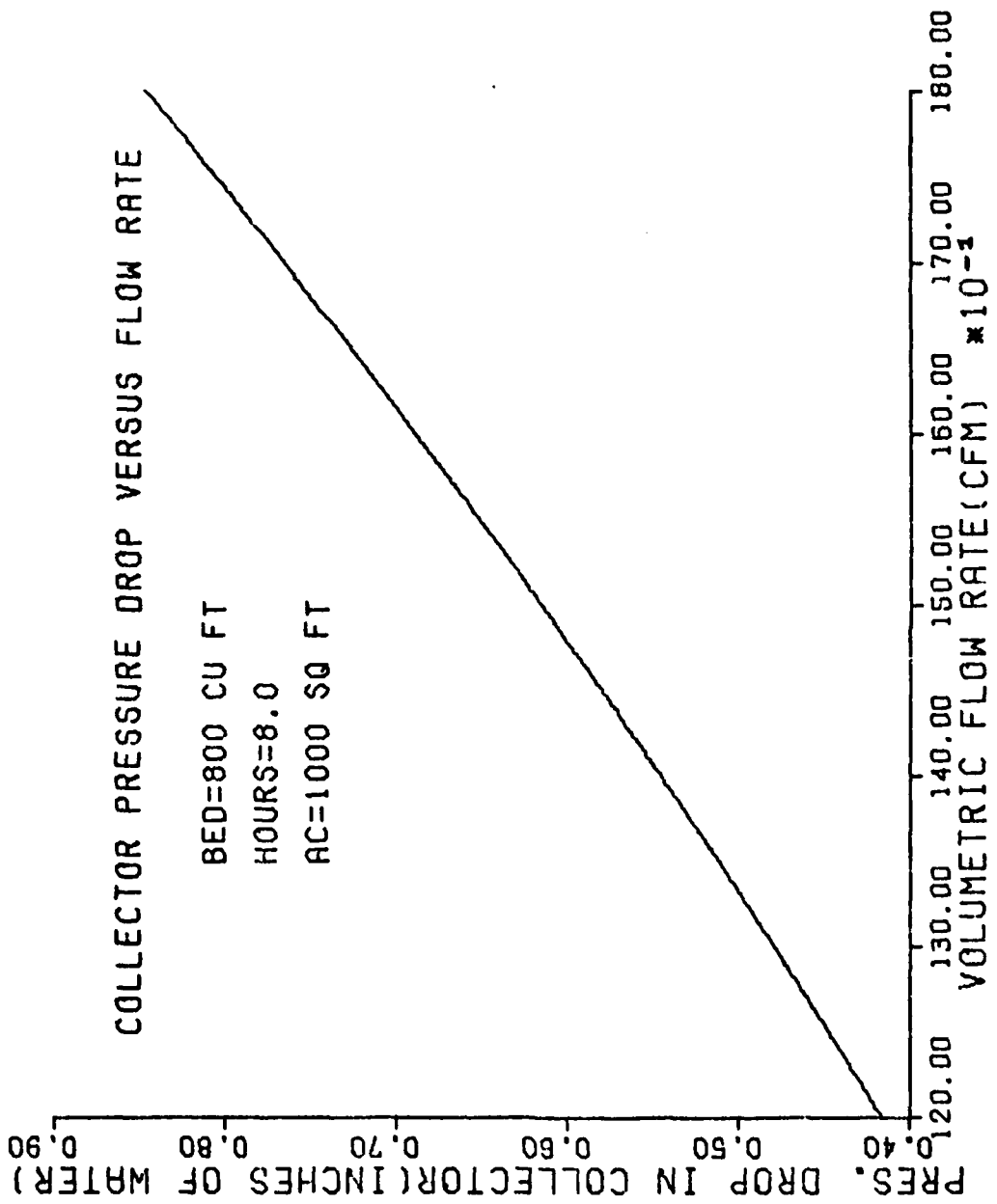


Fig 19. Collector Pressure Drop

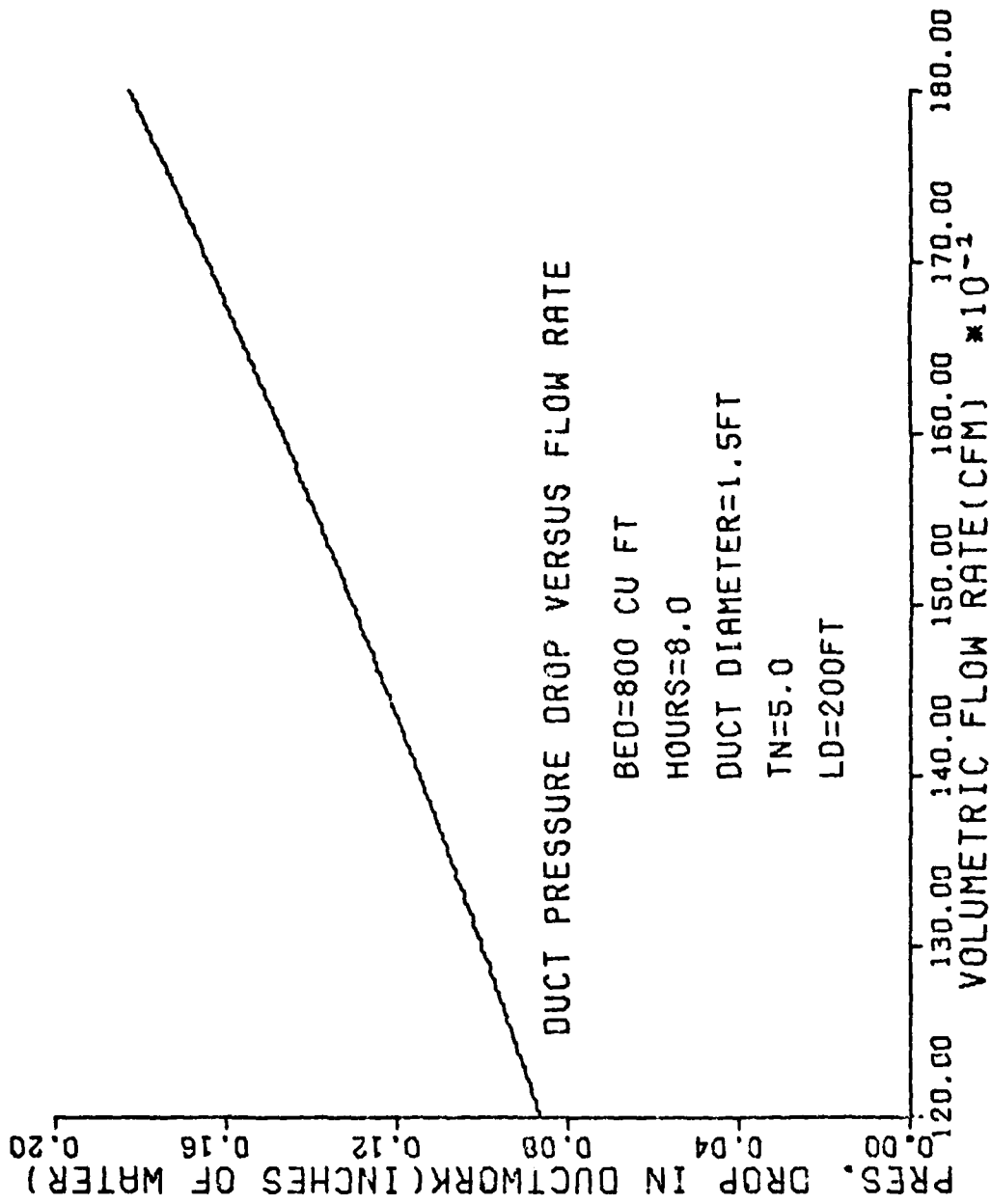


Fig 20. Duct Work Pressure Drop

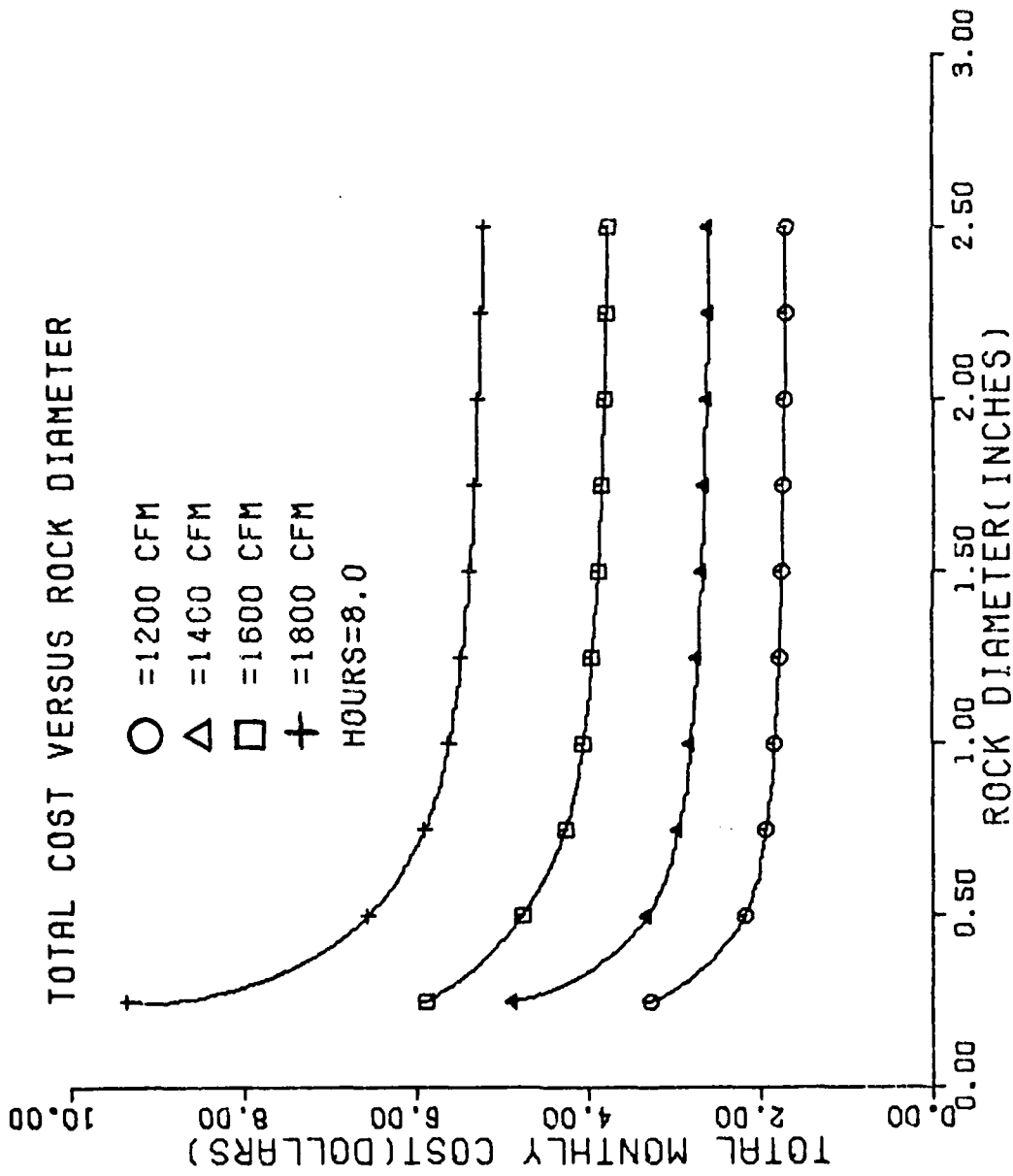


Fig 21. Total Monthly Cost (8 hours of operation)

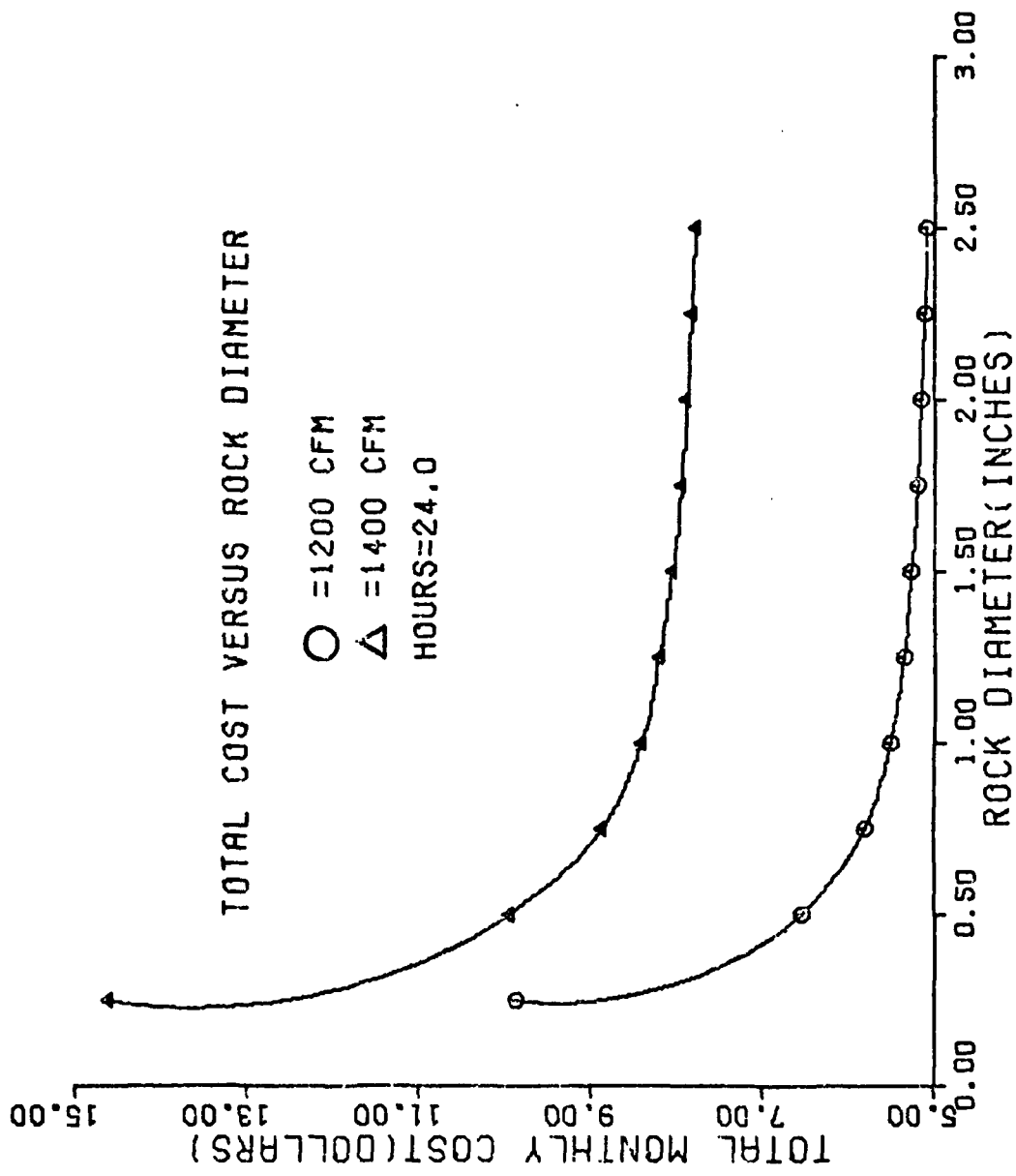


Fig 22. Total Monthly Cost (24 hours of operation)

System Simulation Results

For illustrative purposes the computer program was used to simulate a residence in Columbus, Ohio. Data for the weather, position and orientation of the collector is the same as that used in Prins' program (Ref 16). The parameter values used are as follows:

1. Latitude = 40 degrees
2. Number of covers = 2
3. Slope of collector = 55 degrees
4. Azimuth angle = 0 degrees
5. Area of collector (varied parameter) = 400, 500, 600 and 700 sq. ft.
6. Thickness of cover material = .23 cm
7. Extinction coefficient of cover material = .161/cm
8. Index of refraction of cover material = 1.526
9. Absorptivity of the absorber plate = .92
10. Heat removal efficiency = .62
11. Heat loss coefficient = .60
12. Mass flowrate of fluid through collector = 5112 lbm/hr
13. Specific heat of collector fluid = .24 B/lbm-F
14. Dirt factor = .02
15. Initial temperature of air in bed = 70.0F
16. Efficiency of heat exchanger = 1.0
17. System in use = 4.0
18. Number of months program is to run = 8
19. Time increment for discharge = 2.0 minutes
20. Epsilon for time increment = .01 hours
21. Minimum pump energy = 275.0 B/hr
22. Structure conductance = 1000.0 B/hr-F

23. Time step = 1.0 hours
24. Volumetric flowrate = 20.1 cfs
25. Bed height = 8.0 ft
26. Bed width = 10.0 ft
27. Air density = .071 lbm/ft³
28. Rock diameter = .08333 ft
29. Prandtl number for air = .711
30. Conductivity of air = .0155 B/hr-ft-F
31. Momentum diffusivity of air = .649 ft²/hr
32. Specific heat of air = .24 B/lbm-F
33. Air temperature outside bed = 70.0F
34. Rock density = 165 lbm/ft³
35. Specific heat of rock = .21 B/lbm-F
36. Bed length = 10.0 ft
37. Number of nodes in bed = 21
38. Void fraction of bed = .42
39. Conductivity of rock = 1.0 B/hr-ft-F
40. Initial bed temperature = 70.0F
41. Conductivity of insulation = .023 B/hr-ft-F
42. Thickness of insulation = 1.0 ft
43. Surface area of insulation = 420.0 ft²
44. Dynamic viscosity of air = .046 lbm-hr/ft²
45. Fan efficiency = .55
46. Collector air gap spacing .3333 ft
47. Width of collector = 4.0 ft
48. Length of collector = 8.0 ft
49. Length of duct work = 200.0 ft

50. Duct diameter = 1.5 ft
51. Number of elbows = 5.0
52. Hours of operation = 8.0 hours
53. Primary Federal tax credit = .40
54. Secondary Federal tax credit = .30
55. Ohio tax credit = .10
56. Initial tax credit amount = 2000.0 dollars
57. Secondary tax credit amount = 1000.0 dollars
58. Maximum tax credit amount = 4000.0 dollars
59. Annual mortgage interest rate = .12
60. Down payment = .10
62. Backup furnace cost = \$3.26/million Btu (Gas)
63. Conventional furnace cost = \$3.26/million Btu (Gas)
64. Efficiency of solar backup furnace = .55
65. Efficiency of conventional furnace = .55
66. Property tax rate = 0.0
67. Income tax bracket = .40
68. Extra insurance and maintenance costs = .01
69. General inflation rate = .08
70. Fuel inflation rate = .12
71. Discount rate (varied parameter) = .10 and .20
72. Term of economic analysis = 20.0 years
73. Area dependent costs (air collector) = \$15/sq. ft
74. Area independent costs (fans, etc.) = 1000.0 dollars

Three parameters were varied in this simulation while the others were held fixed. The varied parameters were the collector size, the discount rate and the mortgage loan term. Varying the collector area was necessary to determine the optimum collector size for maximum savings. A cost performance curve is shown below.

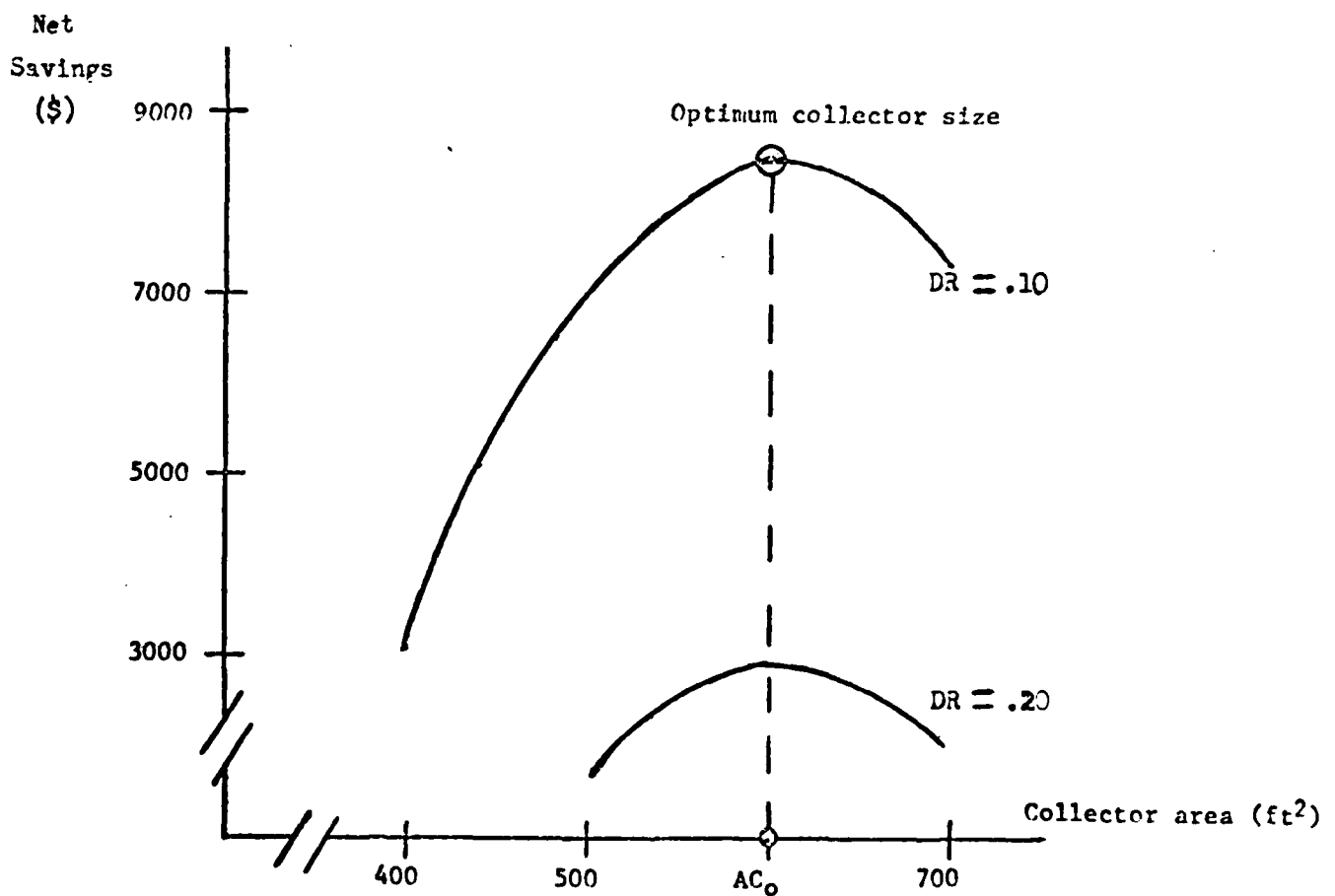


Fig 23. Net Savings

Net savings refers to the total fuel savings minus investment costs.

For this simulation, the optimum collector area was approximately 600 square feet, this corresponded to a maximum savings of 8572 dollars for a discount rate of 10 per cent and a 20 year mortgage term. At a discount rate of 20 per cent a slight savings was still achieved, therefore the system provided at least a 20 per cent return on investment. In this case, it is interesting to note that the amount of savings actually increases with longer mortgage periods. This is due to the fact that the rate of return (20%) is greater than the interest rate for the mortgage loan. It is also important to note that fuel costs were based on natural gas prices, the cheapest of the fossil fuels.

For other key results of our simulation refer to Tables 2 and 3. A plot of solar energy percentage versus collector area is presented below. Note that the slope of the curve begins to drop off at higher collector areas. Because a substantial portion of the solar system cost increases linearly with collector area and thermal performance increases less than linearly, a maximum amount of savings results at some optimum collector size.

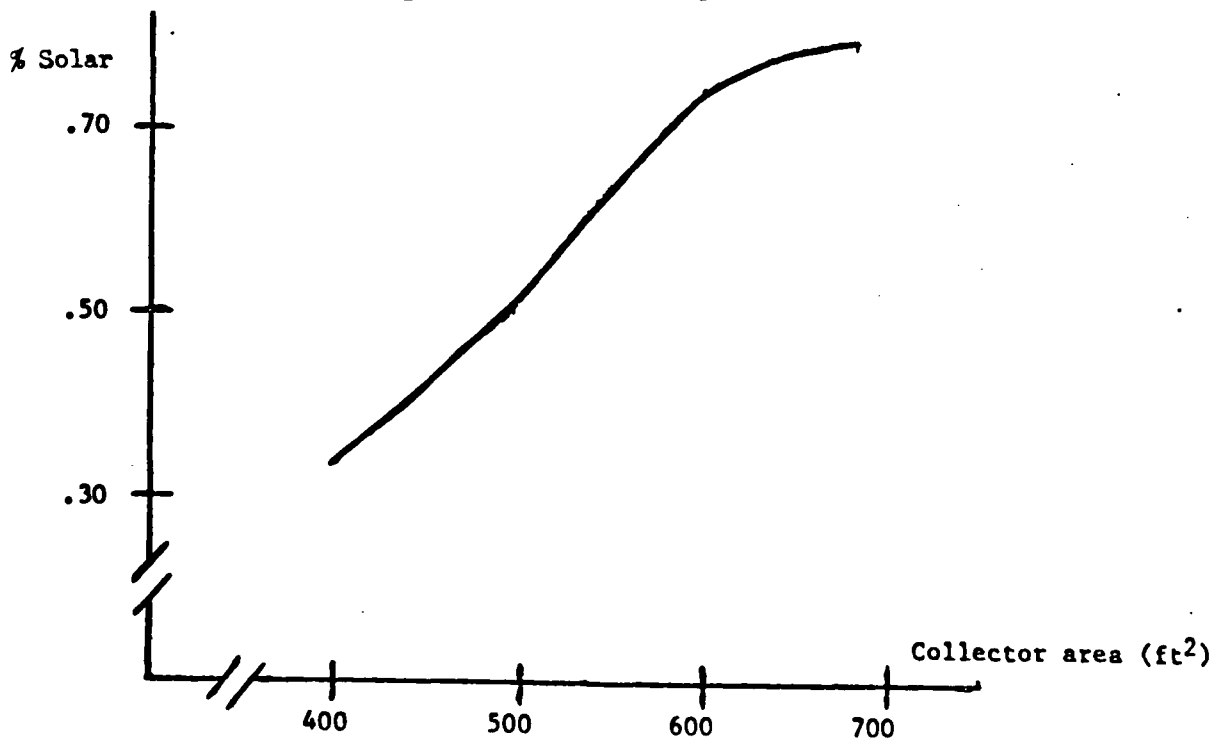


Fig 24. Per Cent Solar Energy

Table 2. Solar Energy Savings

Collector are (ft ²)	400	500	600	700
Mortgage term (years)	5	5	5	5
Discount rate				
.10 Fuel savings	\$6996	\$10653	\$14437	\$14718
Expenses	\$4354	\$ 5334	\$ 6531	\$ 8164
Net savings	\$2642	\$ 5319	\$ 7905	\$ 6554
.20 Fuel savings	\$3017	\$ 4594	\$ 6226	\$ 6547
Expenses	\$3311	\$ 4057	\$ 4967	\$ 6209
Net Savings	\$-294	\$ 537	\$ 1258	\$ 158
Mortgage term (years)	20	20	20	20
Discount rate				
.10 Fuel savings	\$6996	\$10653	\$14437	\$14718
Expenses	\$3909	\$ 4790	\$ 5865	\$ 7330
Net savings	\$3086	\$ 5863	\$ 8572	\$ 7387
.20 Fuel savings	\$5017	\$ 4594	\$ 6226	\$ 6547
Expenses	\$2288	\$ 2802	\$ 3432	\$ 4290
Net savings	\$ 2729	\$ 1791	\$ 2793	\$ 2057

Structure Conductance = 1000 B/hr-F

Average Computer Costs = \$1.00 per run

Table 3. Solar Energy Data

Collector area (ft ²)	400	500	600	700
Maximum temperature out of collector (F)				
Oct	102.0	110.0	120.0	129.0
Nov	95.0	100.0	109.0	118.0
April	95.0	102.0	119.0	131.0
May	97.0	104.0	128.0	139.0
Total solar energy collected (BTU)	59016704	48615485	56853358	65190400
Total backup energy used (BTU)	79027744	50589481	21162806	18969620
Per cent of energy supplied by solar	.33	.49	.72	.78

Structure Conductance = 1000 B/hr-F

Average Computer Costs = \$1.00 per run

General Remarks on Rock Bed Air Systems

The basic advantages of a solar air heating system are that the heat transfer fluid, air, will not freeze or boil and materials used in the system generally have a long life expectancy. Maintenance of the system is expected to be low if quality collectors are used, and corrosion problems are usually quite minimal when compared to water systems. Normal maintenance is confined to cleaning or replacement of filters and proper care of the blowers or fans. Another advantage of the air system is that the house can be heated directly from the collector, the mode 1 operation.

The rock bed storage has the following advantages (Ref 17):

- a. Rocks are plentiful and cheap to purchase.
- b. They are non-toxic, non-corrosive and non-flammable.
- c. Rocks have a high heat storage capacity.
- d. Thermal energy is efficiently transmitted to the rocks by air cir-

culating through the bed due to the large heat transfer area. Also, heat conduction through the bed of rocks is low, because the area of contact between the rocks is small; this leads to low heat losses from the bed. These advantages make the rock bed a fairly efficient storage unit because air can leave the bed at a temperature nearly equal to that of the rocks at that point, which in turn is nearly equal to the temperature of the hot air entering the bed.

The disadvantages of a rock bed air system are:

- a. Significant blowing power may result at high volumetric flowrates.

For water systems, pumping power requirements are usually minimal.

- b. Rock beds generally require a larger volume for thermal storage than water storage tanks.

For design purposes a rule of thumb of 1 to 4 cfm per square foot of

collector area is recommended (Ref 2). Also, the economic optimum storage capacity is 0.50 to 2.00 cubic feet of rock storage per square foot of collector area (Ref 17). Washed stones or crushed rock one half inch to two inches in diameter should be used. The type of rock does not affect the performance of the storage unit as long as the density is approximately 160 lbm/ft^3 (Ref 17). There are two kinds of rocks: igneous rocks and sedimentary rocks. Table 4 shows the various densities of these two types of rocks. Also, Table 5 provides a list of some common heat storage materials (Ref 17).

Conclusions

In conclusion, a solar air heater can effectively provide space heating in residential buildings. Even when natural gas prices were used, the air system still remained cost effective. For this particular simulation, greater than 20 per cent rate of return on investment was achieved. The numerical method proved to be stable and convergent and showed satisfactory agreement in comparison to an analytical solution for constant-inlet air temperatures. Also, the three-modal simulation model demonstrated the capability of estimating the long term response of both the air system and the rock bed. In addition, blowing costs proved to be relatively insignificant in this particular simulation, resulting in a total operating cost of only about two dollars per month. Lastly, computer costs were relatively low, approximately one dollar per simulation.

Table 4. Types of Rocks and Their Densities

IGNEOUS ROCK		SEDIMENTARY ROCKS	
Name	Density (lbm/ft ³)	Name	Density (lbm/ft ³)
Granite	163-172	Limestone	162-169
Syenite	163-172	Dolomite	162-169
Ryolite	163-172	Sandstone	156-169
Trachyte	160-172	Conglomerate	155-169
Diorite	175-181		
Quartz diorite	169-178		
Dacite	169-178		
Andesite	169-178		
Basalt	181-194		
Obsidian	144-169		

Table 5. Properties of Some Common Heat Storage Materials

Substance	Specific Heat c_p (B/lbm-F)	Density ρ (lbm/ft ³)	Thermal Diffusivity $\alpha = \frac{k}{\rho c_p}$ (ft ² /hr) ^D
Air	.240	.075	.850
Asbestos	.250	9.40	.032
Alcohol	.55-.65	50.0	.0035
Brine	.71	75.0	.0100
Brick	.200	106.0	.0128
Charcoal	.242	25.0	.0660
Concrete	.200	137.0	.320
Glass	.16-.20	157.0	.174
Gasoline	.530	50.0	.0031
Ice	.500	57.3	.1132
Porcelain	.255	144.0	.0160
Rock	.210	160.0	.550
Sand (dry)	.191	100.0	.0100
Steel	.120	490.0	.482
Water	1.00	62.4	.0054
Wood (oak)	.570	48.0	.0044

References

1. ASHRAE Handbook, 1977 Fundamentals, American Society of Heating, Refrigerating and Air Conditioning Engineers, New York (1977).
2. Beckman, W.A., Klein, S.A. and Duffie, J.A., Solar Heating Design, Wiley and Sons, New York (1977).
3. Beek, W.J. and Muttzall, K.M.K., Transport Phenomena, Wiley and Sons, New York (1975).
4. Bird, R.B., Stewart, W.E. and Lightfoot, E.N., Transport Phenomena, Wiley and Sons, New York (1960).
5. Clark, J.A. and Arpaci, V.S., "Dynamic Response of a Packed Bed Energy Storage System to a Time Varying Inlet Temperature", Proceedings of the Solar Coding and Heating Forum, December 13-15, 1976, Miami Beach, Florida, U.S.A.
6. Duffie, J.A. and Beckman, W.A., Solar Energy Thermal Processes, Wiley and Sons, New York (1974).
7. Eshleman, W.D., Baird, C.D. and Mears, D.R., "A Numerical Simulation of Heat Transfer in Rock Beds", Proceedings of the 1977 Annual Meeting, Vol. 1, American Section of the International Solar Energy Society, Florida, U.S.A.
8. Holman, J.P., Heat Transfer, 4th Edition, McGraw-Hill, New York (1976).
9. Jeffreson, C.P., "Prediction of Breakthrough Curves in Packed Beds", AIChE Journal, Vol. 18, No. 2, pg. 409 (March 1972).
10. Kays, W.M., Convective Heat and Mass Transfer, McGraw-Hill, New York (1966).
11. Klein, S.A., Beckman, W.A. and Duffie, J.A., "A Design Procedure for Solar Air Heating System", Solar Energy, Vol. 19, No. 5, (1977).
12. Klein, S.A., Beckman, W.A. and Duffie, J.A., "A Design Procedure for Solar Heating Systems", Solar Energy, Vol. 18, No. 1, (1976).
13. Liu, B.Y.H. and R.C. Jordan, "The Interrelationship and Characteristic Distribution of Direct, Diffuse and Total Solar Radiation", Solar Energy, Vol. 4, No. 3, (1960).
14. Manuel Collares-Pereira and Ari Rabl, "The Average Distribution of Solar Radiation-Correlations Between Diffuse and Hemispherical and Between Daily and Hourly Insolation Values", Solar Energy, Vol. 22, No. 2, (1979).
15. McAdams, W.H., Heat Transmission, 3rd Edition, McGraw-Hill, New York (1954).

16. Prins, B.E., "Computer Simulation of a Solar Energy System which Utilizes Flat-Plate Solar Collectors", Master Thesis in Aeronautical Engineering, A.F.I.T., Dayton, Ohio, (1979).
17. Sayigh, A.A.M. and Shaalan, M.R., "Some Experimental Data for Thermal Pile Energy Storage", University of Riyadh, Riyadh, Saudi Arabia.
18. Whitaker, Stephen, "Flow in Packed Beds", AIChE Journal, Vol. 18, No. 2, pg. 366, (March 1972).

Appendix A

Review of Method for Determining Useful Energy Collected

The collector heat removal factor, F_R , of equation (1) from Chapter II is defined as a quantity that relates the actual useful energy gain of a collector to the useful gain if the whole collector surface were at the fluid inlet temperature. F_R is represented by (Ref 2)

$$F_R = \frac{\dot{m}_f c_{pf} (T_{f,o} - T_{f,i})}{[(\bar{\tau}\bar{\alpha})\bar{I}_{Tt} - U (T_{f,i} - T_a)]} \quad (A1)$$

where:

$(\bar{\tau}\bar{\alpha})\bar{I}_{Tt}$ = amount of solar energy absorbed by collector plate

U = energy loss coefficient of collector

The effect of F_R is to reduce the calculated useful energy gain from what it would have been had the whole collector been at $T_{f,i}$ to what actually is using a fluid that increases in temperature as it flows through the collector (Ref 2). As the mass flowrate through the collector increases, the temperature rise through the collector decreases.

\bar{I}_{Tt} in equation (A1) is given by

$$\bar{I}_{Tt} = \bar{R}_t \bar{H} \quad (A2)$$

where r_t is the ratio of hourly total radiation on a horizontal surface to daily total radiation on a horizontal surface. A much better approximation of r_t than the one Prins used has now become available (Ref 14). The new equation is:

$$r_t = \frac{\pi}{24} (a+b \cos w) \frac{\cos w - \cos ws}{\sin ws - ws \cos ws} \quad (A3)$$

where

$$a = .409 + .5016 \sin (ws-1.047)$$

$$b = .6609 - .4767 \sin (ws-1.047)$$

and w is the hour angle and ws is sunset hour angle. In equation (A2), \bar{R} is the monthly average ratio of total radiation on a tilted surface to total radiation on a horizontal surface; therefore, $\bar{R} \bar{H} = \bar{H}_T$. \bar{R} is a function of both the beam and diffuse radiation incident on a horizontal surface. Since these measurements are generally unavailable they are estimated (as discussed in Prins' program) at hourly intervals from \bar{H} by using the results of Liu and Jordan (Ref 13). They found that the ratio of the monthly average daily total radiation (\bar{D}/\bar{H}) was related to \bar{K}_T , the monthly average long term clearness index. \bar{K}_T is the ratio of \bar{H} to H_0 , is the extraterrestrial radiation on a horizontal surface. To find the incident beam radiation on a tilted surface when the incident amount is known on a horizontal surface, the ratio R_b is used. R_b is the ratio of beam radiation on a tilted surface to that on a horizontal surface. If the tilted surface is oriented towards the equator, then

$$R_b = \frac{\cos (\phi-s) \cos \delta \cos w + \sin (\phi-s) \sin \delta}{\cos \phi \cos \delta \cos w + \sin \phi \sin \delta} \quad (A4)$$

where w is the hour angle, ϕ the latitude of the collector, s the slope of the collector from the horizontal, and δ the declination angle.

The utilizability, UT , is a function of the $(\tau\alpha)$ product, the average instantaneous total radiation, \bar{I}_{Tt} , and U , the energy loss coefficient of the collector. UT is the fraction of incident radiation that can be collected, or utilized, by an idealized collector. Utilizability is less than unity because of the heat loss through the sides, back and cover plates of the col-

lector (Ref 16). The overall energy loss coefficient, U , is a function of the collector construction and its operating conditions.

The $(\overline{\tau\alpha})$ product is a function of the dirt factor (DF), the shading factor (SF), and the angle of incidence for both beam and diffuse radiation.

$$(\overline{\tau\alpha}) = .98 (1-DF)(1-SF)(\tau\alpha) \quad (A5)$$

The factor of .98 was used to account for diffuse radiation, and $(\tau\alpha)$ is evaluated for beam radiation.

For a more complete and detailed discussion of energy collection one can refer directly to Captain Prins thesis (Ref 16).

Appendix B

Alternate Methods for Determining Heat Transfer Coefficients and Pressure Drop

Rock Bed

Löf and Hawley (Ref 6) also investigated packed bed energy storage, they arrived at the following expression for the volumetric heat transfer coefficient in $W/m^3 \cdot ^\circ C$, h_v :

$$h_v = 650 \left[\frac{G}{D} \right]^{0.7} \quad (B1)$$

where G is the superficial mass velocity in $Kg/s \cdot m^2$, and D is the equivalent spherical diameter of the particles in meters given by:

$$D = \left[\frac{6}{\pi} \times \frac{\text{net volume of particles}}{\text{number of particles}} \right]^{1/3} \quad (B2)$$

As before

$$h = \frac{h_v A \Delta x}{A_h} = \frac{h_v D_p}{6(1-\epsilon_g)}$$

Another empirical correlation for packed bed heat transfer coefficients is (Ref 4):

$$j_H = 0.91 Re^{-0.51}; \text{ for } Re < 50 \quad (B3)$$

and

$$j_H = 0.61 Re^{-0.41}; \text{ for } Re > 50 \quad (B4)$$

where the Colburn factor, j_H , and Reynolds number, Re , are defined by:

$$j_H = \frac{h}{C_p G} [Pr]_f^{2/3} \quad (B5)$$

and

$$Re = \frac{G}{(A_p/V_p)\mu_g c \phi} \quad (B6)$$

where

$$Pr = \frac{\mu_g c c_p}{k_f} = \text{Prandtl number}$$

$G = \rho V_o =$ superficial mass velocity

$\phi =$ empirical coefficient which depends on the shape of the particle
(See Table B1).

$$\frac{A_p}{V_p} = \frac{6}{D_p} (1 - \epsilon_g) = \text{solid particle surface area per unit volume}$$

The subscript of f denotes properties evaluated at the film temperatures, t_f .

Table B1: Particle Shape Factors for Packed Bed Correlations (Ref 4)

Shape	ϕ
Spheres	1.00
Cylinders	0.91
Flakes	0.86
Rasching rings	0.79
Partition rings	0.67
Berl Saddles	0.80

Tube Bundles

A tube bundle arrangement may also be used for thermal storage. The empirical relationship for air flowing normal to a bank of staggered tubes is (Ref 15)

$$Nu_m = \frac{h_m D_o}{K_f} = 1.12 b_2 (Re)^n (Pr)^{1/3} \quad (B7)$$

where

$$Re = \text{Reynolds number} = \rho V_{\max} D_o / \mu g_c$$

V_{\max} = velocity based on minimum flow area

Pr = Prandtl number of fluid

h_m = mean heat transfer coefficient

D_o = outside tube diameter

K_f = thermal conductivity of air

b_2 and n are the Grimison coefficients; evaluated from tables (Ref 15) and dependent on tube spacing.

This equation normally holds true for tube banks with ten or more rows. However, for smaller number of rows a correction factor exists; these factors are listed in tables for row numbers of ten or less (Ref 15).

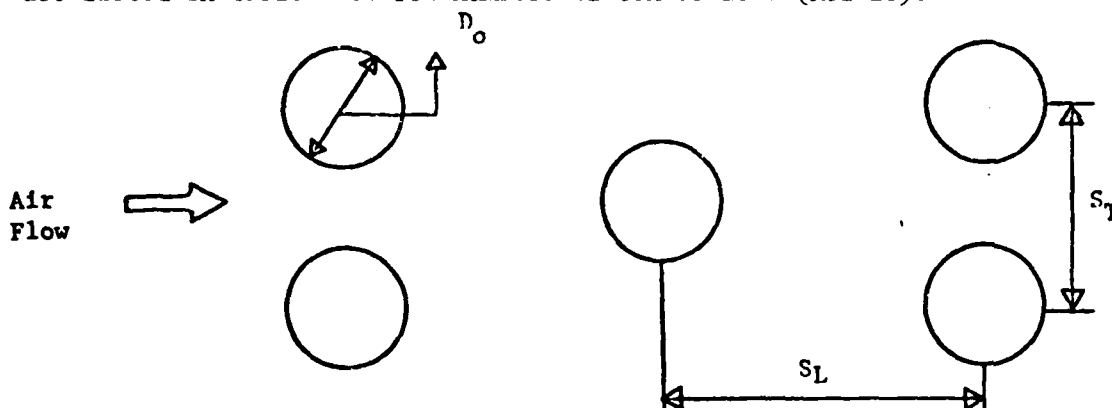


Fig B1. Staggered Tube Arrangement (Top View)

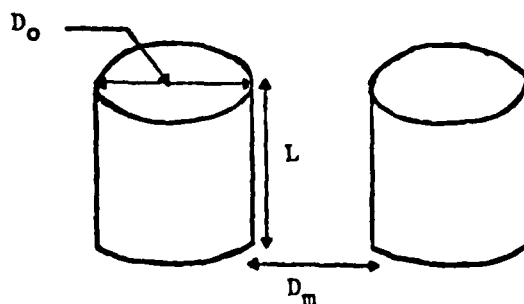


Fig B2. Tube Bundle (Side View)

$$V_{\max} = Q/A_m = Q/D_m L \quad (B8)$$

where:

$A_m = D_m L =$ minimum flow area

$D_m = S_T - D_o =$ minimum clearance distance

$L =$ tube length

$Q =$ volumetric flow rate

To determine the Grimson coefficients, b_2 and n , two more parameters, x_L and x_T must be defined.

$$x_L = S_L/D_o \quad (B9)$$

and

$$x_T = S_T/D_o \quad (B10)$$

where:

$S_L =$ center to center longitudinal distance in direction of flow

$S_T =$ center to center transverse distance perpendicular to flow;

coefficients b_2 and n are presented in tabulated form (Ref 15) as functions of x_L and x_T .

Equation (B7) is valid for turbulent flows and for a Reynolds number range of 2,000 to 40,000.

A pressure drop relationship for the flow of air over a bank of tubes also exist (Ref 8):

$$P = \frac{f^1 G_{\max}^2 N}{\rho (2.09 \times 10^8)} \left(\frac{\mu_w}{\mu_b} \right)^{0.14} \quad (B11)$$

where

$G_{\max} = V_{\max} =$ mass velocity at minimum flow area

$\rho =$ density evaluated at free stream conditions

N = number of transverse rows

μ_w = wall-surface temperature dynamic viscosity of air

μ_b = bulk-temperature dynamic viscosity of air

and the empirical friction factor, f^1 , for staggered tube arrangements is;

$$f^1 = \left[0.25 + \frac{0.118}{[(S_T - D_o)/D_o]^{1.53}} \right] Re_{\max}^{-0.16} \quad (B12)$$

where

$$Re_{\max} = \frac{\rho V_{\max} D_o}{\mu_g} = \text{Reynolds number based on minimum flow area.}$$

Appendix C

Duct Heat Transfer Relationships

In the introduction it was mentioned that the inlet air temperature for the bed during its charging mode was approximately the same as the temperature out of the collector. However, it is only when duct heat losses are at a minimum can this assumption be made.

Therefore, to validate this statement a prediction of heat transfer from circular ducts is necessary. The following diagram is used for this purpose.

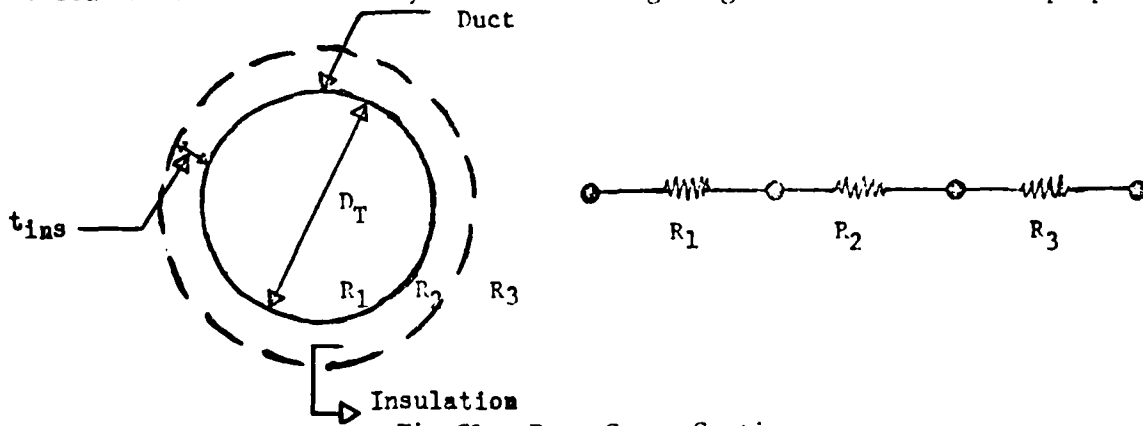


Fig C1. Duct Cross Section

where:

R_1 = forced convective resistance

R_2 = conductive resistance (insulation)

R_3 = free convective resistance

For the fully developed turbulent flow region the forced convective heat transfer within the circular duct can be represented by the following relationship (Ref 10).

$$\bar{Nu} = CRe^{.08}Pr^n = \frac{h_i D_T}{K_f} \quad (C1)$$

where the value of the constant is:

$C = .021$ for constant axial surface temperature

or $C = .022$ for constant axial heat flux

and

h_i = forced convective heat transfer coefficient

K_f = thermal conductivity of fluid (air)

Therefore,

$$Nu_T = .021Re \cdot Pr^n \quad (C2)$$

$$; .4 < n < .6$$

$$Nu_H = .022Re \cdot Pr^n \quad (C3)$$

and $n = .6$ is commonly used for circular ducts exposed to outside ambient conditions. Also, these two algebraic equations are valid for $.5 < Pr < 1.0$: or normally for gases, such as air.

The first two resistances are:

$$R_1 = \frac{1}{h_i} \quad (C4)$$

$$R_2 = \frac{t_{ins}}{K_{ins}} \quad (C5)$$

where

t_{ins} = thickness of insulation

K_{ins} = conductivity of insulation

and h_i is determined from either equation (C2) or (C3). The recommended thickness of insulation (Ref 1) is usually one inch of fiberglass insulation for duct work in the heated area and about 1-2 inches for ducts near the collector or storage unit.

To complete the design calculation of heat losses from a duct to an ambient fluid the outside resistance due to free convection must also be taken into account. For free convection the mean Nusselt number can be represented by the following equation (Ref 8).

$$\bar{Nu}_D = C(Gr_D Pr)^m \quad (C6)$$

where the constants C and m depend on geometry and whether the flow is laminar or turbulent. Also, it is recommended that fluid properties should be evaluated at a mean-film temperature, t_f .

$$t_f = (t_w + t_\infty)/2$$

where:

t_w = wall temperature

t_∞ = ambient (free-stream) temperature

Also, Gr_D = Grashof number (based on diameter)

where:

$$Gr_D = \frac{g \beta (t_w - t_\infty) D_T^3}{\nu^2} \quad (C7)$$

and β = coefficient of volumetric expansion = $\frac{1}{T_\infty}$; for an ideal gas.

For horizontal ducts, the following results may be used:

	$\frac{Gr_D Pr}{C}$	$\frac{m}{C}$	Approximate Mean Coefficients
Laminar	$10^4 - 10^9$.525	$\bar{h}_o = .27 \frac{\Delta t}{D}^{1/4}$ (C8)
Turbulent	$10^9 - 10^{12}$.129	$h_o = .18 (\Delta t)^{1/3}$ (C9)

where: $\Delta t = t_2 - t_3$

$$D = D_T + 2 (t_{ins})$$

and $R_3 = \frac{1}{\bar{h}_o}$; " \bar{h}_o " can be found from either equations (C8) and (C9) or

equation (C6). The total heat loss relationship can now be expressed as:

$$Q_L = UA_s (\Delta t)_{overall} \quad (C10)$$

where: $U =$ overall heat transfer coefficient $= \frac{1}{\sum R}$

or
$$U = \frac{1}{R_1 + R_2 + R_3} = \frac{1}{R_{eff}}$$

and $A_s =$ total surface area $= \pi (D_T + 2 t_{ins}) L_D$. Therefore, the heat loss per unit length can be written as:

$$\frac{Q_L}{L_D} = \frac{\pi (D_T + 2 t_{ins}) (\Delta t)_{overall}}{R_{eff}} \quad (C11)$$

where: $L_D =$ duct length

and $(\Delta t)_{overall} = t_1 - t_3$ or the overall temperature difference.

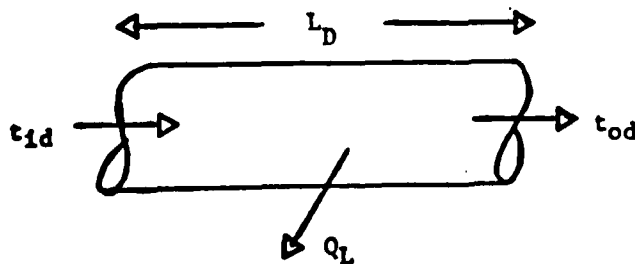


Fig C2. Duct Length Section

Q_L can also be expressed in the following form:

$$Q_L = \dot{m}_a c_{pa} (t_{id} - t_{od}) \quad (C12)$$

where:

t_{id} = air temperature into duct

t_{od} = air temperature out of duct

Solving equation (C12) for " t_{od} " we get:

$$t_{od} = t_{id} - Q_L / \dot{m}_a c_{pa} \quad (C13)$$

where Q_L is determined from equation (C11).

To examine the changes in temperature through a straight duct, several test cases with variable duct lengths were carried out. In all cases a negligible temperature difference, $t_{id} - t_{od}$, resulted. Therefore, the assumption the " t_{od} " is essentially the same as the outlet collector temperature proves to be fairly valid for our particular purposes.

Appendix D

Explicit and Modified-Implicit Schemes

The governing differential air equation is the same as that derived in Chapter II, equation (35).

$$\frac{dT_a}{dx} = \frac{-h_v A}{\dot{m}_a c_{pa}} (T_a - T_b) \quad (D1)$$

Finite-differencing equation (D1) explicitly:

$$\frac{T_{a,i+1} - T_{a,i}}{\Delta x} = \frac{-h_v A}{\dot{m}_a c_{pa}} (T_{a,i} - T_b) \quad (D2)$$

and rearranging gives

$$T_{a,i+1} = \left(1 - \frac{h_v A \Delta x}{\dot{m}_a c_{pa}}\right) T_{a,i} + \frac{h_v A \Delta x}{\dot{m}_a c_{pa}} T_b \quad (D3)$$

For stability purposes

$$\frac{h_v A \Delta x}{\dot{m}_a c_{pa}} < 1 \quad (D4)$$

or

$$\Delta x < \frac{\dot{m}_a c_{pa}}{h_v A} = \frac{\rho_a V_o c_{pa}}{h_v} \quad (D5)$$

Equation (D1) in a modified-implicit form becomes

$$\frac{T_{a,i+1} - T_{a,i}}{\Delta x} = \frac{-h_v A}{\dot{m}_a c_{pa}} \left[\left(\frac{T_{a,i} + T_{a,i+1}}{2} \right) - T_b \right] \quad (D6)$$

Therefore

$$T_{a,i+1} = \frac{\left[1 - \frac{h_v A \Delta x}{2 \dot{m}_a c_{pa}}\right] T_{a,i} + \frac{h_v A \Delta x}{\dot{m}_a c_{pa}} T_b}{1 + \frac{h_v A \Delta x}{2 \dot{m}_a c_{pa}}} \quad (D7)$$

In this case, stability is achieved when

$$\frac{h_v A \Delta x}{2 \dot{m}_a c_{pa}} < 1 \quad (D8)$$

or

$$\Delta x < \frac{2 \dot{m}_a c_{pa}}{h_v A} = \frac{2 \phi_a V_o c_{pa}}{h_v} \quad (D9)$$

Here, Δx is twice that of the explicit result.

For these two schemes, the bed equation is derived in the same manner as the air equation, the result is:

$$\frac{dT_b}{dt} = \frac{h_v A \Delta x}{(1-\epsilon_g) \rho_s c_{ps} A \Delta x} (T_a - T_b) - \frac{Q_L}{(1-\epsilon_g) \rho_s c_{ps} A \Delta x} \quad (D10)$$

In explicit form, letting $B = \frac{h_v \Delta t}{(1-\epsilon_g) \rho_s c_{ps} A \Delta x}$,

equation (D10) becomes

$$T_{b,i}^{j+1} - T_{b,i}^j = B(T_{a,i}^j - T_{b,i}^j) - \frac{Q_L \Delta t}{(1-\epsilon_g) \rho_s c_{ps} A \Delta x} \quad (D11)$$

or

$$T_{b,i}^{j+1} = (1 - B) T_{b,i}^j + B T_{a,i}^j - \frac{Q_L \Delta t}{(1-\epsilon_g) \rho_s c_{ps} A \Delta x} \quad (D12)$$

For stability, $B < 1$ or

$$\Delta t < \frac{(1-\epsilon_g) \rho_s c_{ps}}{h_v} \quad (D13)$$

Now letting $C = \frac{h_v A \Delta x}{\dot{m}_a c_{pa}}$, equation (D3) becomes

AD-A094 771

AIR FORCE INST OF TECH WRIGHT-PATTERSON AFB OH SCHOO--ETC F/6 9/2
COMPUTER SIMULATION OF SOLAR AIR HEATING SYSTEMS USING ROCK BED--ETC(U)
DEC 80 D B FANT
AFIT/GAE/AA/80D-4

NL

UNCLASSIFIED

2 OF 2

436477



END

3-81

$$T_{a,i+1}^j = (1-C) T_{a,i}^j + CT_{b,i}^j \quad (D14)$$

Therefore, equations (D12) and (D14) may be used when an explicit solution scheme is desired.

The bed equation in a modified-implicit form is

$$T_{b,i+1}^{j+1} - T_{b,i+1}^j = B (T_{a,i}^{*j} - T_{b,i+1}^j) - \frac{Q_L \Delta t}{(1-\epsilon_g) \rho_s c_{ps} \Delta x} \quad (D15)$$

where

$$T_{a,i}^{*j} = \frac{T_{a,i}^j + T_{a,i+1}^j + T_{a,i}^{j+1} + T_{a,i+1}^{j+1}}{2} \quad (D16)$$

Substituting for $T_{a,i}^{*j}$ from equation (D16) into equation (D15) and rearranging yields

$$T_{b,i+1}^{j+1} = T_{b,i+1}^j [1-B] + B/4 [T_{a,i}^j + T_{a,i+1}^j + T_{a,i}^{j+1} + T_{a,i+1}^{j+1}] - \frac{Q_L \Delta t}{(1-\epsilon_g) \rho_s c_{ps} \Delta x} \quad (D17)$$

Since $C = \frac{h_v \Delta x}{\dot{m}_a c_{pa}}$, equation (D7) can also be written as:

$$T_{a,i+1}^j = \frac{[1-C/2]}{[1+C/2]} T_{a,i}^j + \left[\frac{C}{1+C/2} \right] T_{b,i+1}^j \quad (D18)$$

Therefore, the modified-implicit solution scheme is represented by equations (D17) and (D18).

Appendix E

Program Instructions

A revision of Captain Prins' computer program for solar water heaters was necessary to deal with the simulation of solar air systems. The modified program can handle both water and air systems, and is relatively easy to operate. However, when an air system simulation is desired some new data cards must be added; consisting of rock bed and pressure drop parameters.

Whenever the air system is in effect any type of water system analysis is overridden. To do this, A PROG=4.0 data card is all that is needed; the exact location of this card will be further explained in the next section.

To use this program, one must also input data about the weather, position and orientation of the collector and the Earth as explained in the Prins' program (Ref 16).

For the air system, rock bed parameters are used to determine the characteristic heat transfer coefficients between the air and the rock; the pressure drop parameters are used to determine pressure drop and blowing costs for the bed, collector and duct work. Next, Prins' part of the program is used to calculate the amount of useful energy collected from a flat-plate solar collector. Once this is done, the three modal operation of an air heating system can be analyzed.

This is accomplished by calculating a space heating load using the degree-day model; then for each hour of the day the useful energy collected is compared to the heating load requirement, and based on this criteria a particular mode of operation is chosen in order to satisfy the load.

The charging and discharging modes, modes 2 and 3 respectively, are the most important. Here, the differential equations which describe the storage

bed are needed to accurately simulate the system. As explained earlier in Chapter IV, the charging mode is used when the useful energy collected is greater than the space load; the load is satisfied first and any excess energy is stored in the bed. The time required to satisfy the load and the time spent charging the bed are both calculated. Also, if the discharging mode was previously in effect, a complete bed temperature distribution reversal is performed before charging the unit.

Mode 3 becomes operational whenever solar energy is no longer available for collection, in this case energy is taken from storage in order to meet the heating load. Again, if the charging mode was previously in effect a bed temperature distribution reversal is necessary before discharging. As in mode 2, the times needed to satisfy the load are also calculated.

In addition, energy losses from the bed are calculated for each period it is not in use; updated bed temperatures are then determined at each nodal point of the storage unit.

To accurately determine fuel savings, a yearly space heating load calculation is needed. Also, a tax credit calculation is necessary to obtain the net investment in a particular type of solar heating system, that is total investment minus the tax credit break. The additional parameters needed for this cost analysis and other modifications are fully explained in the next section.

This last section contains the extra parameters needed to operate an air system simulation. The required input data cards are explained along with the proper nomenclature and input format. All input data is real except where noted. Do not skip any data cards. Input all data in the following order.

<u>Card #</u>	<u>Symbol</u>	<u>Input Format</u>	<u>Units</u>	<u>Explanation</u>
1-15	(First 15 data cards are the same as in Prins' program, Ref 16).			
16	EFF	x.xx	none	Efficiency of heat exchanger. Air systems with no heat exchanger enter 1.
17	PROG	x.	none	If PROG = 4.0, air system is in effect. For water system refer to Prins' work (Ref 16).
18	INT	xx	none	Number of intervals desired on K_T curve (INTEGER). Explained in Prins' program (Ref 16).
19	ND	x	none	Number of consecutive days the simulation is to run (INTEGER).
20	MON	xx	none	Number of months program is run (INTEGER).

Cards 21 through 46 are necessary for the rock bed analysis.

21	TMIN	xx.xxx	minutes	Time increment used in discharging mode. Used in a Do-Loop to determine when load is satisfied or how long hot air should be drawn from the bed to meet the load.
22	EPSIL	xx.xxxxx	hours	Tolerance use to leave Do-Loop after 1 hour of discharging (1 hour plus or minus tolerance). A value of .01 is normally used.
23	QMIN	xxxx.xx	B/hr	Minimum collected energy required before fan turned on.
24	UA	xxxx.xxx	B/hr-F	Overall structure conductance.
25	DELTA S	xx.xxx	hours	Desired time step.
26	Q	xx.xxx	cfs	Volumetric flowrate.
27	HB	xx.xxx	feet	Bed height.
28	WB	xx.xxx	feet	Bed width.
29	RHOA	xxx.xxxx	lbm/ft ³	Air density.

<u>Card #</u>	<u>Symbol</u>	<u>Input Format</u>	<u>Units</u>	<u>Explanation</u>
30	DP	xx.xxxx	lbm/ft ³	Rock diameter.
31	PRN	xx.xxxx	none	Prandtl number of air.
32	CONDA	xxx.xxxx	B/hr-ft-F	Conductivity of air.
33	NEUA	xxx.xxxx	ft ² /hr	Momentum diffusivity of air.
34	CPA	xx.xxxx	B/lbm-F	Specific heat of air.
35	TOB	xx.xx	Degrees-F	Temperature of air outside the bed.
36	RHOS	xxx.xxx	lbm/ft ³	Density of rock.
37	CPS	xxx.xxxx	B/lbm-F	Specific heat of rock.
38	LB	xx.xx	feet	Bed length.
39	KJ	xxx	none	Number of nodes in bed (INTEGER).
40	EG	xx.xxx	none	Void fraction of bed.
41	KS	xx.xxx	B/hr-ft-F	Thermal conductivity of rock.
42	PDIA	xx.xxx	inches	Rock diameter.
43	TBI	xx.xx	Degrees-F	Initial bed temperature.
44	KINS	xxx.xxx	B/hr-ft-F	Thermal conductivity of insulation.
45	TINS	xx.xxx	feet	Insulation thickness.
46	AINS	xxxx.xxx	sq ft	Surface area of bed (top and sides only).

Cards 47 through 55 are needed for pressure drop calculations.

47	UG	xx.xxxx	$\frac{\text{lbm-hr}}{\text{ft}^2}$	Dynamic viscosity of air.
48	EFFP	x.xxxx	feet	Fan efficiency.
49	ACC	xx.xxxxx	feet	Collector air gap spacing.
50	BC	xx.xxx	feet	Width of collector.
51	LC	xx.xxx	feet	Length of collector.
52	LD	xx.xxx	feet	Length of duct work.

<u>Card #</u>	<u>Symbol</u>	<u>Input Format</u>	<u>Units</u>	<u>Explanation</u>
53	DTD	xx.xxx	feet	Duct diameter.
54	TN	xx.xxx	none	Number of turns or elbows.
55	NH	xx.xxx	hours	Hours of operation
56	DDAY	xxxxx.xx	Degrees-F	Number of Degree-Days. (for the average number of Degree-Days corresponding to each month of the year in Vandalia, Ohio refer to Table E1).

57-63 (Same as cards 28-35 in Prins' program, Ref 16).

Cards 64 through 85 are for the cost analysis portion. If a cost analysis is not desired, do not enter any more data cards and the program will stop automatically.

64	FTC1	xx.xxxx	none	Primary Federal tax credit percentage (ex., 40% of the first 2000 dollars invested; per cent is entered in decimal form, 40% = .40).
65	FTC2	xx.xxxx	none	Secondary Federal tax credit percentage (per cent is entered in decimal form).
66	OTC	xx.xxxx	none	Ohio tax credit percentage (per cent in decimal form).
67	STCA	xxxxx.xx	dollars	Initial tax credit amount (i.e., first 2000 dollars).
68	LTCA	xxxxx.xx	dollars	Secondary tax credit amount.
69	TMAYC	xxxxx.xx	dollars	Maximum return from tax credit (i.e., amount from tax credit can not exceed 4000 dollars).

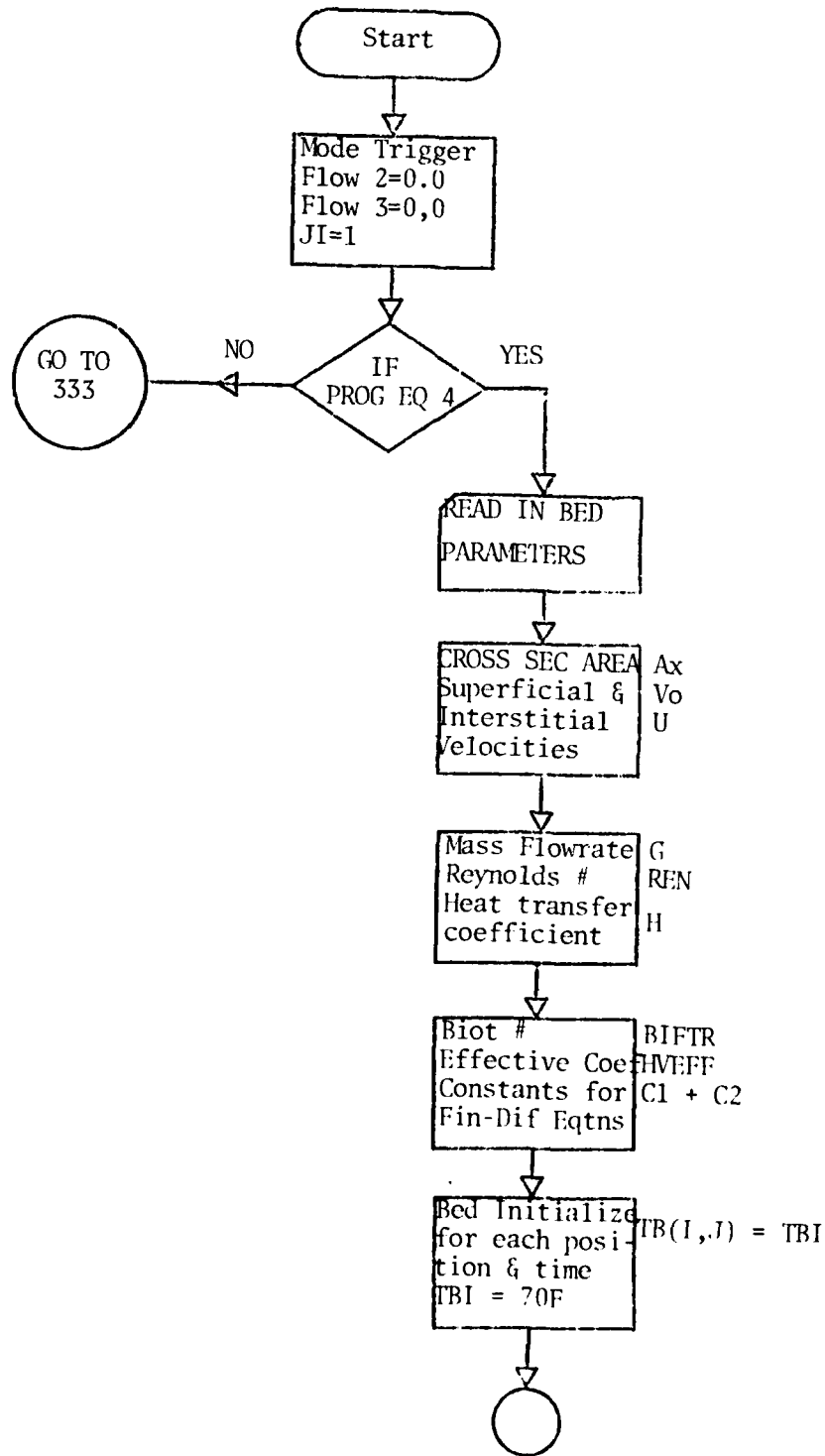
70-85 (Same as cards 36-51 in Prins' program, Ref 16).

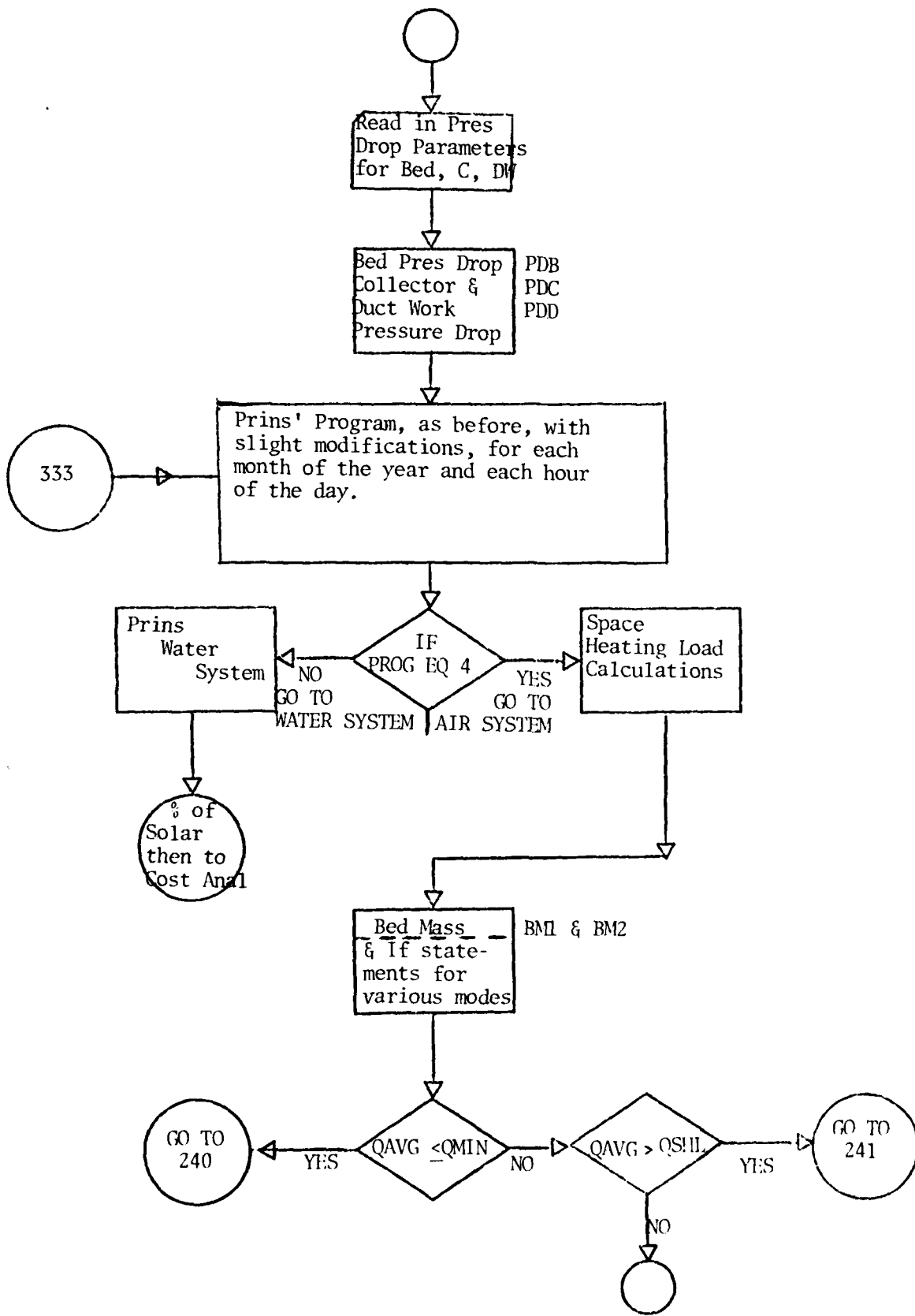
	1973	1974	1975	1976	1977	1978	23 Yr Ave to 74
JAN	1066	1007		1265	1624	1387	1157
FEB	955	993		782	1038	1284	977
MAR	515	655		621	630	891	804
APR	458	352		409	326	427	410
MAY	228	170	↑	217	68	206	171
JUN	0	44		16	28	14	23
JUL	0	0	268	3	0	3	2
AUG	5	0		33	6	22	7
SEP	61	182	↓	137	35	62	81
OCT	231	393		567	390	428	328
NOV	612	621		921	584	617	691
DEC	1061	962		1206	1072	940	1023
TOTAL	5192	5379	5362	6177	5801	6281	5673

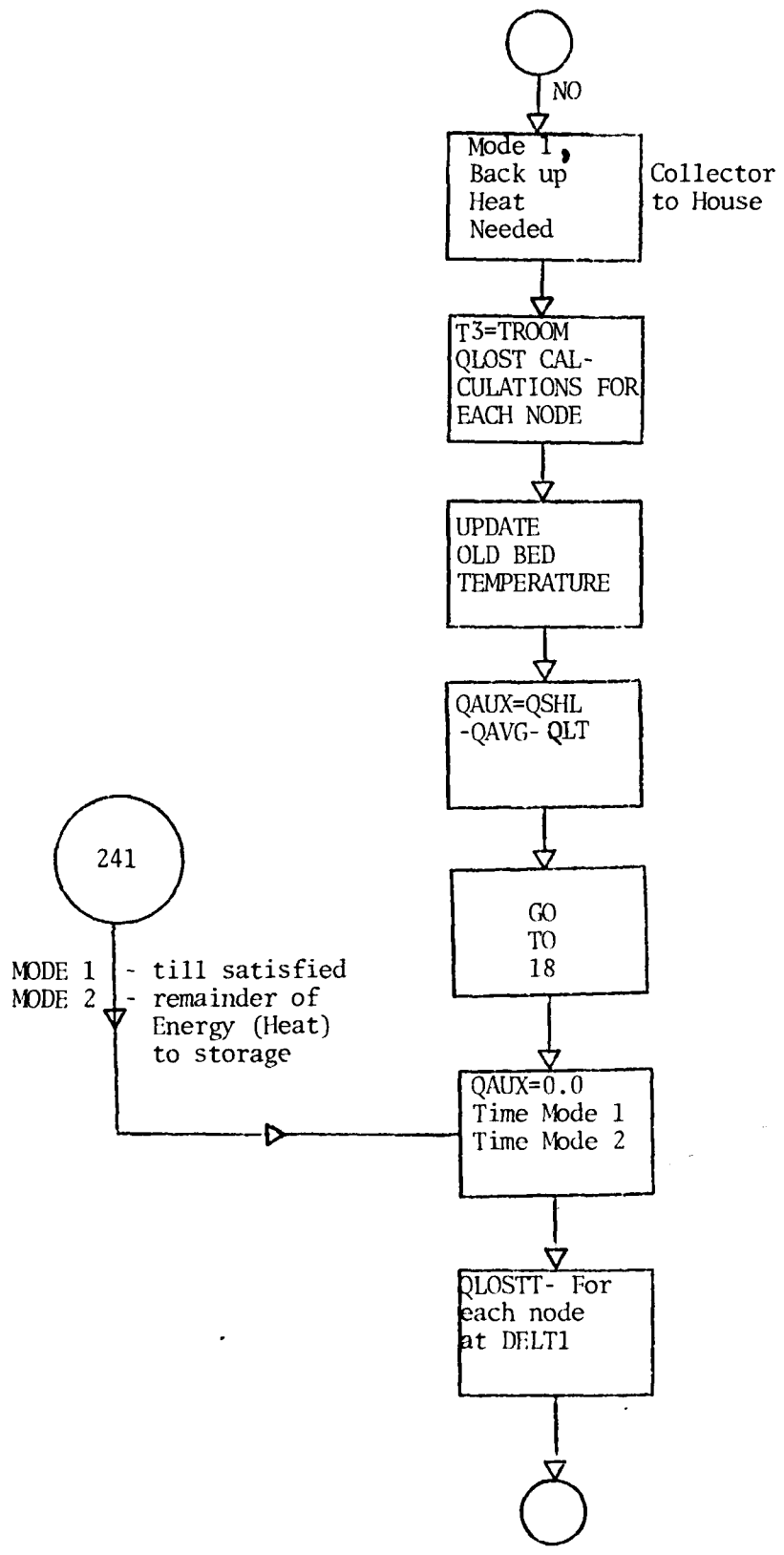
Table E1. Degree-Days, Vandalia, Ohio, Dayton Power and Light Cpy.

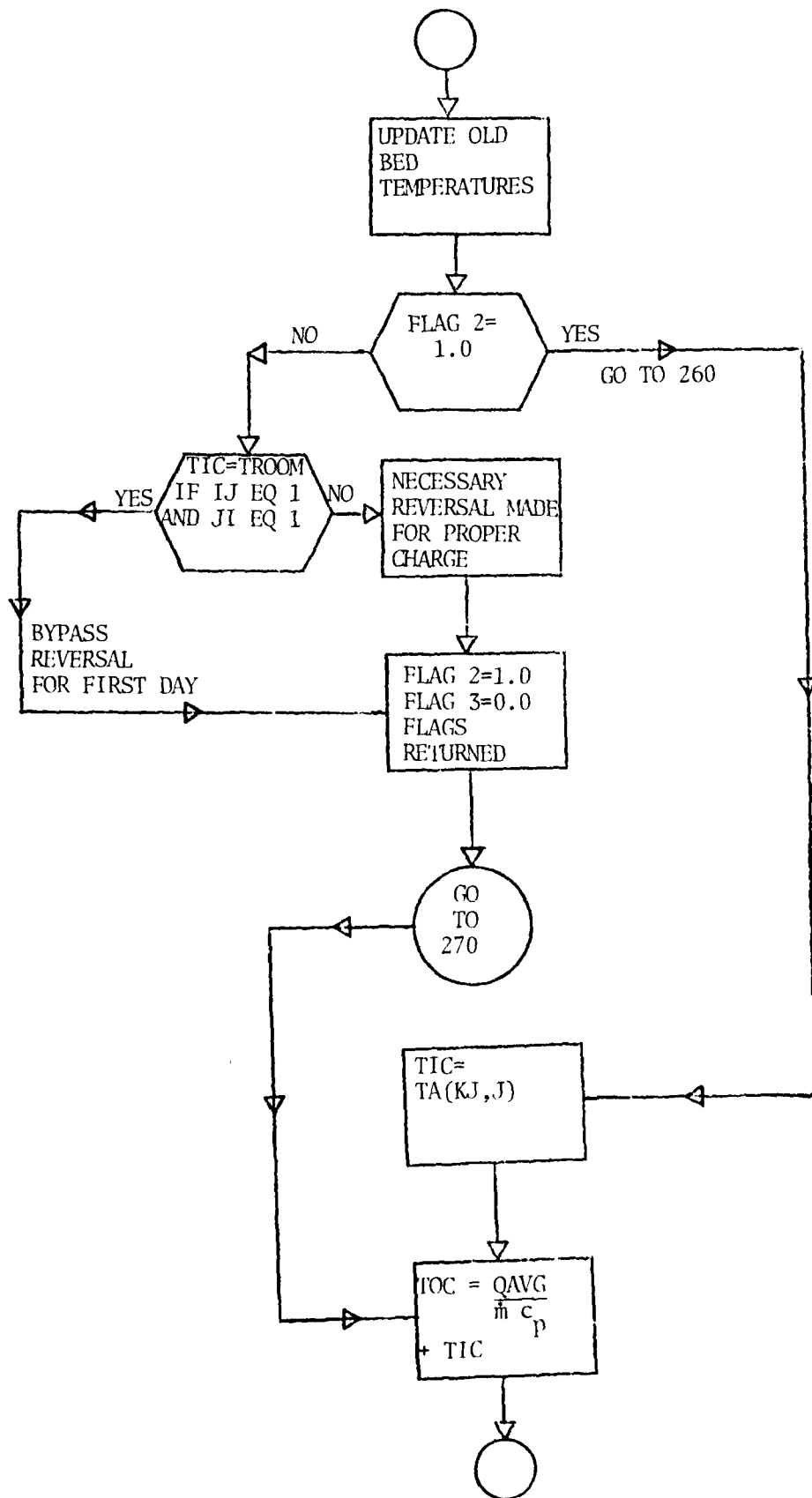
Appendix F

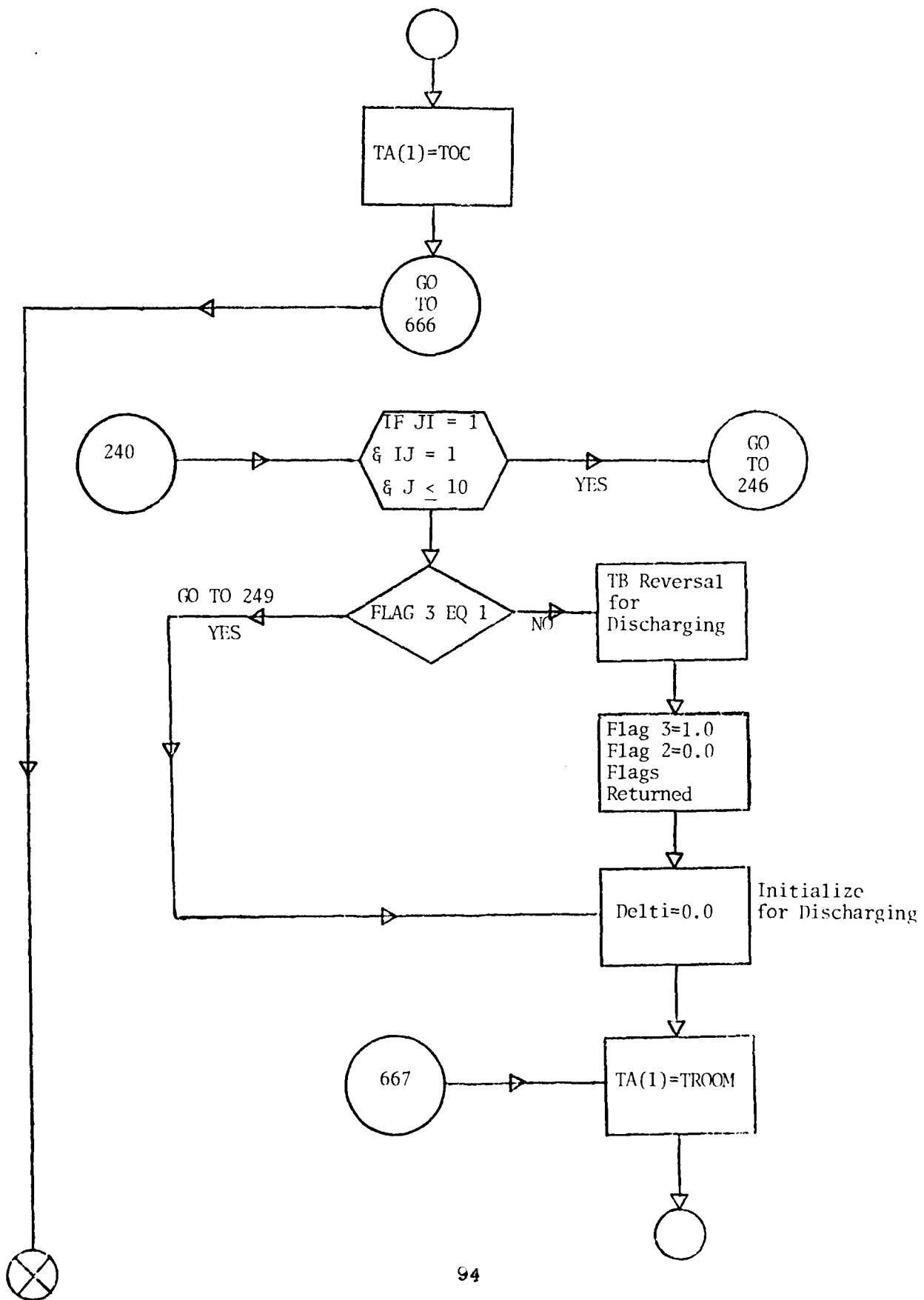
Air System Flowchart

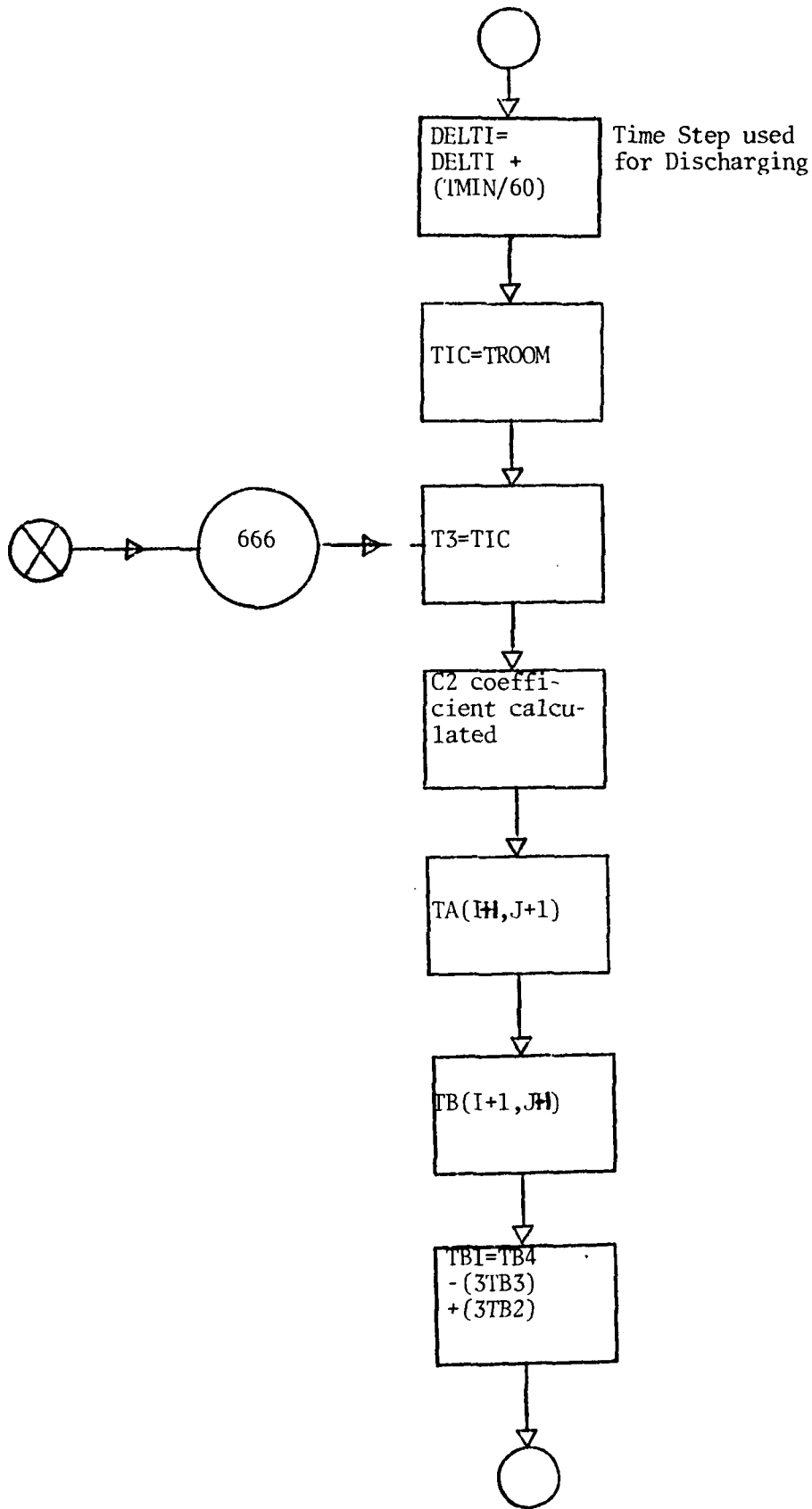


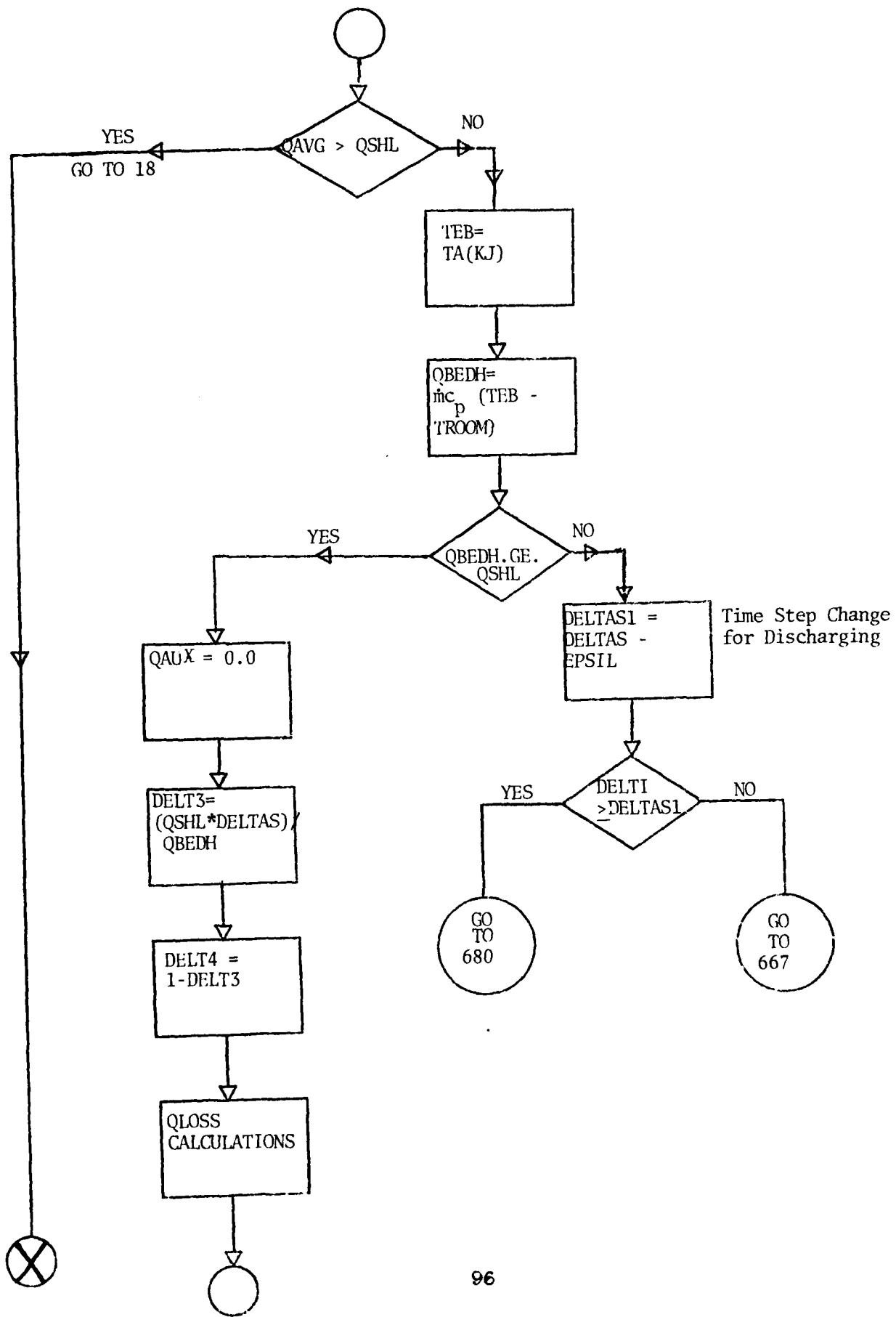


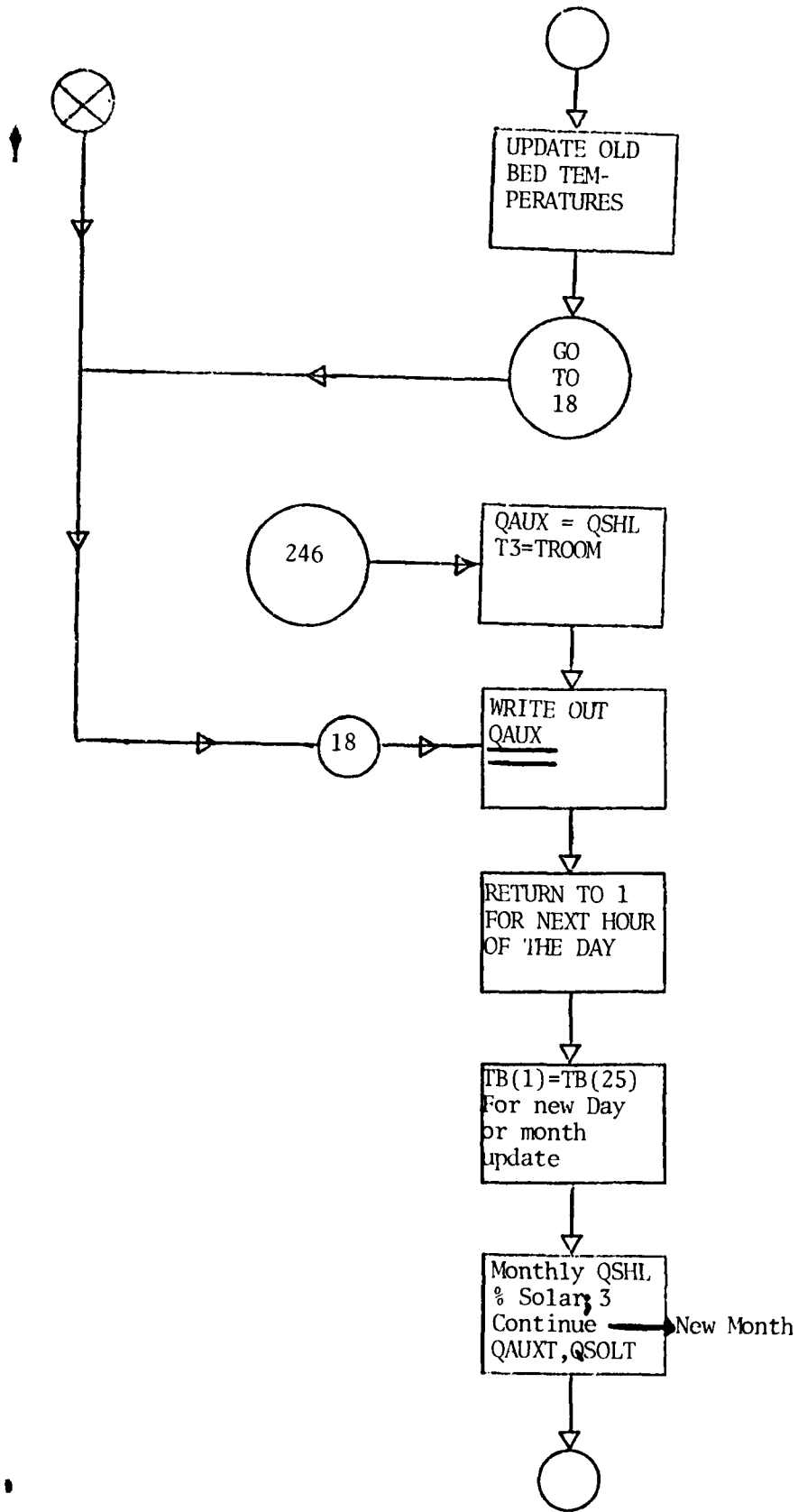


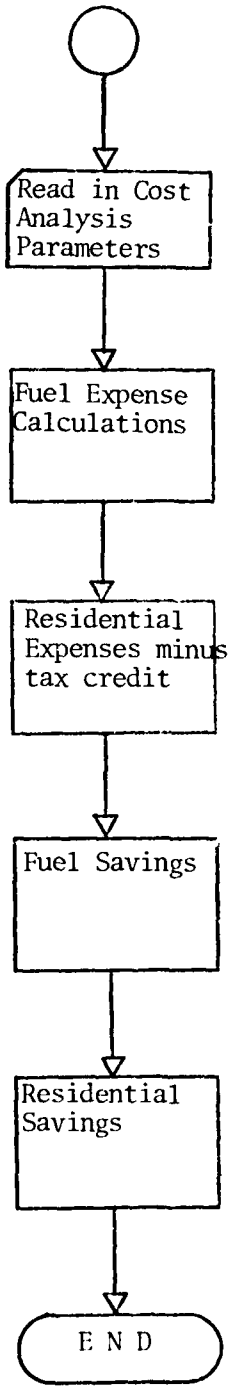












Appendix G

Computer Program Listing


```

YELJMET.
YRUFEC.
YOTOTEI.
OSHLTEI.
IF (P(10), NE(4)) GO TO 333
C READ IN ROCK BED PARAMETERS
  READ*, TMIN
  WRITE(6,905) TMIN
  READ*, EPSIL
  WRITE(6,907) EPSIL
  READ*, OMIN
  WRITE(6,911) OMIN
  READ*, UA
  WRITE(6,915) UA
  READ*, DELTAS
  WRITE(6,921) DELTAS
  READ*, Q
  WRITE(6,925) Q
  READ*, HR
  WRITE(6,931) HR
  READ*, WB
  WRITE(6,935) WB
  READ*, RHOA
  WRITE(6,941) RHOA
  READ*, DP
  WRITE(6,945) DP
  READ*, PRN
  WRITE(6,951) PRN
  READ*, CO(10)
  WRITE(6,955) CO(10)
  READ*, NEUA
  WRITE(6,959) NEUA
  READ*, CPA
  WRITE(6,965) CPA
  READ*, TOR
  WRITE(6,971) TOR
  READ*, RHOS

```

```

WRITE (5, 875) RHOS
READ, DP5
WRITE (5, 880) DPS
READ, LB
WRITE (5, 885) L3
READ, KJ
WRITE (5, 890) KJ
READ, EG
WRITE (5, 895) EG
READ, KS
WRITE (5, 900) KS
READ, PDIA
WRITE (5, 905) PDIA
READ, FBI
WRITE (5, 910) FBI
READ, KINS
WRITE (5, 915) KINS
READ, TINS
WRITE (5, 920) TINS
READ, AINS
WRITE (5, 925) AINS
C DETERMINE THE EFFECTIVE REYNOLDS NUMBER AND THE EFFECTIVE
C HEAT TRANSFER COEFFICIENT TO TAKE INTO ACCOUNT INTERNAL TEMP. GRADIENTS
AX=4R*WR
VD=0/AX
V=VJ/EG
AV=EG*AX
GERHA*V5
VOLP=(1./V)*((3.1416)*DP**3.)
DEP=(5.*VOLP)/(3.1416)**((L./3.1416))
LSTAR=DP*(EG/(1.-EG))
USTAR=(Q/(2000.))/(EG*AX)
RENE=(USTAR*LSTAR)/NEUA
H=(0.5*((REN)**.5)+1.)*.2*((REN)**(2./3.1416))**((CONDG/DP)**
1((1.-EG)/EG))
HV=(H*.5**((1.-EG)))/DP
BI=(H*(DP/2.0))/KS

```

```

HCS=HCS*CPA*(1. -CB)
HCA=HCA+CPA*ES
B=HCS/(HCS+HCA)
BIFF=(1.0+R1/3.0)*(B**2.0)
HVEFF=HV/BIFF
DELX=LR/(FLOAT(KJ)-1.0)
MFLOA=(Q-3511.0)*B*HCA
C1=(HVEFF*AX*DELX)/(MFLOA*CPA)
NH=20
N1=(KJ)-1
N2=NV-1
DO 1 1 J=1,NV
DO 1 1 I=1,KJ
101 T(I,J)=THI
102 CONTINUE
C READ IN PRESSURE DROP PARAMETERS FOR BED, COLLECTOR AND DUCT WORK
READ,UG
WRITE(5,110) UG
READ,EEFF
WRITE(5,111) EEFF
READ,ACC
WRITE(5,112) ACC
READ,BC
WRITE(5,113) BC
READ,LC
WRITE(5,114) LC
READ,LD
WRITE(5,115) LD
READ,OTD
WRITE(5,116) OTD
READ,TN
WRITE(5,117) TN
READ,NH
WRITE(5,118) NH
337 DO 3 IJ=1,40N

```

```

IF (PROG.NE.4.) GO TO 334
C READ IN THE NUMBER OF DEGREE-DAYS FOR EACH MONTH TO BE USED IN
C FINDING THE SPACE-HEATING LOAD
      READ,DDAY
      WRITE(5,999) DDAY
334  READ, DAY
      WRITE(5,1000) DAY
      READ, JAMB
      WRITE(5,1100) JAMB
      READ, HAVG
      WRITE(5,1135)
      WRITE(5,1140) HAVG
      READ, KTRVS
      WRITE(5,1020) KTRVS
      READ, CP
      WRITE(5,1150)
      WRITE(5,1155) CP
      READ, TROOM
      WRITE(5,1235) TROOM
      READ, DAYMON
      WRITE(5,1290) DAYMON
IF (PROG.NE.4.) GO TO 335
C REQ PRESSURE DROP AND PUMPING COST DETERMINED
      V1=V0/350.
      A=((177.7/(EG*43.))+(1.0-EG)/DP)**2.3)*LB
      B=((1.75*(1.-EG)-LB)/((EG*3.7)*CP))
      DELPR=(A+UG*V1)/(32.2*(3600.**2.7))+(3.54CA*(V0**2.5))
      A/(32.2*(3600.**2.7))
      DPA=(DELPR/1.1)**.8*(27.673)
      WRITE(5,500) DPA
      FORMAT('X',1X,'PRES. DROP OF 850 IN INCHES OF WATER= ',F10.4)
      WK=DELPR/RHCA
      P=DELPR*0.367.
      P1=P/778.
      P11=P1*11NH
      PCR=(P01-15.33)/(1.00015.0)

```

```

001170
011044
011210
011221
011230
011234
011270
011260
011270
011300
011370
011710
011650
011670

```

```

PC4=PC0R*DAYM0N
PC03=PC0N/EEF3
WRITE(6, 1) PC03
+1. FORMAT(" ", 1, X, "PUMPING COST OF $FD PER MONTH IN DOLLARS=", F10.4)
C COLLECTOR PRESSURE DROP AND PUMPING COST DETERMINED
NH=(2. *ACC02)/(ACC+PC)
VC=(0.30 *V0)/(30+ACC)
REQ=(RHQA+VD*TH)/UG
MFLOC=RHQA*V0*357.
DELPO=((0.079*LC)/32.2*(360. *2.11))*(MFLOC* 2.0)*(ACC+30))/
B(PECA*.25)*(RHQA*(ACC+BC)*3.0)
PC02=(DELPO/1.4)*(AC/(PC+LC))*2.573
WRITE(6, 2) PC02
+2. FORMAT(" ", 1, X, "PRES. DROP IN GALL. IN INCHES OF WATER=", F10.4)
PC0=(DELPO*MFLOC)/(RHOA
PC01=(PC/778.0)*NH*(AC/(PC+LC))
PC02=(PC0*15.38)/(1000000)
PC03=PC00/DAY40N
PC04=PC00N/EEF3
WRITE(6, 3) PC03
+3. FORMAT(" ", 1, X, "PUMP COST OF COL. PER MONTH IN DOLLARS=", F10.4)
C DUCT WORK PRESSURE DROP AND PUMPING COST DETERMINED
VD=((V0*0)/(3.14*10*(DID**2.0)))*75.15.
VED=(RHQA*VD*TH)/US
DELPO1=((0.079*(VED**2.0)))/(2.0*(32.2*(
R(30. *2.0)))*DID)
DELPO2=(IN*(.1)*RHOA*(VD**2.0))/(2.0*(32.2*(REL. *2.0))
DELPO=DELPO1+DELPO2
PC0=(0.450/1.4) *27.673
WRITE(6, 4) PC0
+4. FORMAT(" ", 1, X, "PRES. DROP IN DUCT NK IN INCHES OF WATER=", F10.4)
PC0=(DELPO*0.35*100)
PC01=(PC/778.0)*NH
PC02=(PC01*15.38)/(1000000)
PC03=PC00/DAY40N
PC04=PC00N/EEF3

```

```

WRITE(6,450) *PCO
451 FORMAT('C',1X,'PUMP COST OF DUCT WK. PER MONTH IN $ ',F10.4)
C TOTAL(RED,COLLECTOR,AND DUCTS) MONTHLY PUMPING COST IS CALCULATED
TCO=PPC*RT*PCO
WRITE(6,460) TCO
461 FORMAT(' ',1X,'TOTAL PUMP COST PER MONTH IN DOLLARS= ',F10.4)
C FIRST, DETERMINE THE AMOUNT OF RADIATION STRIKING THE COLLECTOR SURFACE.
C FIND THE DECLINATION(Delta), THE SUNSET HOUR ANGLE (WS), THE
C EXTRATERRESTRIAL RADIATION ON A HORIZONTAL SURFACE (HO), THE LONG
C TERM CLEARNESS INDEX (KTAVG), AND THE MONTHLY AVERAGE DAILY DIFFUSE
C RADIATION ON A HORIZONTAL SURFACE (DAVG)
IF(PCOS.EQ.0.) GO TO 511
375 DAST=CONST*AREAST/THICKST
501 PI=ACOS(-1.)
RAD=17.2987733131
LAT=LATD/RAD
D=2.*PI*(20.+DAY)/365.
DEL=23.45*SIN(D)
DELTA=DELT/RAD
WRITE(6,1005)DEL
WS=ACOS(-TAN(LAT)*TAN(DELTA))
WS=MS*PI
WRITE(6,1015)WS
O=1.33*(COS(DELTA)*COS(LAT)*SIN(WS))+(WS*SIN(LAT))*SIN(DELTA)
O=(2./PI)*O
HO=(O+GC)*DS
WRITE(6,1020)HO
IF(KTAVG.GT.0.) GO TO 4
KTAVG=HAVG/HO
WRITE(6,1025)KTAVG
IF(KTAVG.LE.0.32) GO TO 5
DAVG=HAVG*(.73-(.93-KTAVG))

```

```

101000
101010
101020
101030
101040
101050
101060
101070
101080
101090
101100
101110

```

```

01120
01130
01140
01150
01160
01170
01180
01190
01200
01210
01220
01230
01240
01250
01260
01270
01280
01290
01300
01310
01320
01330
01340
01350
01360
01370
01380
01390
01400
01410
01420
01430
01440
01450
01460
01470
01480
01490
01500
01510
01520
01530
01540
01550
01560
01570
01580
01590
01600
01610
01620
01630
01640
01650
01660
01670
01680
01690
01700
01710
01720
01730
01740
01750
01760
01770
01780
01790
01800
01810
01820
01830
01840
01850
01860
01870
01880
01890
01900
01910
01920
01930
01940
01950
01960
01970
01980
01990
02000

```

```

5 GO TO 10
10 DAVS=H*AVG*(1.2-(2.*K*AVG))
CONTINUE
INTV=INT+1
DO 5 L=L1,INTV,1
READ,DKT(L)
N=L-1
WRITE(6,1230) N,DKT(L)
CONTINUE
WRITE(6,1025)
WRITE(6,1035) DAVG
S=SD/PAD
GA 44A=36AMMA/RAD
DO 2 N=1,ND,1
WD=-3.147
CSUM=0.0
CRUE=0.0
C DO LOOP 1 IS COMPLETED FOR EACH HOUR OF THE DAY
HP=12.
HP=1.
DO 1 J=1,NA
IF(HP.GT.12.) GO TO 66
HR=HP
GO TO 87
85 HK=HP-12.
87 IF(HP.GT.12.) GO TO 88
HP=HP
GO TO 89
89 HP=HP-12.
WRITE(6,1000) HR,HP
HP=HP+1.
HP=HP+1.
C FIND THE ANGLE BETWEEN THE COLLECTOR SURFACE NORMAL AND THE SUN'S RAYS
C (THETA) AND THE SOLAR ZENITH ANGLE (THETA7)
IF(DCA4MA)/.E.0

```

```

7
AS1=COS(LAT)/(SIN(GAMMA)*TAN(S))
AS2=SIN(LAT)/TAN(GAMMA)
ASR=AS1+AS2
BS1=COS(LAT)/TAN(GAMMA)
BS2=SIN(LAT)/(SIN(GAMMA)*TAN(S))
BSR=TAN(DELTA)*(PS1-BS2)
ABSQT=SQRT((ASR*ASR)-(BSR*BSR)+1.)
WSM=ACOS(((ASR*BSR)+ABSQT)/(ASR*ASR+1.))
WSO=ACOS(((ASR*BSR)-ABSQT)/(ASR*ASR+1.))
WSR=-WSM
WSS=WSO
IF(WD.LT.WSR) GO TO 13
IF(WD.GT.WSS) GO TO 13
GO TO 21
9
AS1=COS(LAT)/(SIN(GAMMA)*TAN(S))
AS2=SIN(LAT)/TAN(GAMMA)
ASR=AS1+AS2
BS1=COS(LAT)/TAN(GAMMA)
BS2=SIN(LAT)/(SIN(GAMMA)*TAN(S))
BSR=TAN(DELTA)*(BS1-BS2)
ABSQT=SQRT((ASR*ASR)-(BSR*BSR)+1.)
WSM=ACOS(((ASR*BSR)+ABSQT)/(ASR*ASR+1.))
WSO=ACOS(((ASR*BSR)-ABSQT)/(ASR*ASR+1.))
WSR=-WSO
WSS=WSM
IF(WD.LT.WSR) GO TO 13
IF(WD.GT.WSS) GO TO 13

```

```

      GO TO 21
      WA=ABS(WD)
      IF(WA.GT.WS) GO TO 13
      W=W
      A1=SIN(DELTA)*SIN(LAT)*COS(S)
      A2=SIN(DELTA)*COS(LAT)*SIN(S)+COS(GAMMA)
      A3=COS(DELTA)*COS(LAT)*COS(S)+COS(W)
      A4=COS(DELTA)*SIN(LAT)*SIN(S)+COS(GAMMA)*COS(W)
      A5=COS(DELTA)*SIN(LAT)*SIN(GAMMA)*SIN(W)
      A6=A1-A2+A3+A4+A5
      THETA=ACOS(A6)
      THETA=THETA*PI/180
      WRITE(6,1035)THETA
      IF(THETA.GT.85.) GO TO 13
      THETA=ACOS(COS(LAT)*COS(DELTA)*COS(N)+SIN(DELTA)*SIN(LAT))
      THETA7=THETA*PI/180
      WRITE(6,1036)THETA7
      RR=COS(THETA)/COS(THETA7)
      C FIND THE MONTHLY AVERAGE RATIO OF TOTAL RADIATION ON A TILTED SURFACE TO
      C TOTAL RADIATION ON A HORIZONTAL SURFACE (RAVG)
      RD=(PI/24.)*((COS(W)-COS(WS))/(SIN(NS)-COS(WS))-(WS*COS(WS))))
      ANGE=WS-1.117
      COEF1=.9+.5*15*SIN(ANGF)
      COEF2=.6*CO1+.757*SIN(ANGF)
      ANGL=(COS(W)-COS(WS))/(SIN(NS)-COS(WS))
      RT=(PI/24.)*(COEF1+COEF2+COS(W)/AN5)
      C=CP/100.
      RHOG=(.2*(1.-C))+(.7*C)
      WRITE(6,1037)RHOG
      RA=(R/RT)*C*W/G/HAVG
      RAVG=((1.-RA)*R8)+(.5*(1.+COS(S))^2)+.5*(1.-COS(S))*RHOG
      C FIND THE MONTHLY AVERAGE INSTANTANEOUS TOTAL RADIATION ON A TILTED
      C SURFACE (ITT)
      ITT=RAVG*RT*HVG
      IF(ITT.GE.0.) GO TO 12
      ITT=0.

```

01215
01221
01223
01230
01234
01237
01239
01243

01244
01247
01311

01720
01730
01730

01730
01730
01730

01730
01740
01740
01740
01740

01740
01740
01740

```

12 GO TO 13
CONTINUE
WRITE(6,1050)
WRITE(6,1051)IT
C SECOND, FIND THE AMOUNT OF RADIATION UTILIZED BY THE COLLECTOR SYSTEM
C FIND THE TRANSMITTANCE (TAUI) OF THE COVERS, ACCOUNTING FOR REFLECTION
C (TAUR) AND FOR ABSORPTANCE (TAUAI)
IF(THETAR.GT.1.0) GO TO 15
THETAC=0.0
GO TO 21
THETAC=ASIN(SIN(THETAR))/ETAC)
THETAC=THETAC*3.14159
CONTINUE
IF(THETAR.GT.1.0) GO TO 25
RH02=((ETAC-1.0)/(ETAC+1.0))**2
TAUR1=(1.-RH02)/(1.+((2.*CN)-1.)*RH02)
GO TO 27
TCR=ABS(THETAC-THETAR)
TCC=THETAC+THETAR
RH01=(SIN(TCR)/SIN(TCC))**2
RH02=(TAN(TCR)/TAN(TCC))**2
TA1=(1.-RH01)/(1.+((2.*CN)-1.)*RH01)
TA2=(1.-RH02)/(1.+((2.*CN)-1.)*RH02)
TAURI=(TA1+TA2)/2.
TAUAI=EXP(-(COP*ETC*THC)/COS(THETAC))
TAUI=TAURI*TAUAI
WRITE(6,1052) TAUI
C FIND THE EFFECTIVE TRANSMITTANCE-ABSORPTANCE PRODUCT (TAUAA)
C THEI=(COS(THETAR))**2
ALPHA=ALPHAN*GTHET
DE=CN-2.
IF(CD)35,40,45
RH02=.16
GO TO 50
RH02=.2+
GO TO 50

```

011700
011710
011720
011730

011740
011750
011760
011770

011780
011790
011800
011810

011820
011830
011840

011850
011860
011870
011880
011890
011900
011910

```

45 RHO2=.29
50 CONTINUE
TAUA=(TAUI*ALPHA)/(1.-((1.-ALPHA)**RHO2))
IF(DN)55,6,65
55 B1=.27
B2=.7
R3=.7
GO TO 70
60 B1=.15
R2=.52
B3=.7
GO TO 70
70 B1=.14
R2=.5
R3=.75
CONTINUE
IF(THETA*.51.) GO TO 42
T1=((1.-RHO2)/(1.+RHO2))*EXP((-ED*TD)/COS(THETA))
T2=((1.-RHO2)/(1.+RHO2))*EXP((-2.*ED*THC)/COS(THETA))
GO TO 43
42 RHO1=(SIN(TDR)/SIN(TCC))**2
PHO2=(TAN(TDR)/TAN(TCC))**2
T11=(1.-RHO1)/(1.+RHO1)
T12=(1.-RHO2)/(1.+RHO2)
TP1=(T11+T12)/2.
T1=TR1*EXP((-ED*THC)/COS(THETA))
T21=(1.-RHO1)/(1.+RHO1)
T22=(1.-RHO2)/(1.+RHO2)
TR2=(T21+T22)/2.
TC=TR2*EXP((-2.*ED*THC)/COS(THETA))
TAUAM=TAUA+(1.-TAUAI)*(B1+(B2+T1)+(B3*T2))
SF=(CNI*.6)*TAN(THETA)
WRITE(5,137)SF
TAUAA=.98*(1.-DF)*(1.-SF)*TAUAM
WRITE(5,137E)TAUAA

```

```

161910
161920
161930
161940
161950
161960
161970
161980
161990
162000
162010
162020
162030
162040
162050
162060
162070
162080
162090
162100
162110
162120
162130
162140
162150
162160
162170
162180
162190
162200
162210
162220
162230
162240
162250
162260
162270
162280
162290
162300
162310
162320
162330
162340
162350
162360
162370
162380
162390
162400
162410
162420
162430
162440
162450
162460
162470
162480
162490
162500
162510
162520
162530
162540
162550
162560
162570
162580
162590
162600
162610
162620
162630
162640
162650
162660
162670
162680
162690
162700
162710
162720
162730
162740
162750
162760
162770
162780
162790
162800
162810
162820
162830
162840
162850
162860
162870
162880
162890
162900
162910
162920
162930
162940
162950
162960
162970
162980
162990
163000

```

C FIND THE RATIO OF OPTICAL RADIATION TO MONTHLY AVERAGE INSTANT TOTAL
C TOTAL RADIATION (PCRIT) AND THEN INTEGRATE THE AREA UNDER THE KT CURVE

```

C TO FIND THE UTILIZABILITY
RCRIT=(U*(I3-TAMB))/(TAUAA*IT)
WRITE(6,1031)
WRITE(6,1032) RCRIT
TNI=1./INT
K=0
E=0.
DO 35 M=1,INTV,1
KT=JKT(M)
IF(KT.GT.0.75) GO TO 80
DH=(2.32*KT-3.22)*KT*KT+1.
GO TO 95
DH=.17
CONTINUE
KT=RO/PT
S=.5*(1.-COS(S))*RHUG
P=(1.-(P7*DH))*KP*(.5*(1.+COS(S))*R7*DH)+S
ITTE=(K/RAVS)*KT/KTAVG
AVG(K)=ITTE
IF(K.EQ. ) GO TO 91
IF(K.EQ.INT) GO TO 91
UT(K)=(AVG(K)-RCRIT)*TNI
GO TO 92
UT(K)=(AVG(K)-RCRIT)*TNI/2.
CONTINUE
IF(UT(K).GT.0.) GO TO 96
UT(K)=0.
CONTINUE
K=K+1
E=E+TNI
CONTINUE
UTIL=E*0.
DO 35 M=1,INTV,1
L=L+1
UTIL=UTIL+UT(L)
CONTINUE

```

```

002151
002152
002153
002154
002155
002156
002157
002158
002159
002160
002161
002162
002163
002164
002165
002166
002167
002168
002169
002170
002171
002172
002173
002174
002175
002176
002177
002178
002179
002180
002181
002182
002183
002184
002185
002186
002187
002188
002189
002190
002191
002192
002193
002194
002195
002196
002197
002198
002199
002200
002201
002202
002203
002204
002205
002206
002207
002208
002209
002210
002211
002212
002213
002214
002215
002216
002217
002218
002219
002220
002221
002222
002223
002224
002225
002226
002227
002228
002229
002230
002231
002232
002233
002234
002235
002236
002237
002238
002239
002240
002241
002242
002243
002244
002245
002246
002247
002248
002249
002250
002251
002252
002253
002254
002255
002256
002257
002258
002259
002260
002261
002262
002263
002264
002265
002266
002267
002268
002269
002270
002271
002272
002273
002274
002275
002276
002277
002278
002279
002280
002281
002282
002283
002284
002285
002286
002287
002288
002289
002290
002291
002292
002293
002294
002295
002296
002297
002298
002299
002300
002301
002302
002303
002304
002305
002306
002307
002308
002309
002310
002311
002312
002313
002314
002315
002316
002317
002318
002319
002320
002321
002322
002323
002324
002325
002326
002327
002328
002329
002330
002331
002332
002333
002334
002335
002336
002337
002338
002339
002340
002341
002342
002343
002344
002345
002346
002347
002348
002349
002350
002351
002352
002353
002354
002355
002356
002357
002358
002359
002360
002361
002362
002363
002364
002365
002366
002367
002368
002369
002370
002371
002372
002373
002374
002375
002376
002377
002378
002379
002380
002381
002382
002383
002384
002385
002386
002387
002388
002389
002390
002391
002392
002393
002394
002395
002396
002397
002398
002399
002400
002401
002402
002403
002404
002405
002406
002407
002408
002409
002410
002411
002412
002413
002414
002415
002416
002417
002418
002419
002420
002421
002422
002423
002424
002425
002426
002427
002428
002429
002430
002431
002432
002433
002434
002435
002436
002437
002438
002439
002440
002441
002442
002443
002444
002445
002446
002447
002448
002449
002450
002451
002452
002453
002454
002455
002456
002457
002458
002459
002460
002461
002462
002463
002464
002465
002466
002467
002468
002469
002470
002471
002472
002473
002474
002475
002476
002477
002478
002479
002480
002481
002482
002483
002484
002485
002486
002487
002488
002489
002490
002491
002492
002493
002494
002495
002496
002497
002498
002499
002500

```

```

13 13 02150
14 14 02150
15 15 02150
16 16 02150
17 17 02150
18 18 02150
19 19 02150
20 20 02150
21 21 02150
22 22 02150
23 23 02150
24 24 02150
25 25 02150
26 26 02150
27 27 02150
28 28 02150
29 29 02150
30 30 02150
31 31 02150
32 32 02150
33 33 02150
34 34 02150
35 35 02150
36 36 02150
37 37 02150
38 38 02150
39 39 02150
40 40 02150
41 41 02150
42 42 02150
43 43 02150
44 44 02150
45 45 02150
46 46 02150
47 47 02150
48 48 02150
49 49 02150
50 50 02150
51 51 02150
52 52 02150
53 53 02150
54 54 02150
55 55 02150
56 56 02150
57 57 02150
58 58 02150
59 59 02150
60 60 02150
61 61 02150
62 62 02150
63 63 02150
64 64 02150
65 65 02150
66 66 02150
67 67 02150
68 68 02150
69 69 02150
70 70 02150
71 71 02150
72 72 02150
73 73 02150
74 74 02150
75 75 02150
76 76 02150
77 77 02150
78 78 02150
79 79 02150
80 80 02150
81 81 02150
82 82 02150
83 83 02150
84 84 02150
85 85 02150
86 86 02150
87 87 02150
88 88 02150
89 89 02150
90 90 02150
91 91 02150
92 92 02150
93 93 02150
94 94 02150
95 95 02150
96 96 02150
97 97 02150
98 98 02150
99 99 02150
100 100 02150

```

```

WRITE(6,1105)UTIL
C FIND THE ENERGY TRANSFERRED TO STORAGE (QAVG)
G=FLOWC/AC
FRPRIME=FR/(1.+(FR*U)/(G*CPO))**((1./EFF)-1.)
QAVG=AC*FRPRIME*TAUA+ITT*UTIL
WRITE(6,1120)QAVG
GO TO 14
QAVG=1.0
WRITE(6,1110)
CONTINUE
C THIRD, FIND THE AMOUNT OF ENERGY TRANSFERRED TO STORAGE.
C WHEN PRUG EQUALS 1.0 THE SOLAR AIR HEATING PROGRAM IS IN EFFECT AND THE
C WATER-SYSTEM ANALYSIS IS SURPASSED
IF(PRUG.EQ.1.) GO TO 213
HLOAD=FLOW(I)-DAYFLOW*CPS*(T3-TT4)*3.335
IF(PRUG.EQ.1.)GO TO 16
IF (PRUG.EQ.2.)GO TO 17
IF (PRUG.EQ.3.) GO TO 18
GO TO 13
C SYSTEM 1 IS A SIMPLE WATER HEATING SYSTEM WITH NO BACKUP HEAT
T4=T3+(QAVG-UAST*(T3-TROOM))/MASS
T3=T4
GO TO 11
C SYSTEM 2 IS A WATER HEATING SYSTEM WITH A CONVENTIONAL WATER HEATER THAT
C PROVIDES ITS SUPPLY FROM A SOLAR HEATED STORAGE TANK
T4=T3+(QAVG-HLOAD-(UAST*(T3-TROOM)))/MASS
T5=(T3+T4)/2.
T3=T4
QAVX=FLOW(I)+DAYFLOW*CPS*(140.-T5)*9.335
T5=QAVX/GT.0) GO TO 41
QAVX=1.0
GO TO 11
C SYSTEM 3 IS LIKE SYSTEM 2 EXCEPT THAT AN ANTI-FREEZE TYPE SOLUTION IS
C USED AS THE COLLECTOR FLUID
T4=T3+(QAVG-HLOAD-(UAST*(T3-TROOM)))/MASS
T5=(T3+T4)/2

```

```

T3=T4
QAJX=FLOW(I)*DAYFLOW*CPS*(1+0.-T5)*9.335
IF(QAJX.GT.0.) GO TO 41
QAJX=9.9
+1 WRITE(6,1115)T4
C SPACE-HEATING LOAD IS CALCULATED ALONG WITH VARIOUS "IF" STATEMENTS
C NECESSARY TO OBTAIN THE AMOUNT OF AUXILIARY ENERGY REQUIRED
217 QSHL=(UA*DDAY)/DAYMON
      BHI=((AX*L3)/(FLOAT(KJ-1)))*RHOS*(L.-EG)
      B42=(RM1/2.1)
      IF(QAVG.LE.0MIN) GO TO 24J
      IF(QAVG.GT.CSHL) GO TO 24I
C MODE 1
      T3=TRDM
      QLOST=0.0
      DO 226 I=1,KJ
      QLOSS1=(KINGS*AINS)/(FLOAT(KJ)*TINS)*(TB(I,J)-TOP)*DELTA5
      IF((I.EQ.1).OR.(I.EQ.KJ)) GO TO 211
      TQLOSS1=QLOSS1/(RM1+CPS)
      GO TO 214
212 TQLOSS1=QLOSS1/(RM2*CPS)
213 QLOST=QLOST+QLOSS1
226 TR(I,J+1)=TB(I,J)-TQLOSS1
      QAJX=QSHL-QAVG-QLOST
      GO TO 18
C MODE 2 AND RED REVERSAL
241 QAJX=1.
      DELT1=(QSHL*DELTA5)/QAVG
      WRITE(6,340) DELT1
      DELT2=1.-DELT1
      WRITE(6,312) DELT2
      DELT1=DELT2
      DELT2=DELT1
      QLOSTT=0.9
      DO 234 I=1,KJ
      QLOSS2=(KINGS*AINS)/(FLOAT(KJ)*TINS)*(TB(I,J)-TOP)*DELT1

```

```

IF(I.EQ.1).OR.(T.EQ.KJ) GO TO 215
TBLOSS2=QBLOSS2/(R41+CPS)
GO TO 217
215 TBLOSS2=QBLOSS2/(R42+CPS)
217 QBLOSS2=QBLOSS2+QBLOSS2
236 TB(I,J)=TB(I,J)-TBLOSS2
IF(FLAG2.EQ.1.) GO TO 266
TTC(J)=TROOM
IF((T1.EQ.1).AND.(J1.EQ.1)) GO TO 231
DO 27 I=1,KJ
MH=KJ-I
27 TBT(MN+1,J)=TB(I,J)
GO 218 I=1,KJ
218 TB(I,J)=TBT(I,J)
251 FLAG2=1.
FLAG3=.7
GO TO 276
26 TIG(J)=TA(KJ,J)
C TEMPERATURE OUT OF THE COLLECTOR IS DETERMINED
270 TDC(J+1)=(QAVG7(MFLOA*CPA))+TIG(J)
WRITE(5,347) TDC(J+1)
TA(1,J+1)=TDC(J+1)
GO TO 566
247 CONTINUE
IF((J1.EQ.1).AND.(LJ.EQ.1).AND.(J.LE.17)) GO TO 245
IF(FLAG3.EQ.1.) GO TO 249
C MODE 3 AND REF REVERSAL
DO 28 I=1,KJ
MH=KJ-I
24 TBT(MN+1,J)=TB(I,J)
GO 219 I=1,KJ
219 TBT(I,J)=TBT(I,J)
FLAG2=1.
FLAG3=.7
249 DELTI=.0
56 TBT(I,J+1)=TROOM

```

```

DELTA=DELTA+(TMIN/60.)
TIC(J)=TROOM
T=TIC(J)
C2=(MELDA*CPA*DELTA)/((1.-EG)*RHO*CP*AX*DELX)
DO 23 I=1,JI
C IMPLICIT FINITE-DIFFERENCED AIR TEMPERATURE EQUATION AS A
C FUNCTION OF TIME AND BED POSITION IS DEVELOPED, ENERGY LOSSES FROM
C THE BED ARE ALSO TAKEN INTO ACCOUNT
      TA(I+1,J+1)=((1.+C1-C2)/(1.+C1+C1*C2))*TA(I,J+1)+
      2*((C1)/(1.+C1+C1*C2))*TB(I+1,J)-((C1)/(1.+C1+C1*C2))*
      3*((KINS*AINS)/TINS)*(TB(I+1,J)-T0)*((DELTA)/(1.-EG))* (RHO*CP*
      4(AX*DELX))
C IMPLICIT FINITE-DIFFERENCED BED TEMPERATURE EQUATION AS A FUNCTION
C OF TIME AND POSITION IS ALSO DEVELOPED
      TB(I+1,J+1)=((C1-C2)/(1.+C1+C1*C2))*TA(I,J+1)+
      5*((1.+C1)/(1.+C1+C1*C2))* (TB(I+1,J))-(((KINS*AINS)/TINS)*
      6(TB(I+1,J)-T0))* (DELTA)/((1.-EG))* (RHO*CP* (AX*DELX)))
23 CONTINUE
C BED TEMP AT NODE 1, CURVE FIT SOLUTION
      T(1,J+1)=TB(1,J+1)-(3.*TB(3,J+1))+ (3.*TB(2,J+1))
      IF (DAYS.GT.OSHL) GO TO 18
      T=TA(KJ,J+1)
      WRITE(6,343) T
      C=7445104*CPA*(T-TROOM)
      T=(70504.6E-034L) GO TO 67
      DELTAS1=DELTA3-EPSIL
      T=(DELTA1.GT.DELTAS1) GO TO 503
      GO TO 587
57 CONTINUE
      DELTAS=(OSHL*DELTA4)/OREDH
      WRITE(6,343) DELTAS
      DELT4=1.-DELTA
      DO 235 I=1,KJ

```

```

      QLOSS=((KINS*AINS)/(FLOAT(KJ)+TINS))*(TB(I,J+1)-103)*0.114
      IF((I.EQ.1).OR.(I.EQ.KJ)) GO TO 239
      TLOSS=QLOSS/(3M1+CPS)
      GO TO 239
278  TLOSS=QLOSS/(742*CPS)
279  TR(I,J+1)=TB(I,J+1)-TLOSS
280  CONTINUE
      GO TO 19
      QAIH=QSHL-QRECH
      GO TO 13
286  QAIH=QSHL
      T3=TCOOL
      CONTINUE
      WIND=0.2512
      WRITE(6,1315) QAIH
      IF((J.EQ.1).AND.(IJ.EQ.1)) GO TO 1
      QSUM=QSUM+QAIH
      Q3)=QRU+QAIH
      CONTINUE
      IF((J.EQ.1).AND.(IJ.EQ.1)) GO TO 332
      WRITE(6,1316) QRU
332  CO 327 T=1,KJ
333  TR(I,1)=TB(I,24)
      IF((J.EQ.1).AND.(IJ.EQ.1)) GO TO 112
      GO TO 2
103  J=J+1
      GO TO 50
      CONTINUE
2  MONTHLY SPACE-HEATING LOAD AND MONTHLY SOLAR ENERGY
3  ACCUMULATED SOLAR LOAD
      QSHL=QSHL+DAY40*24.0
      Q3)=QSUM+DAY40N
      WRITE(6,1235) QTOT
      IF(PROG.EQ.1) GO TO 271
      MFLOW=DAYFLOW+DAY40N
      WRITE(6,1315) MFLOW

```

112350
112570

127

102710

```

PMFLOW=YFLOW*3.355*(141.-TIN)
WRITE (5,1325) RMFLOW
GO TO 24
271 OSHLT=OSHLT+OSHLM
280 O3UM=ORU DAY4DN
WRITE (5,1326) ORUM
YQTOT=YQTOT+YQTJ
YBUQ=YBUQ+YBUQ
IF (PROG.NE.3.) GO TO 299
PERSOL=YQTOT/(YQTOT+YBUQ)
UQTOT=OSHLT-YBUQ
GO TO 3
290 YFLOW=YFLOW+RMFLOW
UQTOT=YFLOW-YBUQ
CONTINUE
3 IF (PROG.EQ.4.) GO TO 295
WRITE (5,1330) YFLOW
295 WRITE (5,1331) YQTOT
WRITE (5,1332) YBUQ
WRITE (5,1333) UQTOT
IF (PROG.NE.4.) GO TO 298
WRITE (5,1332) PERSOL
WRITE (5,1340) OSHLT
298 CONTINUE
3 FOURTH, DO A COST ANALYSIS TO DETERMINE THE ECONOMIC FEASIBILITY
3 THE COST ANALYSIS IS A LIFE CYCLE COST ANALYSIS PROGRAM
READ*,FTC1
IF (EOF(5)INPUT).NE.0.) GO TO 93
WRITE (5,750) FTC1
READ*,FTC2
WRITE (5,711) FTC2
READ*,OTC
WRITE (5,721) OTC
READ*,STCA
WRITE (5,731) STCA

```

```
READ*,LICA  
WRITE(5,740) LICA  
READ*,TMAXC  
WRITE(6,745) TMAXC  
READ*,AMIR  
WRITE(6,2000) AMIR  
READ*,YRMORT  
WRITE(6,2005) YRMORT  
READ*,DNFMT  
WRITE(5,2010) DNFMT  
READ*,BUFCOST  
WRITE(6,2015) BUFCOST  
READ*,CONFCS  
WRITE(6,2020) CONFCS  
READ*,BUEFF  
WRITE(5,2025) BUEFF  
READ*,CONEFF  
WRITE(5,2030) CONEFF  
READ*,TAXRT  
WRITE(6,2035) TAXRT  
READ*,TAXPRKT  
WRITE(5,2040) TAXPRKT  
READ*,XTRINS  
WRITE(5,2045) XTRINS  
READ*,GENINF  
WRITE(6,2050) GENINF  
READ*,FLINF  
WRITE(6,2055) FLINF  
READ*,DISCRT  
WRITE(6,2060) DISCRT  
READ*,ANALTRM  
WRITE(6,2065) ANALTRM  
3 COST ANALYSIS MODIFIED FOR AIR HEATER  
IF (PROG.EQ.4.) GO TO 505
```

```

YR1FL=(YFLOW/(19.**6))*(CONF CST/CONF EFF)
GO TO 51
505 YR1FL=(OSHLT/(19.**6.))*(CONF CST/CONF EFF)
517 WRITE(6,2170) YR1FL
READ*,AREACST
WRITE(6,2120) AREACST
READ*,ARINCST
WRITE(6,2125) ARINCST
C THE INFLATION-DISCOUNT FACTOR IS USED TO REDUCE COSTS TO PERCENT YEAR COSTS
CALL DI(ANALTRM,FLINF,DISCRT,AA)
CALL DI(ANALTRM,GENINF,DISCRT,BB)
IF(YRMORT.GT.ANALTRM) GO TO 115
CALL DI(YRMORT,AMIR,DISCRT,CC)
CALL DI(YRMORT,J.J,DISCRT,FF)
GO TO 116
115 CALL DI(ANALTRM,AMIR,DISCRT,CC)
116 CALL DI(ANALTRM,J.J,DISCRT,FF)
CONTINUE
CALL DI(YRMORT,J.J,AMIR,EE)
WRITE(6,3000) AA
WRITE(6,3005) BB
WRITE(6,3010) CC
WRITE(6,3015) EE
WRITE(6,3020) FF
GG=FF/EE
WRITE(6,2180) GG
HH=SG+(CC*(AMIR-(1./EE)))
WRITE(6,2035) HH
II=DNPMI+((1.-DNPMI)*(GG-(HH*TAXBKTI)))
WRITE(6,2130) II
JJ=(XTRINS*BB)
WRITE(6,2155) JJ
KK=TAXRT*BB*(1.-TAXBKTI)
OO=II+JJ+KK
WRITE(6,2100) KK

```

```

WRITE (6,2115) 00
RTC=(ARFACSI*AC)+ARINCST
IF(RTC.GT.LICA) GO TO 600
C INVESTMENT IN SOLAR MINUS TAX CREDIT
OFTC1=((FTC1+OTC)*(STCA)+(FTC2+OTC)*(RTC-STCA))
IF(OFTC1.GT.TMAXC) GO TO 612
R3=RTC-OFTC1
GO TO 611
500 OFTC2=((FTC1+OTC)*(STCA)+(FTC2+OTC)*(LICA-STCA))
IF(OFTC2.GT.TMAXC) GO TO 612
R3=RTC-OFTC2
GO TO 611
512 R3=RTC-TMAXC
510 IF(PROG.EQ.4.) GO TO 530
R2=UOTOT/YFLOW
R4=YFLOW*(1.-R2)*BUCFST/(BUEFF*(10.**6))
GO TO 541
530 R2=UOTOT/OSHLT
R4=OSHLT*(1.-R2)*BUCFST/(BUEFF*(10.**6))
540 R5=(YR1FL-R4)*AA
R5=00*R3
R8=R5-RE
WRITE (6,2160) R2
WRITE (6,2130) R3
WRITE (6,2135) R4
WRITE (6,2140) R5
WRITE (6,2145) R6
WRITE (6,2150) R8
CONTINUE
99 340 FORMAT(" TIME TO HOUSE,MODE 2",35X,F9.5)
342 FORMAT(" TIME TO BED,MODE 2",35X,F9.5)
344 FORMAT(" TEMP OUT OF COLLECTOR",35X,F9.3)
346 FORMAT(" TIME TO SATISFY LOAD",35X,F8.5)
348 FORMAT(" TA AT EXIT,MODE 3",35X,F9.3)

```

717 FORMAT(" FEDERAL TAX CREDIT PERCENTAGE INITIALLY",3CX,F8.4)
 718 FORMAT(" FEDERAL TAX CREDIT PERCENTAGE SECONDARY",3CX,F8.4)
 720 FORMAT(" OHIO TAX CREDIT PERCENTAGE",3CX,F6.4)
 730 FORMAT(" INITIAL TAX CREDIT AMOUNT",3CX,F10.2)
 740 FORMAT(" SECONDARY TAX CREDIT AMOUNT",3CX,F10.2)
 745 FORMAT(" MAX TAX CREDIT AMT.",3CX,F10.2)
 905 FORMAT(" MINUTE TIME INCREMENT FOR DISCHARGE",35X,F7.3)
 907 FORMAT(" EPSILON FOR TIME INCREMENT",37X,F8.5)
 910 FORMAT(" MINIMUM PUMP ENERGY",40X,F9.2)
 915 FORMAT(" STRUCTURE CONDUCTANCE",40X,F9.3)
 920 FORMAT(" TIME STEP",45X,F6.3)
 925 FORMAT(" VOLUMETRIC FLOW RATE (CFS)",40X,F5.3)
 930 FORMAT(" BED HEIGHT",45X,F6.3)
 935 FORMAT(" BED WIDTH",45X,F6.3)
 940 FORMAT(" AIR DENSITY",45X,F9.5)
 945 FORMAT(" PARTICLE DIAMETER(FT)",42X,F10.5)
 950 FORMAT(" POROSITY NUMBER",45X,F3.3)
 955 FORMAT(" CONDUCTIVITY OF AIR",42X,F9.5)
 960 FORMAT(" MOMENTUM DIFFUSIVITY",42X,F9.5)
 965 FORMAT(" SPECIFIC HEAT(AIR)",42X,F9.5)
 970 FORMAT(" OUTSIDE BED TEMP.",42X,F5.2)
 975 FORMAT(" SOLID DENSITY",45X,F9.3)
 980 FORMAT(" SOLID SPECIFIC HEAT",42X,F9.5)
 985 FORMAT(" BED LENGTH",45X,F6.2)
 990 FORMAT(" NUMBER OF NODES",43X,I3)
 995 FORMAT(" VOID FRACTION OF BED",4CX,F3.4)
 999 FORMAT(" NUMBER OF DEGREE-DAYS",40X,F9.3)
 1100 FORMAT(" DAY OF YEAR",49X,F5.0)
 1105 FORMAT(" DECLINATION (DEGREES)",4X,F8.4)
 1110 FORMAT(" EXTRATERRESTRIAL RADIATION ON A HORIZ SURFACE",13X,F9.4)
 1115 FORMAT(" SUNSET HOUR ANGLE (DEGREES)",33X,F8.4)
 1120 FORMAT(" LONGTERM CLEARNESS INDEX",37X,F5.4)
 1125 FORMAT(" MONTHLY AVERAGE DIFFUSE RADIATION ON A")
 1130 FORMAT(" HORIZONTAL SURFACE",42X,F9.4)
 1135 FORMAT(" ANGLE BETWEEN SUN AND COLLECTOR NORMAL",22X,F8.4)
 1140 FORMAT(" SOLAR ZENITH ANGLE",42X,F8.4)

102730
 002740
 002750
 002760
 002770
 002780

1140 FORMAT(" GROUND REFLECTANCE ",4X,F5.4)
1150 FORMAT(" MONTHLY AVERAGE INSTANTANEOUS TOTAL RADIATION")
1160 FORMAT(" ON A TILTED SURFACE ",4X,F8.4)
1170 FORMAT(" TOTAL TRANSMITTANCE",4X,F6.4)
1180 FORMAT(" SHADING FACTOR",4X,F5.4)
1190 FORMAT(" EFFECTIVE TRANSMITTANCE-ABSORPTANCE PRODUCT",20X,F5.4)
1200 FORMAT("RATIO OF CRITICAL RADIATION TO MONTHLY AVERAGE INSTANT")
1210 FORMAT(" TOTAL RADIATION ON A TILTED SURFACE",27X,F7.4)
1220 FORMAT(" FROM ",F4.0," TO ",F4.0," O'CLOCK")
1230 FORMAT(" UTILITY",50X,F6.4)
1240 FORMAT(" NO HEAT GAIN THIS HOUR")
1250 FORMAT(" TEMPERATURE OF FLUID IN STORAGE TANK(DEG F)",17X,F5.1)
1260 FORMAT(" HEAT TRANSFER THIS HOUR(BTJ/HR)",28X,F9.1)
1270 FORMAT(" LATITUDE(DEGREES)",4X,F3.1)
1280 FORMAT(" AVERAGE AMBIENT TEMPERATURE(DEG F)",27X,F5.1)
1290 FORMAT(" AVERAGE DAILY RADIATION ON A HORIZONTAL")
1300 FORMAT(" SURFACE (BTU/HR-SQ FT)",37X,F7.1)
1310 FORMAT(" DIFT FACTOR",52X,F4.2)
1320 FORMAT(" PERCENT OF TIME THE GROUND IS COVERED WITH")
1330 FORMAT(" MORE THAN ONE INCH OF SNOW",35X,F4.0)
1340 FORMAT(" SLOPE OF COLLECTOR (DEGREES)",34X,F2.0)
1350 FORMAT(" NUMBER OF COVERS ON COLLECTOR",34X,F2.0)
1360 FORMAT(" COLLECTOR AZIMUTH ANGLE (DEGREES)",28X,F5.1)
1370 FORMAT(" SURFACE AREA OF COLLECTOR FACE (SQ FT)",22X,F6.1)
1380 FORMAT(" THICKNESS OF ONE LAYER OF COVER MATERIAL",23X,F5.3)
1390 FORMAT(" EXTINCTION COEFFICIENT OF COVER MATERIAL",23X,F5.3)
1400 FORMAT(" INDEX OF REFRACTION OF COVER MATERIAL",26X,F5.3)
1410 FORMAT(" ABSORPTIVITY OF COLLECTOR",38X,F4.2)
1420 FORMAT(" HEAT REMOVAL EFFICIENCY OF COLLECTOR",27X,F4.2)
1430 FORMAT(" COLLECTOR HEAT LOSS COEFFICIENT",22X,F4.2)
1440 FORMAT(" MASS FLOW RATE OF FLUID THROUGH COLLECTOR IN")
1450 FORMAT(" POUNDS-PER-HOUR",45X,F5.1)
1460 FORMAT(" COEFF OF SPECIFIC HEAT OF COLLECTOR FLUID",22X,F4.2)
1470 FORMAT(" NUMBER OF INTERVALS DESIRED ON F-CHART",24X,I2)
1480 FORMAT(" INITIAL TEMPERATURE OF FLUID IN STORAGE TANK",17X,F5.1)
1490 FORMAT(" INITIAL TEMPERATURE INSIDE BUILDING",26X,F5.1)

002810
002820
002830
002850
002850
002870
002890
002930
002950
002960
002970
002990
002990
003000
003010
003020
003030
003040
003050
003060
003070
003080
003090
003100
003110
003120
003130
003140
003150
003160
003170
003180
003190

1247 FORMAT(" EFFICIENCY OF HEAT EXCHANGER",35X,F4.2)
1248 FORMAT(" TYPE OF SYSTEM IN USE",41X,F3.0)
1251 FORMAT("AMOUNT OF FLUID IN STORAGE TANK (GAL)",24X,F7.1)
1252 FORMAT(" SURFACE AREA OF STORAGE TANK (SQ FT)",25X,F5.1)
1253 FORMAT(" INSULATION THICKNESS ON STORAGE TANK (IN)",20X,F4.2)
1254 FORMAT(" CONDUCTIVITY OF STORAGE TANK INSULATION",24X,F4.2)
1255 FORMAT(" COEFFICIENT OF SPECIFIC HEAT OF STORAGE FLUID",13X,F4.2)
1256 FORMAT(" NUMBER OF DAYS PROGRAM IS TO RUN",37X,I2)
1257 FORMAT(" KT(",I2,") = ",F6.4)
1258 FORMAT(" NUMBER OF DAYS IN THE MONTH",38X,F4.0)
1259 FORMAT(" TOTAL USEFUL SOLAR ENERGY FOR MONTH",24X,F10.1)
1260 FORMAT(" AVERAGE DAILY FLOW USED (GAL)",31X,F10.1)
1261 FORMAT(" MONTHLY FLOW USED (GAL)",35X,F11.1)
1262 FORMAT(" BACKUP HEAT USED THIS HOUR(BTU)",27X,F11.1)
1263 FORMAT(" DAILY BACKUP HEAT USED(BTU)",31X,F11.1)
1264 FORMAT(" MONTHLY BACKUP HEAT USED (BTU)",28X,F11.1)
1265 FORMAT(" MONTHLY LOAD USED (BTU)",35X,F11.1)
1266 FORMAT(" YEARLY BACKUP ENERGY USED (BTU)",25X,F13.1)
1267 FORMAT(" PERCENT SOLAR ENERGY",30X,F8.0)
1268 FORMAT(" YEARLY SOLAR ENERGY USED (BTU)",26X,F13.1)
1269 FORMAT(" YEARLY LOAD USED (BTU)",34X,F13.1)
1270 FORMAT(" NUMBER OF MONTHS PROGRAM IS TO RUN",31X,I2)
1271 FORMAT(" YEARLY SOLAR ENERGY ACCOUNTING FOR TANK LOSS",12X,F13.1)
1272 FORMAT(" ANNUAL MORTGAGE INTEREST RATE",36X,F4.2)
1273 FORMAT(" TERM OF MORTGAGE",49X,F4.2)
1274 FORMAT(" DOWN PAYMENT, AS FRACTION OF INVESTMENT",24X,F6.4)
1275 FORMAT(" BACKUP FURNACE COST",41X,F15.2)
1276 FORMAT(" CONVENTIONAL FURNACE COST",34X,F11.2)
1277 FORMAT(" EFFICIENCY OF SOLAR BACKUP FURNACE",31X,F4.2)
1278 FORMAT(" EFFICIENCY OF CONVENTIONAL SYSTEM FURNACE",24X,F4.2)
1279 FORMAT(" TAX RATE, FRACTION OF INVESTMENT",32X,F6.4)
1280 FORMAT(" EFFECTIVE INCOME TAX BRACKET",35X,F5.3)
1281 FORMAT(" EXTRA INS AND MAINT COST, FRACT OF INVESTMENT",21X,F4.2)
1282 FORMAT(" GENERAL INFLATION RATE PER YEAR",33X,F3.3)
1283 FORMAT(" FUEL INFLATION RATE PER YEAR",35X,F6.3)
1284 FORMAT(" DISCOUNT RATE",51X,F5.3)

003249
003250
003260
003270

2165 FORMAT(" TERM OF ECONOMIC ANALYSIS",40X,F10.2)
 2170 FORMAT(" FIRST YEAR NON-SOLAR FUEL EXPENSE",28X,F6.2)
 2180 FORMAT(" LOAN PAYMENT",50X,F7.2)
 2185 FORMAT(" LOAN INTEREST",45X,F10.2)
 2190 FORMAT(" CAPITAL COST",47X,F10.2)
 2195 FORMAT(" INSURANCE AND MAINTENANCE COSTS",28X,F10.2)
 2200 FORMAT(" PROPERTY TAX",47X,F10.2)
 2210 FORMAT(" RESIDENTIAL COSTS",42X,F10.2)
 2220 FORMAT(" COLLECTOR AREA DEPENDENT COSTS",29X,F10.2)
 2225 FORMAT(" COLLECTOR AREA INDEPENDENT COSTS",27X,F10.2)
 2230 FORMAT(" INVESTMENT IN SOLAR MINUS TAX CREDIT",35X,F10.2)
 2235 FORMAT(" FIRST YEAR FUEL EXPENSE",35X,F10.2)
 2240 FORMAT(" FUEL SAVINGS",47X,F10.2)
 2245 FORMAT(" RESIDENTIAL EXPENSES",39X,F10.2)
 2250 FORMAT(" RESIDENTIAL SAVINGS",46X,F10.2)
 2255 FORMAT(" TEMPERATURE OF FLUID FROM SUPPLY",32X,F5.1)
 2260 FORMAT(" PERCENT OF TOTAL LOAD SATISFIED",30X,F5.3)
 3100 FORMAT(" AA =",56X,F8.3)
 3105 FORMAT(" BB =",56X,F8.3)
 3110 FORMAT(" CC =",56X,F8.3)
 3115 FORMAT(" EE =",56X,F8.3)
 3120 FORMAT(" FF =",56X,F8.3)
 4000 FORMAT(" SOLID CONDUCTIVITY",44X,F6.4)
 4010 FORMAT(" PARTICLE DIAMETER(INCHES)",42X,F6.3)
 4020 FORMAT(" INITIAL BED TEMP.",42X,F5.2)
 4030 FORMAT(" INSULATION CONDUCTIVITY",42X,F3.4)
 4040 FORMAT(" INSULATION THICKNESS(FT)",42X,F5.3)
 4050 FORMAT(" SURFACE AREA OF INSULATION",40X,F9.3)
 4100 FORMAT(" DYNAMIC VISCOSITY OF AIR",40X,F10.6)
 4110 FORMAT(" FAN EFFICIENCY",45X,F3.2)
 4120 FORMAT(" COLLECTOR AIR GAP SPACING",40X,F10.6)
 4130 FORMAT(" WIDTH OF SINGLE COLLECTOR",40X,F5.3)
 4140 FORMAT(" LENGTH OF SINGLE COLLECTOR",40X,F6.3)
 4150 FORMAT(" LENGTH OF DUCT WORK",43X,F7.3)
 4160 FORMAT(" DUCT DIAMETER",45X,F6.3)
 4170 FORMAT(" NUMBER OF TURNS(ELBOWS)",40X,F6.3)

```
107  FORMAT(" HOURS OF OPERATION",42X,"6.3")
      STOP"END OF PPROGRAM"
      END
      SUBROUTINE DI(YFS,RTINF,DISC,ZZ)
      IF(RTINF.EQ.DISC) GO TO 105
      ZZ=(1./((DISC-RTINF))+(1.-((1.+RTINF)/(1.+DISC)))*YRS)
      RETURN
105  ZZ=YFS/(1.+RTINF)
      RETURN
      END
```

Vita

Daniel Bartholomew Fant was born on 2 July 1957 in Queens, New York. He attended Newtown High School in Connecticut and graduated in June, 1975. He then attended the University of Connecticut and graduated in May, 1979 with the degree of Bachelor of Science in Mechanical Engineering. Upon graduation, he received a commission in the USAF through the AFROTC program. He then entered the School of Engineering at the Air Force Institute of Technology in June, 1979.

Permanent Address: 35 Appleblossom Lane
Newtown CT 06470

Thesis was typed by Patricia Browder.

UNCLASSIFIED

SECURITY CLASSIFICATION OF THIS PAGE (When Data Entered)

REPORT DOCUMENTATION PAGE		READ INSTRUCTIONS BEFORE COMPLETING FORM
1. REPORT NUMBER AFIT/GAE/AA/80D-4	2. GOVT ACCESSION NO. AD-A094771	3. RECIPIENT'S CATALOG NUMBER
4. TITLE (and Subtitle) Computer Simulation of Solar Air Heating Systems Using Rock Bed Thermal Storage Units		5. TYPE OF REPORT & PERIOD COVERED MS Thesis
		6. PERFORMING ORG. REPORT NUMBER
7. AUTHOR(s) Daniel B. Fant, 2D LT, USAF		8. CONTRACT OR GRANT NUMBER(s)
9. PERFORMING ORGANIZATION NAME AND ADDRESS Air Force Institute of Technology (AFIT/EN) Wright-Patterson AFB OH 45433		10. PROGRAM ELEMENT, PROJECT, TASK AREA & WORK UNIT NUMBERS
11. CONTROLLING OFFICE NAME AND ADDRESS		12. REPORT DATE December 1980
		13. NUMBER OF PAGES 128
14. MONITORING AGENCY NAME & ADDRESS (if different from Controlling Office)		15. SECURITY CLASS. (of this report) Unclassified
		15a. DECLASSIFICATION, DOWNGRADING SCHEDULE
16. DISTRIBUTION STATEMENT (of this Report) Approved for public release; distribution unlimited.		
17. DISTRIBUTION STATEMENT (of the abstract entered in Block 20, if different from Report)		
18. SUPPLEMENTARY NOTES Approved for public release; IAW AFR 190-17 FREDERICK C. LYNCH, MAJOR, USAF 30 DEC 1980 Director of Public Affairs		
19. KEY WORDS (Continue on reverse side if necessary and identify by block number) Solar Air Heating System Simulation Rock Bed Thermal Storage Fully-Implicit Numerical Scheme		
20. ABSTRACT (Continue on reverse side if necessary and identify by block number) This thesis is concerned with the analysis and design of solar air heating systems utilizing rock beds as thermal storage units. A computer simulation model capable of estimating the response of both the solar collector and the rock bed is described.		

Block 20: Abstract (Cont'd)

Differential equations describing the rock bed were approximated in a finite-difference form and solved numerically on a digital computer. The temperature of both the solid (rock) and the fluid (air) is determined as a function of time and distance along the bed. The simulation required both charging and discharging of the rock bed for time-varying inlet fluid temperatures. The numerical method used to solve the rock bed equations proved to be stable and convergent and showed satisfactory agreement in comparison to an analytical solution for constant-inlet air temperatures. A cost-analysis was also incorporated within this program; by varying the collector area one could determine the optimum collector size for maximum savings. Pressure drop relationships for flat-plate collectors, duct work and packed beds were used to determine operating costs. The particular air system tested proved to be cost effective when compared with natural gas fuel costs for an economic term of 20 years.